

**Alzheimer-like pathology in murine transgenic
models: disease modification by
environmental and genetic interventions**

Dissertation
for the award of the degree
“Doctor rerum naturalium”
of the Georg-August-University Göttingen

within the doctoral program *Molecular Physiology of the Brain*
of the Georg-August-University School of Science (GAUSS)

submitted by
Melanie Hüttenrauch

from Heilbad Heiligenstadt, Germany

Göttingen, 2016

Thesis Committee:

PD Dr. Oliver Wirths (Reviewer)

Department of Molecular Psychiatry, Division of Molecular Psychiatry, University Medical Center Göttingen

Prof. Dr. Tiago F. Outeiro (Reviewer)

Department of Neurodegeneration and Restorative Research, University Medical Center Göttingen

Prof. Dr. Dr. Hannelore Ehrenreich

Department of Clinical Neurosciences, Max Planck Institute of Experimental Medicine, Göttingen

Date of oral examination: May 18th, 2016

Affidavit

I hereby declare that my doctoral thesis entitled “Alzheimer-like pathology in murine transgenic models: disease modification by environmental and genetic interventions” has been written independently with no other sources and aids than quoted.

Melanie Hüttenrauch
Göttingen, March 2016

This thesis is dedicated to my beloved Family

List of publications:

Publications included in this thesis:

Hüttenrauch M, Brauß A, Kurdakova A, Borgers H, Klinker F, Liebetanz D, Salinas-Riester G, Wiltfang J, Klafki H, Wirths O. (2016)
Physical activity delays hippocampal neurodegeneration and rescues memory deficits in an Alzheimer disease mouse model.
Transl Psychiatry. 6:e800

Hüttenrauch M, Baches S, Gerth J, Bayer TA, Weggen S, Wirths O. (2015)
Neprilysin deficiency alters the neuropathological and behavioral phenotype in the 5XFAD mouse model of Alzheimer's disease.
J Alzheimers Dis. 44(4):1291-302.

Publications not included in this thesis:

Weissmann R*, **Hüttenrauch M***, Kacprowski T, Bouter Y, Pradier L, Bayer TA, Kuss AW, Wirths O. (2015)
Gene expression profiling in the APP/PS1KI mouse model of familial Alzheimer's disease.
J Alzheimers Dis. 50(2):397-409
* equal contribution

Christensen DZ, **Huettenrauch M**, Mitkowski M, Pradier L, Wirths O. (2014)
Axonal degeneration in an Alzheimer mouse model is PS1 gene dose dependent and linked to intraneuronal A β accumulation.
Front Aging Neurosci. 6:139

Reinert J, Martens H, **Huettenrauch M**, Kolbow T, Lannfelt L, Ingelsson M, Pateau A, Verkkoniemi-Ahola A, Bayer TA, Wirths O. 2014
A β 38 in the brains of patients with sporadic and familial Alzheimer's disease and transgenic mouse models.
J Alzheimers Dis. 39(4):871-81

Abstracts:

Hüttenrauch M, Brauß A, Kurdakova A, Klafki H, Wiltfang J, Wirths O. (2015)
Physical activity ameliorates neuron loss and memory deficits in Tg4-42 mice.
Pharmacopsychiatry. 48(06)

Hüttenrauch M, Baches S, Gerth J, Bayer TA, Weggen Sascha, Wirths O. (2015)
Neprilysin deficiency alters the neuropathological and behavioral phenotype in the 5XFAD mouse model of Alzheimer's disease.
Neurodegenerative Diseases, 2015;15(suppl 1): 352-1969 – Page 1021

Contents

ACKNOWLEDGEMENTS	I
ABSTRACT	III
LIST OF FIGURES	V
LIST OF TABLES	VI
LIST OF ABBREVIATIONS	VII
1 INTRODUCTION	1
1.1 Alzheimer's disease	1
1.2 Clinical features of Alzheimer's disease	1
1.3 Neuropathological hallmarks	2
1.3.1 Amyloid deposits.....	2
1.3.2 Neurofibrillary tangles.....	2
1.3.3 Brain atrophy.....	3
1.3.4 Inflammation	4
1.4 The amyloid precursor protein.....	5
1.4.1 Amyloidogenic and non-amyloidogenic processing of APP	6
1.5 The amyloid hypothesis.....	7
1.6 A β clearance mechanisms.....	9
1.6.1 Non-enzymatic clearance pathways.....	9
1.6.2 Enzymatic clearance pathways.....	10
1.7 Mouse models of Alzheimer's disease.....	12
1.7.1 The Tg4-42 mouse model	13
1.7.2 The 5XFAD mouse model.....	15
1.8 Risk factors for Alzheimer's disease	16
1.8.1 Genetic risk factors.....	16
1.8.2 Environmental risk factors.....	17
1.9 The cognitive reserve hypothesis	18
1.10 The environmental enrichment paradigm	19
1.10.1 Benefits of environmental enrichment in rodents.....	21
1.10.2 Benefits of environmental enrichment in AD mouse models	21
1.11 Project objectives	23
1.11.1 Project I: The effect of long-term environmental enrichment and physical activity on the pathology of Tg4-42 and 5XFAD mice	23

1.11.2	Project II: Neprilysin deficiency alters the neuropathological and behavioural phenotype in the 5XFAD mouse model of Alzheimer's disease	24
2	MATERIALS AND METHODS.....	25
2.1	Chemicals, Reagents and Kits	25
2.2	Laboratory Animals.....	27
2.2.1	Animal care and general conditions	27
2.2.2	Housing conditions.....	27
2.2.2.1	Standard housing.....	27
2.2.2.2	Environmental enrichment housing	27
2.2.2.3	Individual cage housing	28
2.2.3	Tg4-42 transgenic mice	28
2.2.4	5XFAD transgenic mice.....	28
2.2.5	Neprilysin gene-disrupted mice.....	29
2.2.6	Tissue collection and preservation	29
2.3	Behavioural Analysis.....	30
2.3.1	Motor phenotype assessment	30
2.3.1.1	Balance Beam	30
2.3.1.2	String suspension	30
2.3.1.3	Rotarod	31
2.3.2	Y-Maze	31
2.3.3	Cross Maze	31
2.3.4	Elevated plus maze.....	32
2.3.5	Morris water maze.....	32
2.3.6	Novel object recognition	33
2.4	Molecular Biology.....	34
2.4.1	Isolation of genomic DNA and genotyping of transgenic mice.....	34
2.4.2	RNA isolation from mouse brain.....	36
2.4.3	Determination of nucleic acid concentration	37
2.4.4	Reverse transcription.....	37
2.4.5	Quantitative real-time polymerase chain reaction (qRT-PCR)	38
2.4.6	Primers.....	39
2.4.7	Protein isolation from mouse brain.....	41
2.4.8	Protein concentration determination	41
2.4.9	Enzyme-linked immunosorbent assay (ELISA) analysis	41
2.4.10	Electrochemiluminescence A β assay.....	42
2.5	Deep sequencing analysis	43
2.6	Immunohistochemistry.....	43

2.6.1	Paraffin embedding of mouse brain	43
2.6.2	3, 3'-Diaminobenzidine (DAB) immunohistochemistry	44
2.6.3	Free-floating immunohistochemistry	45
2.6.4	Thioflavin S staining of paraffin sections.....	46
2.6.5	Quantification of A β plaque load, Thioflavin S and GFAP immunoreactivity	46
2.6.6	Primary Antibodies	47
2.6.7	Secondary Antibodies.....	47
2.7	Quantification of neuron numbers	47
2.7.1	Sample preparation.....	47
2.7.2	Cresyl violet staining	48
2.7.3	Stereological analysis	48
2.7.3.1	Quantification of total neuron numbers in CA1 area and dentate gyrus of the hippocampus	48
2.7.3.2	Estimation of volume of CA1 area and dentate gyrus of the hippocampus	50
2.8	Statistical analysis.....	51
3	RESULTS	52
3.1	PROJECT I: The effect of long-term environmental enrichment and physical activity on the pathology of Tg4-42 and 5XFAD mice.....	52
3.1.1	Part I: Enriched living conditions and physical activity delays hippocampal neurodegeneration and rescues memory deficits in the Tg4-42 mouse model of Alzheimer's disease	53
3.1.1.1	The impact of environmental enrichment and voluntary exercise on the sensory-motor performance of Tg4-42 ^{het} mice	53
3.1.1.2	Enriched environment and voluntary exercise prevent spatial reference memory deficits in Tg4-42 ^{het} mice.....	54
3.1.1.3	Enriched environment combined with physical activity restores recognition memory in Tg4-42 ^{het} mice.....	57
3.1.1.4	The effect of environmental enrichment and voluntary exercise on hippocampal neuron numbers and volume in Tg4-42 ^{het} mice.....	58
3.1.1.5	Enriched environment and physical activity do not affect subgranular adult neurogenesis in Tg4-42 ^{het} mice	60
3.1.1.6	The effect of long-term cognitive and physical stimulation on A β brain levels in Tg4-42 ^{het} mice.....	61
3.1.1.7	Housing under enriched conditions and physical activity changes the gene expression profile of WT and Tg4-42 ^{het} mice.....	61

3.1.1.8	The effect of physical activity alone on the pathology of Tg4-42 ^{hom} mice	65
3.1.2	Part II: Lifelong environmental enrichment in combination with voluntary exercise has limited effects on the pathology of 5XFAD mice	68
3.1.2.1	The effect of environmental enrichment on the physiological status and the sensory-motor phenotype of 5XFAD mice	68
3.1.2.2	Environmental enrichment fails to restore decreased anxiety levels and spatial working memory deficits in 5XFAD mice	69
3.1.2.3	Long-term physical and cognitive stimulation does not influence amyloid plaque load and A β ₁₋₄₂ levels in brains of 5XFAD mice	71
3.1.2.4	Housing condition has no impact on the inflammatory phenotype of 5XFAD mice	73
3.1.2.5	The effect of voluntary exercise on gene expression in 5XFAD mice	74
3.2	Project II: Neprilysin deficiency alters the neuropathological and behavioural phenotype in the 5XFAD mouse model of Alzheimer's disease	75
3.2.1	Characterization of 5XFAD/NEP ^{+/-} mice	75
3.2.2	The effect of neprilysin deficiency on the spatial working memory performance of 5XFAD mice	76
3.2.3	Region-specific increase in extracellular A β plaque load in aged 5XFAD/NEP ^{+/-} mice	78
3.2.4	Increased astrogliosis in 5XFAD/NEP ^{+/-} mice	81
3.2.5	Amyloid pathology in young 5XFAD/NEP ^{+/-} mice	82
3.2.6	A β -degrading enzyme expression in 5XFAD and 5XFAD/NEP ^{+/-} mice	83
4	DISCUSSION	85
4.1	Project I: The effect of long-term environmental enrichment and physical activity on the pathology of Tg4-42 and 5XFAD mice	85
4.1.1	Part I: Enriched living conditions and physical activity delays hippocampal neurodegeneration and rescues memory deficits in the Tg4-42 mouse model of Alzheimer's disease	85
4.1.1.1	Improved sensory-motor performance in enriched housed Tg4-42 ^{het} mice	85
4.1.1.2	Voluntary exercise decelerates CA1 neuron loss in Tg4-42 mice	86
4.1.1.3	Prolonged physical activity prevents the cognitive decline in Tg4-42 ^{het} mice	88
4.1.1.4	Adult hippocampal neurogenesis is unaffected in enriched housed WT and Tg4-42 ^{het} mice	90
4.1.1.5	Tg4-42 ^{het} SH and EE mice display unaltered brain A β levels	92
4.1.1.6	Gene expression changes underlying the beneficial effects of long-term enriched environment	93

4.1.1.7	Conclusions of Project I, Part I:.....	96
4.1.2	Part II: Lifelong environmental enrichment in combination with voluntary exercise has limited effects on the pathology of 5XFAD mice	96
4.1.2.1	Long-term enriched living conditions have a limited effect on the physiological status and the sensory-motor phenotype of 5XFAD mice.....	96
4.1.2.2	Enriched living conditions do not alter the behavioural phenotype of 5XFAD mice	97
4.1.2.3	Standard- and enriched housed 5XFAD mice display similar levels of amyloid pathology	98
4.1.2.4	Induction of neuroprotective genes in physically active 5XFAD mice	100
4.1.2.5	Conclusions of Project I, Part II:.....	101
4.2	Project II: Neprilysin deficiency alters the neuropathological and behavioural phenotype in the 5XFAD model of Alzheimer's disease	101
4.2.1	Conclusions of Project II:.....	104
5	SUMMARY & CONCLUSIONS	106
6	BIBLIOGRAPHY	109
	CURRICULUM VITAE	128

ACKNOWLEDGEMENTS

First of all, I would like to express my gratitude to my supervisor PD. Dr. Oliver Wirths. Thank you so much for your encouraging guidance and excellent scientific support. I gratefully acknowledge your immense patience, scientific knowledge and teaching skills. Thank you for your trust and for giving me the opportunity to work independently.

Furthermore, I thank Prof. Dr. Thomas Bayer for giving me the opportunity to perform my PhD thesis in his lab and his helpful advices.

I further gratefully thank the members of my thesis committee: Thank you, Prof. Tiago Outeiro for agreeing to be the second reviewer for my thesis and for your helpful comments and valuable input during my progress reports. Thank you, Prof. Hannelore Ehrenreich for your time, support and very helpful discussions.

I would also like to thank Prof. Dr. Gerhard Hunsmann for providing me with a stipend throughout the time of my doctoral studies. Thank you for your considerable interest in my project and for numerous delightful discussions during our annual meetings.

Many thanks to the members of the GGNB office, especially Mirja Blötz, who has always been able to offer assistance.

Many thanks to Petra Tucholla for her laboratory assistance and practical support.

Greg, the last three years would not have been the same without you. Not only are you one of the most humorous persons I have ever met in my life, but also the one with the kindest heart. I would not want to miss a single experience we shared together in the last years. Thank you for always being there.

Berni, our time inside and outside the lab was so much fun. Thank you for being who you are and also for being there in the worst times.

Anika, I joined this lab because of you. Thank you so much! Especially for teaching me in the beginning, but also for lovely times outside the lab.

Nasrin, my dear friend. Thank you for all our chatty lunch breaks and for your delightful personality! You have such a warm heart.

Meike, words are not enough to express how thankful I am that you joined our lab last year. We had this instant connection that makes me feel like I have been knowing you forever. Thank you so much for endless fun hours in the lab, for listening to the same stories all over again, for laughing with me on good days and for cheering me up on the worst ones. Thank you for being who you are.

Adriana & Soc, when you joined the lab, the whole atmosphere lightened up immediately. Thank you for your positive and heart-warming personalities.

Thanks to all the bachelor, master and rotation students who came and went and whom I have taught, especially Anastasia, Jon, Naira and Margie.

Ein ganz besonderer Dank gilt auch meinen lieben Freunden außerhalb des Labors und Göttingen, insbesondere: Doro und Jenny, meine Liebsten, ohne eure Existenz wäre ich aufgeschmissen. Meine lieben Gerbershäuser, danke für eure vielen Besuche, die mich immer so sehr aufheitern. Flori, Mario und Markus, danke für die lustigsten Abende in Göttingen überhaupt (meine finale Antwort ist: heilen :)). Tobi, danke dass du alle Höhen und Tiefen während dieser Doktorarbeit ertragen hast.

Mein größter Dank gilt jedoch meiner lieben Familie: Papa, Mama & Bea, ich bin euch so unglaublich dankbar für alles, was ihr für mich tut. Danke für eure bedingungslose Unterstützung und euer Vertrauen. Eine Familie wie euch zu haben ist das wertvollste Geschenk, das man sich wünschen kann.

Ich schreibe meine Dissertation in liebevollem Gedenken an meinen Großvater Erich und meine Großmutter Waltraut. Ich hoffe, es geht euch gut.

ABSTRACT

As no successful therapeutic approach to treat Alzheimer's disease (AD) has been developed to date, preventative strategies and non-pharmacological interventions increasingly become a major research focus. In recent years, substantial evidence for a protective role of physical and cognitive activity on the risk of AD has been growing. In the present study, the effect of a challenging environment in combination with regular exercise on the Alzheimer-like pathology of the Tg4-42 and 5XFAD mouse models was investigated.

The Tg4-42 model overexpresses N-truncated $A\beta_{4-42}$ without any mutations and develops an age- and dose-dependent neuron loss in the CA1 region of the hippocampus associated with a severe memory decline. It could be shown that long-term cognitive and physical stimulation significantly delay hippocampal neuron loss and completely rescue memory deficits in 12-month-old Tg4-42 mice. Moreover, long-term gene expression profile changes yielding to neuroprotective events could be observed in enriched housed Tg4-42 mice. These effects were irrespective of brain $A\beta_{4-42}$ levels and increased neurogenesis rates. The present findings provide evidence for the first time that neuron loss and memory decline can be counteracted by prolonged physical and cognitive activity in a mouse model that rather reflects the sporadic form of AD.

The 5XFAD model is a well-characterized, commonly used AD model for the familial form of the disease, representing an early and aggressive pathology. In the present work, it could be demonstrated that prolonged cognitive and physical activity has no therapeutic benefit on the pathophysiology of this conventional 5XFAD model. Despite partial improvements in motor performance, no beneficial effects in terms of behavioural deficits, $A\beta$ plaque deposition, $A\beta_{1-42}$ levels or inflammatory phenotype were observed. These results suggest that a rather mild intervention like mental stimulation and regular exercise cannot counteract the aggressive AD pathology seen in 5XFAD mice.

In sporadic AD cases, a decelerated degradation of $A\beta$ is supposed to be the primary cause of an enhanced accumulation of the peptide in the brain. Nephilysin (NEP) represents the major $A\beta$ -degrading enzyme as shown by numerous *in vitro* and *in vivo*

studies and hence is assumed to play a pivotal role in the progression of AD. In order to gain deeper knowledge about the function of NEP, 5XFAD mice were crossed with homozygous NEP knock-out mice. NEP reduction led to an impaired spatial working memory performance in 6-month-old 5XFAD mice. Furthermore, depletion of the enzyme increased extracellular amyloid deposition in specific brain regions and enhanced the inflammatory response in the brain. In young 5XFAD mice, however, NEP knock-out led to a delayed A β plaque deposition accompanied by elevated levels of the NEP homologue endothelin-converting enzyme 1 (ECE1). These data support previous observations showing that NEP is a substantial A β -degrading enzyme and suggest a reciprocal effect between NEP and ECE1 activities in young 5XFAD mice.

LIST OF FIGURES

Figure 1: Amyloid plaques.....	2
Figure 2: Brain atrophy in AD.....	4
Figure 3: Inflammatory response in AD.....	5
Figure 4: APP processing pathways.....	7
Figure 5: The classical and modified amyloid cascade hypothesis.....	9
Figure 6: A β clearance pathways.....	12
Figure 7: Schematic diagram of Tg4-42 transgene.....	15
Figure 8: Schematic diagram of 5XFAD transgenes.....	16
Figure 9: The environmental enrichment paradigm.....	20
Figure 10: Schematic representation of hippocampal counting areas.....	50
Figure 11: Housing conditions and experimental design.....	52
Figure 12: Effects of EE on sensory-motor performance of WT and Tg4-42 ^{het} mice.....	54
Figure 13: Impaired spatial reference memory in Tg4-42 ^{het} mice is restored upon EE housing.	56
Figure 14: The impact of EE and physical activity on recognition memory performance.....	57
Figure 15: The effect of EE on hippocampal neuron numbers and volume.....	59
Figure 16: The impact of EE on adult neurogenesis in WT and Tg4-42 ^{het} mice.....	60
Figure 17: The effect of EE and physical activity on A β brain levels in Tg4-42 ^{het} mice.....	61
Figure 18: Gene expression profile changes upon long-term EE in WT and Tg4-42 ^{het} mice.....	64
Figure 19: Necdin expression analysis.....	65
Figure 20: The effect of physical activity on hippocampal neurodegeneration of Tg4-42 ^{hom} mice.....	67
Figure 21: The effect of EE and physical activity on the survival, body weight and sensory- motor performance of 5XFAD mice.....	69
Figure 22: Anxiety-related behaviour and working memory performance in standard and enriched housed 5XFAD mice.....	71
Figure 23: Housing condition has no effect on A β plaque pathology and A β ₁₋₄₂ levels of 5XFAD mice.....	72
Figure 24: Housing condition has no influence on the inflammatory phenotype of 5XFAD mice.....	73
Figure 25: Gene expression changes in enriched housed 5XFAD mice.....	74
Figure 26: Neprilysin mRNA and protein levels.....	76
Figure 27: Spatial working memory performance of 5XFAD mice upon NEP depletion.....	78
Figure 28: A β plaque deposition and A β ₁₋₄₂ level in 6-month-old 5XFAD and 5XFAD/NEP ^{+/-} mice.....	80
Figure 29: Inflammation status of 6-month-old 5XFAD and 5XFAD/NEP ^{+/-} mice.....	82
Figure 30: A β plaque load quantification in 2.5-month-old 5XFAD and 5XFAD/NEP ^{+/-} mice.....	83
Figure 31: Expression analysis of A β -degrading enzymes.....	84

LIST OF TABLES

Table 1: Chemicals and Reagents.....	25
Table 2: Kits	26
Table 3: Reaction mix for Tg4-42 genotyping PCR.....	35
Table 4: Reaction mixture for 5XFAD genotyping PCR.....	35
Table 5: Reaction mixture for NEP knockout genotyping PCR.....	36
Table 6: Cycling program for genotyping PCR.....	36
Table 7: qRT-PCR reaction mixture	38
Table 8: qRT-PCR cycling program	39
Table 9: List of primers used for genotyping and qRT-PCR.....	39
Table 10: Brain tissue dehydration protocol	44
Table 11: Primary Antibodies.....	47
Table 12: Secondary Antibodies.....	47
Table 13: Parameters for stereological analysis of CA1 and dentate gyrus neuron numbers .	49

LIST OF ABBREVIATIONS

Abbreviation	Description
A β	Amyloid beta
ABC	ATP-binding cassette transporter
ABC	Avidin-biotin complex
ABCB1	ATP-binding cassette subfamily B member 1
ACE	Angiotensin-converting enzyme
AD	Alzheimer's disease
ADAM	A disintegrin and metalloproteinase
ADE	A β -degrading enzyme
AICD	Amyloid precursor protein intracellular domain
ANOVA	Analysis of variance
APH	Anterior pharynx defective
APLP	Amyloid precursor like protein
ApoE	Apolipoprotein E
APP	Amyloid precursor protein
ATP	Adenosine triphosphate
BACE1	Beta-site cleaving enzyme 1
BBB	Blood brain barrier
BDNF	Brain-derived neurotrophic factor
CA1-3	Cornu ammonis area 1-3
cDNA	Complementary DNA
CR	Cognitive reserve
DAB	3,3'-diaminobenzidine
DAPI	4',6-diamino-2-phenylindole
DCX	Doublecortin X
DG	Dentate gyrus
DNA	Deoxyribonucleic acid
ECE-1	Endothelin-converting-enzyme 1
EE	Environmental enrichment
ELISA	Enzyme-linked immunosorbent assay
EO-AD	Early-onset Alzheimer's disease
ER	Endoplasmic reticulum
FAD	Familial Alzheimer's disease
FCS	Fetal calf serum

GFAP	Glial fibrillary acidic protein
GO	Gene ontology
GOI	Gene of interest
GWAS	Genome-wide association studies
Het	Heterozygous
Hom	Homozygous
HRP	Horseradish peroxidase
HSP	Heat shock protein
icv	intracerebroventricular
IDE	Insulin-degrading enzyme
ISF	Interstitial fluid
KEGG	Kyoto encyclopaedia of genes and genomes
LDLR	LDL receptor family
LOAD	Late-onset Alzheimer's disease
LRP2	low-density lipoprotein receptor-related protein-1
LTP	Long-term potentiation
MAPT	Microtubule-associated tau
MCI	Mild cognitive impairment
mGluR5	Metabotropic glutamate receptor 5
MRI	Magnetic resonance imaging
mRNA	Messenger RNA
MTL	Medial temporal lobe
MWM	Morris water maze
NCT	Nicestrin
NDN	Necdin
NEP	Nepriylsin
NFT	Neurofibrillary tangle
NGF	Nerve growth factor
NOR	Novel object recognition
NT-3/4	Neurotrophin 3/4
PAXIP1	PAX-interacting protein 1
PBS	Phosphate buffered saline
PCR	Polymerase chain reaction
PEN-2	Presenilin enhancer 2
PFA	Paraformaldehyde
PHF	Paired helical filament
PICALM	Phosphatidylinositol binding clathrin assembly protein

PSEN 1/2	Presenilin 1/2
RAGE	Receptor for advanced glycation end products
RNA	Ribonucleic acid
ROS	Reactive oxygen species
RT	Room temperature
sAPP	soluble APP
SDS	Sodium dodecyl sulfate
SEM	Standard error of the mean
SGZ	Subgranular zone
SH	Standard housing
SPF	Specific-pathogen-free
STZ	Streptozotolin
TAE buffer	Tris base/acetic acid buffer
TBE buffer	Tris/borate/EDTA buffer
TREM2	Triggering receptor expressed on myeloid cells 2
TRH	Thyrotropin-releasing hormone
WT	Wildtype
α 2M	α 2-macroglobulin

1 INTRODUCTION

1.1 Alzheimer's disease

Alzheimer's disease (AD) is an irreversible, progressive brain disorder representing the most common cause of dementia in the elderly population (Barker et al., 2002). According to the Alzheimer's association report, AD is the sixth-leading cause of natural death in the United States and evolved to be an enormous public health problem (Alzheimers Association, 2015). For those aged 65 and older, the risk to develop AD doubles every five years (Querfurth and LaFerla, 2010). Currently, there are approximately 1.5 million people suffering from dementia in Germany, with two-thirds of them being diagnosed with AD. This number is estimated to increase up to 3.0 million by 2050 due to the demographic development (Bickel, 2012).

1.2 Clinical features of Alzheimer's disease

The course of AD is slowly progressive and can be separated in different stages. Before clinical symptoms become apparent, neurodegenerative processes in the brain start and accumulate. This time period is referred to as preclinical AD and can last several years (Backman et al., 2004). When neurodegeneration reaches a certain level, neuropsychological tests can reveal the stage of mild cognitive impairment (MCI). In this stage, a person still lives independently but learning and memory abilities start to decline. Patients tend to forget recent events and appointments and develop difficulties in performing tasks in work and social settings. In the moderate stage of AD, patients require supervision as they develop impairments of language, motor deficits, disorientation and strong memory decline. Furthermore, personality and behavioural changes such as aggression, suspiciousness and delusions develop (Forstl and Kurz, 1999). In the late stage of AD, patients lose the ability to interact with their environment and require full-time assistance. Next to extreme lethargy and apathy, language skills are minimized and motor impairments, including rigidity, poor posture and bradykinesia become apparent (Scarmeas et al., 2004). Ultimately, patients lose their ability to swallow and become prone to infections like pneumonia (Frank, 1994;Forstl and Kurz, 1999).

1.3 Neuropathological hallmarks

1.3.1 Amyloid deposits

The extracellular deposition of amyloid beta ($A\beta$) in form of plaques represents one of the major hallmarks of AD. Based on their morphology, senile amyloid plaques can be categorized in either neuritic or diffuse plaques (Yamaguchi et al., 1988; Small, 1998) (Figure 1). Neuritic plaques, or dense-core plaques, are composed of highly aggregated filamentous $A\beta$ surrounded by dystrophic neurites, micro- and astrogliosis (Selkoe, 2001; Duyckaerts et al., 2009). These plaques can be detected with β -sheet binding dyes like Thioflavin S and Congo Red and range in size from 10 to 120 μm . Being primarily formed in the neocortex, neuritic plaques later spread to the hippocampus, amygdala, subcortical layers and brain stem (Arnold et al., 1991; Thal et al., 2002). In contrast, diffuse plaques are not detectable with β -sheet binding dyes as they consist of amorphous, less aggregated $A\beta$ depositions. They vary in size from 50 μm to several hundred μm and they are suggested to be precursors for neuritic plaques (Yamaguchi et al., 1988; Dickson, 1997). Intriguingly, diffuse plaques are not only detectable in AD patients, but also in cognitively normal, healthy individuals (Morris et al., 1996).

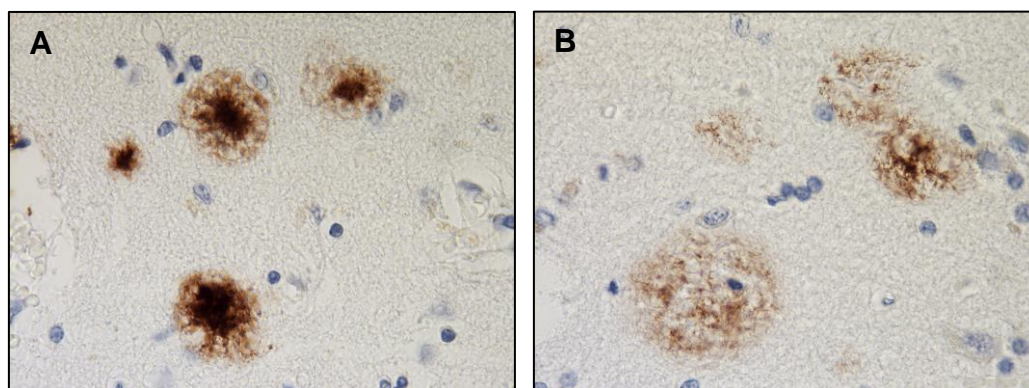


Figure 1: Amyloid plaques. Neuritic plaques (A) and diffuse amyloid plaques (B) visualized by immunohistochemistry.

1.3.2 Neurofibrillary tangles

Neurofibrillary tangles (NFTs) represent another major histopathological hallmark of AD (Alzheimer, 1907). These intracellular aggregates are present in the perikarya or apical dendrites of neurons and consist of paired helical filaments (PHFs) wound into

a helical structure. PHFs are composed of hyperphosphorylated, microtubule-associated tau (MAPT) (Kidd, 1963). Tau, under physiological conditions, supports the assembly of microtubules and therefore stabilizes the cytoskeleton (Drechsel et al., 1992). However, upon phosphorylation by diverse kinases, tau dissociates from the microtubules and aggregates into NFTs. Hyperphosphorylated tau aggregates cause diverse cellular dysfunctions including protein mistrafficking and loss of neuronal integrity (Ittner and Gotz, 2011). Unlike amyloid pathology, the localization of NFTs correlates well with the severity of AD progression. Therefore, tau pathology is used to stage the severity of AD into the Braak stages I-VI (Braak and Braak, 1991; Braak et al., 2006).

1.3.3 Brain atrophy

Next to amyloid plaques and NFTs, brain atrophy represents one of the most prominent pathological features of AD (Figure 2). This atrophy is caused by neuron loss in a region specific manner and is characterized by enlarged ventricles, widening of cortical sulci and shrinkage of gyri. Using magnetic resonance imaging (MRI), brain volume and weight reductions can be detected even at early stages of disease progression and are therefore predictable for the progression from MCI to AD (Jack et al., 2005). Atrophy is predominantly affecting the medial temporal lobe including the hippocampus, amygdala and entorhinal cortex (Bottino et al., 2002). The underlying cause of neuron death is still not known in great detail. Very early studies suggested a correlation between NFTs and neuron loss (Cras et al., 1995). Other findings reported evidence for apoptosis as one of the mechanisms contributing to cell death in AD (Shimohama, 2000). However, more recent studies link the neurotoxicity of intraneuronal and/or oligomeric A β with cell death (Bayer and Wirths, 2010).

In addition to neuron death, loss of synapses contributes to the cortical atrophy in AD brains. Synaptic loss is supposed to be an early pathological alteration that precedes neuron death (Serrano-Pozo et al., 2011). Accordingly, patients with mild AD display significantly fewer synapses in the cornu ammonis area 1 (CA1) region of the hippocampus when compared to healthy controls or patients with MCI (Scheff et al., 2007). The loss of synapses represents the structural correlate to early cognitive decline as supported by the fact that synaptic counts significantly correlate with the severity of dementia (DeKosky and Scheff, 1990; Ingelsson et al., 2004).

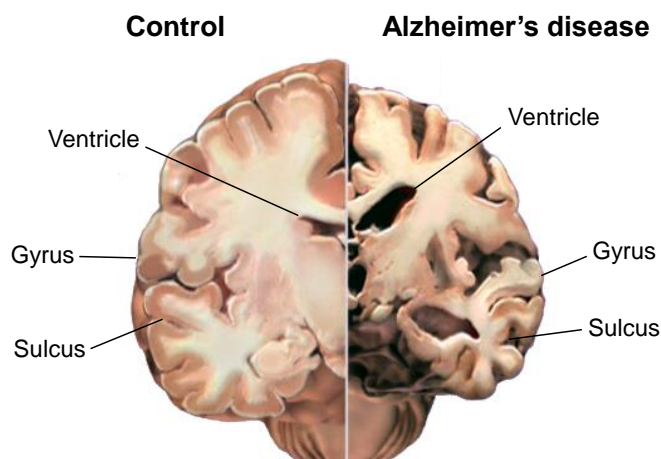


Figure 2: Brain atrophy in AD. Compared to the control subject (left), a patient with AD (right) shows enlargement of ventricles, widening of sulci and shrinkage of gyri. Tissue loss is specifically evident in the hippocampal region and entorhinal cortex. Modified from <http://www.alz.org/braintour.asp>.

1.3.4 Inflammation

Neuroinflammation represents an additional pathological hallmark of AD. Inflammatory processes are consistently found in brains of AD patients and also occur in transgenic AD mouse models (Hoozemans et al., 2006; Schwab et al., 2010). As astro- and microgliosis are predominantly present in close proximity of neuritic plaques, it is suggested that $A\beta$ promotes the inflammatory profile (Itagaki et al., 1989). Activated astrocytes (Figure 3) and microglia release proinflammatory as well as potentially neurotoxic substances such as cytokines, complement factors, reactive oxygen intermediates and chemokines. However, activated microglia have also been shown to phagocytose $A\beta$ deposits and remove soluble forms of $A\beta$, therefore exerting a neuroprotective role (Mandrekar-Colucci and Landreth, 2010). Moreover, activated astrocytes can internalize and degrade $A\beta_{42}$ deposits (Wyss-Coray et al., 2003). In support of this, it is still controversy whether inflammatory processes are causative for AD or if it is a protective reaction in response to $A\beta$ toxicity (Wyss-Coray and Rogers, 2012).

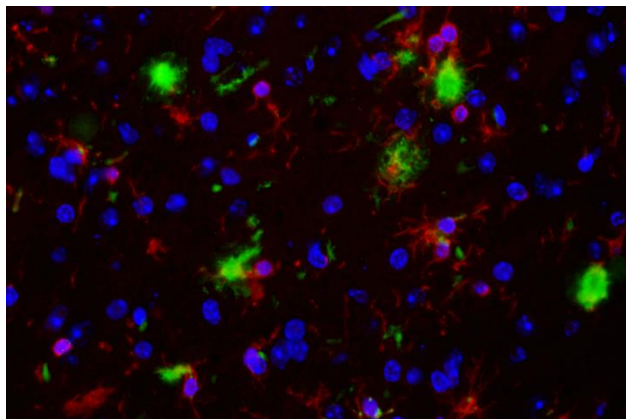


Figure 3: Inflammatory response in AD. Confocal image of activated astrocytes in 5XFAD mice. A neuritic plaque (green) is surrounded by activated astrocytes (red).

1.4 The amyloid precursor protein

The amyloid precursor protein (APP) is a ubiquitously expressed, type I integral membrane protein that is encoded by a gene located on chromosome 21 (Yoshikai et al., 1990). APP is part of a large evolutionary conserved gene family with two mammalian homologs, APLP1 and APLP2 (Wasco et al., 1992). These proteins display a high degree of homology in extracellular domains and intracellular C-terminal portions, but the A β containing trans- and juxtamembrane domains are unique to APP (Bayer et al., 1999). Through alternative splicing, different isoforms of APP are being generated. While APP695 is primarily expressed in neurons, longer isoforms like APP751 and APP770 are also being expressed in other tissues and cell types (Mattson, 1997). In the endoplasmatic reticulum (ER) and Golgi networks, immature APP undergoes posttranslational modifications before it is transported and integrated to the plasma membrane (Weidemann et al., 1989). During development, APP expression is found at growth cones of developing neurites, while in mature neurons, the protein is localized within pre- and postsynaptic structures and at focal adhesion sites (Yamazaki et al., 1997; Sabo et al., 2003). Although the precise physiological role of uncleaved APP remains unclear, the protein has been implicated in processes such as synapse formation (Priller et al., 2006), cell growth (Saitoh et al., 1989), neurite outgrowth (Allinquant et al., 1995) and neural plasticity (Turner et al., 2003).

1.4.1 Amyloidogenic and non-amyloidogenic processing of APP

APP is physiologically processed in two alternative pathways, which constantly compete with each other (Figure 4). In the non-amyloidogenic pathway, α -secretases cleave APP within the A β domain, thereby preventing its generation. Numerous members of the “a disintegrin and metalloprotease” (ADAM) family can function as α -secretases with ADAM10 being the physiologically most relevant, constitutive secretase in neurons (Kuhn et al., 2010). The ADAM10 cleavage induces the release of the soluble sAPP α fragment into the lumen/extracellular space (Sisodia, 1992). The remaining C-terminal fragment (C83) is subsequently cleaved by γ -secretase which liberates the soluble fragment p3 and the APP intracellular domain (AICD) (Zheng and Koo, 2011). The p3 fragment is rapidly degraded while the physiological role of AICD remains unclear. Controversial studies have implicated AICD in the regulation of gene transcription (Haass et al., 1993).

In the amyloidogenic pathway, A β is produced by the consecutive action of β - and γ -secretase. β -site APP cleavage enzyme 1 (BACE1) releases a large part of the ectodomain of APP (sAPP β) and generates the membrane-bound APP C-terminal fragment C99 (Vassar et al., 1999). C99 is subsequently cleaved by the γ -secretase protein complex at various cleavage sites, resulting in the liberation of A β peptides and AICD (Annaert and De Strooper, 2002). As the final γ -secretase cleavage is not precise, generated A β peptides can range from 37 to 43 amino acids in length, with A β ₁₋₄₀ being the most common isoform under physiological conditions (Haass et al., 1992; Citron et al., 1995). The γ -secretase protease complex consists of four trans-membranous subunits: presenilin (PSEN) 1 or PSEN2, nicastrin (NCT), anterior pharynx defective (APH)-1a or APH-1b and the PSEN enhancer (PEN)-2. While PSEN1/2 contain the catalytic active domain for APP cleavage, little is known about the biological function of NCT, APH-1 and PEN-2 (Wolfe et al., 1999; Francis et al., 2002; Edbauer et al., 2003).

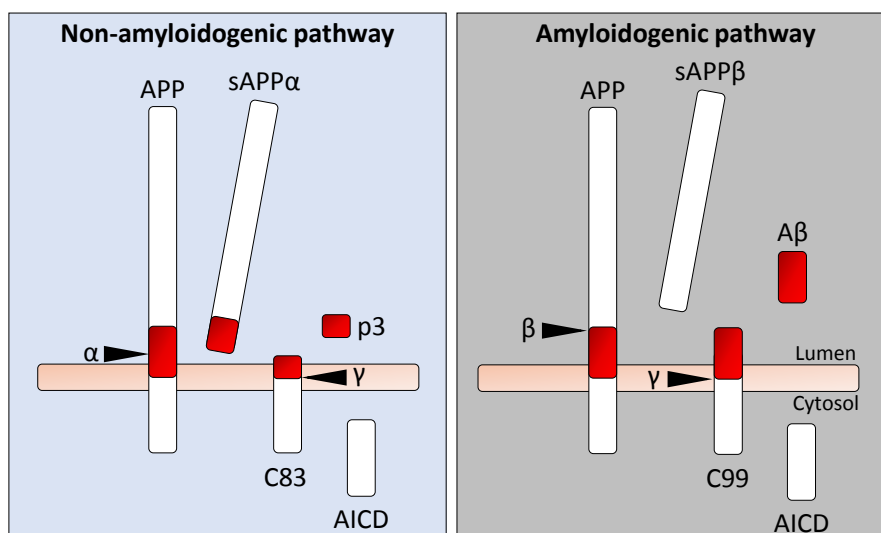


Figure 4: APP processing pathways. During the non-amyloidogenic pathway (left), APP is sequentially cleaved by α - and γ -secretase, resulting in the release of p3 and AICD. The $A\beta$ -liberating amyloidogenic way (right) is initiated by a BACE1 cleavage of APP. Subsequently, the γ -secretase complex induces the release of $A\beta$ and AICD. Adapted from (Haass et al., 2012).

1.5 The amyloid hypothesis

The amyloid cascade hypothesis (Figure 5) was first described by Hardy and Allsop in 1991 and is based on the idea that $A\beta$ has a central role in the pathological cascade of AD (Hardy and Allsop, 1991). The hypothesis states that an increase of extracellular $A\beta$ levels is the causative event of AD pathology leading to the formation of NFTs, neuron and synapse loss, vascular damage, memory loss and other clinical AD symptoms. Numerous observations support the classical amyloid cascade hypothesis. For example, mutations in APP and PS increase the production of $A\beta$ thereby leading to the familial form of AD (FAD) (Rademakers and Rovelet-Lecrux, 2009). Furthermore, transgenic rodent models that express mutations linked to FAD recapitulate numerous aspects of AD pathology including $A\beta$ plaque deposition, gliosis and memory deficits (Duyckaerts et al., 2008). In addition, Down-Syndrome patients harbour a triplication of the *APP* gene on chromosome 21 which ultimately leads to AD pathology formation at young ages (Wisniewski et al., 1985). However, over time, some major controversies against the classical amyloid hypothesis have evolved. First of all, studies in humans and AD mouse models revealed that plaque load does not correlate consistently with the severity of cognitive decline (Snowdon, 2003; Walsh and Selkoe, 2007). Accordingly, cognitively normal individuals who do not show any signs of dementia can display strong amyloid plaque deposition (Pimplikar, 2009). In addition, many AD

mouse models develop cognitive deficits and neuropathological changes before showing extracellular plaques (Walsh and Selkoe, 2007;Lesne et al., 2008).

In consideration of these observations, a modified amyloid hypothesis has been proposed. The revised version emphasizes intraneuronal A β accumulation prior extracellular plaque deposition as a key contributor in AD pathology (Wirhth et al., 2004). Intraneuronal A β was observed already 30 years ago by Masters et al. (Masters et al., 1985) and has later been shown to accumulate specifically in brain regions vulnerable to AD (Aoki et al., 2008;Hashimoto et al., 2010). It is hypothesized that intracellular A β has two potential origins. Next to its production through intracellular APP cleavage, A β can be secreted and re-uptake might occur from the extracellular space. Intraneuronal A β , particularly A β_{42} variants, accumulate to toxic oligomers which ultimately cause neuronal and synaptosomal dysfunction, brain atrophy and dementia (Wirhth et al., 2004). The hypothesis is supported by observations in Down syndrome patients, where intracellular A β was found to accumulate at young ages before extracellular plaque pathology is present. With age, intraneuronal A β decreases and plaques begin to deposit (Gyure et al., 2001). Furthermore, numerous mouse models reflect typical pathological AD hallmarks such as plaque deposition and inflammation, however, without showing neuron loss (Wirhth et al., 2004). In contrast, more recently developed AD models such as APP/PS1KI (Casas et al., 2004), 5XFAD (Oakley et al., 2006) and Tg4-42 (Bouter et al., 2013) show an early accumulation of intracellular A β , which correlates with a neuron loss as well as behavioural deficits. All of these findings imply that soluble intracellular and extracellular A β oligomers are key players in the development and progression of AD.

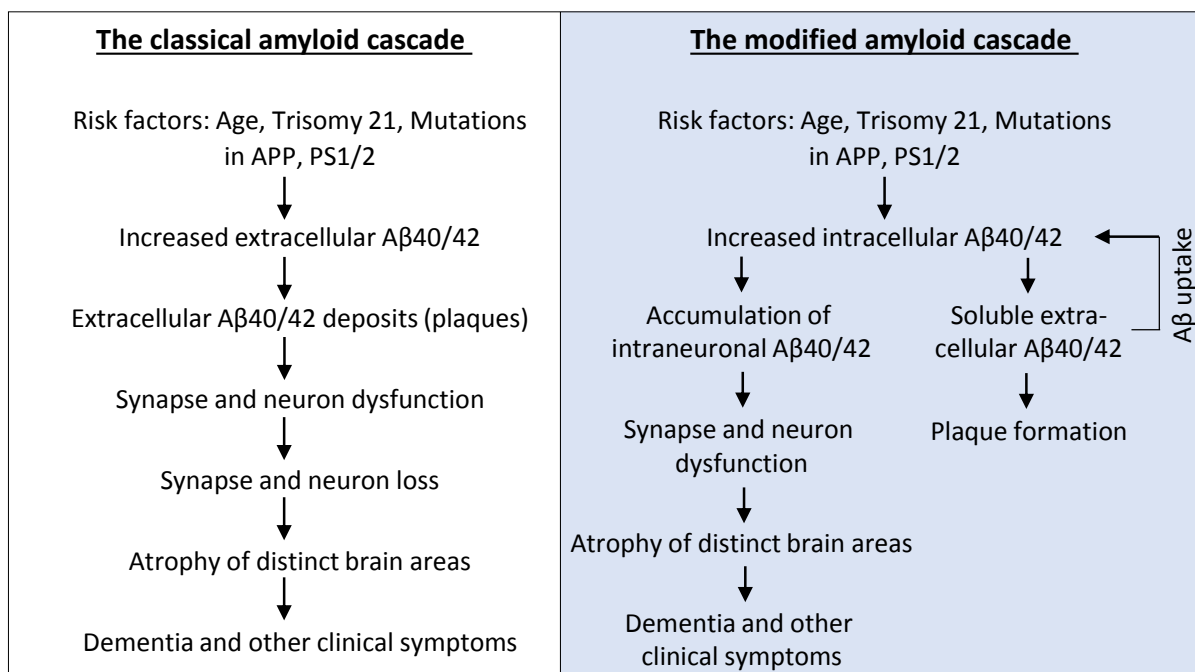


Figure 5: The classical and modified amyloid cascade hypothesis. Adapted from (Wirhns et al., 2004).

1.6 A β clearance mechanisms

Under physiological conditions, constant levels of A β in the brain are maintained by a dynamic balance between synthesis, clearance and re-uptake of the peptide. While familial forms of AD are characterized by both increased A β synthesis rates and decreased A β clearance, sporadic AD is characterized by an impaired clearance of A β (Mawuenyega et al., 2010; Tarasoff-Conway et al., 2015). These clearance mechanisms implicate non-enzymatic and enzymatic pathways (Figure 6).

1.6.1 Non-enzymatic clearance pathways

Non-enzymatic clearance pathways of A β include the transport across the blood brain barrier (BBB) by clearance receptors. These specialized transporters are necessary as endothelial cells of the BBB are connected through tight junctions, which prevent A β and other proteins to freely pass into the blood (Deane and Zlokovic, 2007). The transporters being mainly responsible for the efflux of A β from the brain belong to the LDL receptor (LDLR) family and include LRP-1 (low-density lipoprotein receptor-related protein-1) as well as ABC transporters (ATP-binding cassette transporters) (Shibata et al., 2000).

LRP-1 binds multiple ligands including A β , secreted APP, ApoE and α 2-macroglobulin and was originally described to regulate the metabolism and transport of cholesterol (Harris-White and Frautschy, 2005). LRP-1 rapidly transports A β ₁₋₄₀ across the BBB while A β ₁₋₄₂ is removed at a much slower rate. Additionally, A β ₁₋₄₀ variants harbouring the Dutch mutation are cleared with less efficiency than the non-mutated version, delineating the role of LRP-1 function in AD pathogenesis (Monro et al., 2002).

ABCB1 is the main ABC transporter exporting A β into the blood circulation. ABCB1 does not bind A β directly, but transports the peptide in an ApoE-dependent manner. However, the precise mechanism of ABCB1-mediated A β clearance remains to be elucidated. Next to LRP1 and ABCB1, A β can be cleared from the brain by LRP2 and α 2-macroglobulin. The receptor being predominantly responsible for the re-entry of A β from the circulation into the brain is RAGE (receptor for advanced glycation end products) (Deane et al., 2003). In plasma, A β is bound by numerous proteins including albumin, α 2-macroglobulin and the soluble form of LRP (sLRP) (Bates et al., 2009). After being transported to the liver and kidney, unbound A β as well as complexes of sLRP-A β become systematically cleared (Sagare et al., 2007). Next to BBB transport mechanisms, A β can be eliminated from the brain through the perivascular interstitial fluid (ISF) drainage pathway (Weller et al., 2000) and phagocytosis by activated astrocytes and microglia followed by lysosomal degradation (Rogers et al., 2002).

1.6.2 Enzymatic clearance pathways

Amyloid- β can be catabolized by a diversity of proteolytic enzymes which have specific regional and subcellular localizations, pH optima and target specificities. Hence, A β -degrading enzymes (ADEs) are capable to target distinct pools of intra- and extracellular A β (Leissring, 2014; Nalivaeva et al., 2014). ADEs include, among others, neprilysin (NEP), endothelin-converting enzyme (ECE)-1, insulin-degrading enzyme (IDE), angiotensin-converting enzyme (ACE) and cathepsin D (Wang et al., 2006). In the following paragraph, NEP, ECE-1 and IDE will be introduced in more detail.

The type-II metallo-endopeptidase neprilysin is ubiquitously expressed and has been reported to be the major ADE in the brain, where it is mainly present within neurons (Matsas et al., 1986; Iwata et al., 2000). NEP is also named CD10, enkephalinase or neutral endopeptidase and belongs to the M13 family of zinc peptidases. It is an integral membrane protein regulating the degradation of extracellular peptides, as its

active centre is facing the extracellular side of the membrane (Fukami et al., 2002). Besides A β , NEP is responsible for the degradation of diverse biologically active peptides such as tachykinins, enkephalins and natriuretic and chemotactic peptides (Turner et al., 2001). Numerous NEP cleavage sites have been identified within the A β sequence using *in vitro* assays (Wang et al., 2006;Miners et al., 2011), however, the ability of the peptidase to degrade oligomeric A β is still under controversial discussion (Kanemitsu et al., 2003;Leissring et al., 2003). Genetic depletion of NEP in AD mouse models results in an impaired degradation of both endogenous and exogenously administered A β (Iwata et al., 2001). In addition, inhibition of the protease by thiorphan results in increased accumulation of A β , cognitive dysfunction and a reduction in cholinergic activity in rats (Zou et al., 2006). On the contrary, overexpression of NEP ameliorates A β -induced spatial memory deficits in AD mouse models, inhibits extracellular plaque deposition and reduces A β accumulation (Poirier et al., 2006;Iijima-Ando et al., 2008;Meilandt et al., 2009). Intriguingly, it has been demonstrated in aged *D. melanogaster*, rodents and humans that NEP levels diminish during aging in AD vulnerable brain regions such as hippocampus, temporal gyrus and cortex. In contrast, brain regions rather unaffected by amyloid deposition display increased or unaltered steady-state levels of the protease (Yasojima et al., 2001;Caccamo et al., 2005). Furthermore, NEP levels have been shown to be significantly lower in AD patients when compared to healthy controls, leading to the hypothesis that decreased levels of the endopeptidase and a resulting diminished A β clearance significantly contribute to the progression of the disease (Yasojima et al., 2001).

The endothelin-converting enzyme (ECE) induces the conversion of the inactive form of the potent vasoconstrictive peptide endothelin into its active version. Two different isoforms of ECE have been described (ECE-1 and ECE-2), however, only ECE-1 is supposed to act as an ADE. Like NEP, ECE-1 is a type II metallo-endopeptidase being predominantly localized in plasma membranes, but also in intracellular compartments. At the amino acid level, ECE-1 shares approximately 38% sequence homology with NEP (Wang et al., 2006). ECE-1 is active at a pH of 7 and has been shown to degrade A β within intracellular compartments (Eckman et al., 2001). A study in SH-SY5Y cells recently reported that ECE-1 degrades at least two distinct pools of A β , consisting of one that is degraded in the endosomal-lysosomal pathway and the other being destined

for secretion (Pacheco-Quinto and Eckman, 2013). In addition, mice lacking ECE-1 and ECE-2 display significantly higher levels of $A\beta_{40}$ and $A\beta_{42}$ when compared to controls, further emphasizing the importance of ECE in $A\beta$ clearance (Eckman et al., 2003). IDE represents another zinc metallo-endopeptidase which, in addition to $A\beta$, has numerous substrates including AICD, insulin, glucagon, β -endorphin and transforming growth factor- α (Duckworth et al., 1998). IDE is expressed in liver, blood cells, skeletal muscle and brain and is active at a neutral pH. The protease is predominantly located in the cytosol, however, it has also been found in plasma membranes and peroxisomes (Wang et al., 2006). Like NEP and ECE-1, IDE has been shown to successfully degrade $A\beta$. Overexpression of IDE in mice results in a massive reduction of amyloid deposition and a prolonged survival rate (Hama et al., 2004). On the contrary, genetic depletion of IDE elevates brain $A\beta$ levels (Farris et al., 2003). Like NEP, IDE mRNA and protein levels display region-dependent, reduced expression levels in aged healthy individuals as well as AD patients (Cook et al., 2003; Caccamo et al., 2005). Hence, IDE is another crucial ADE potentially playing a role in AD pathology.

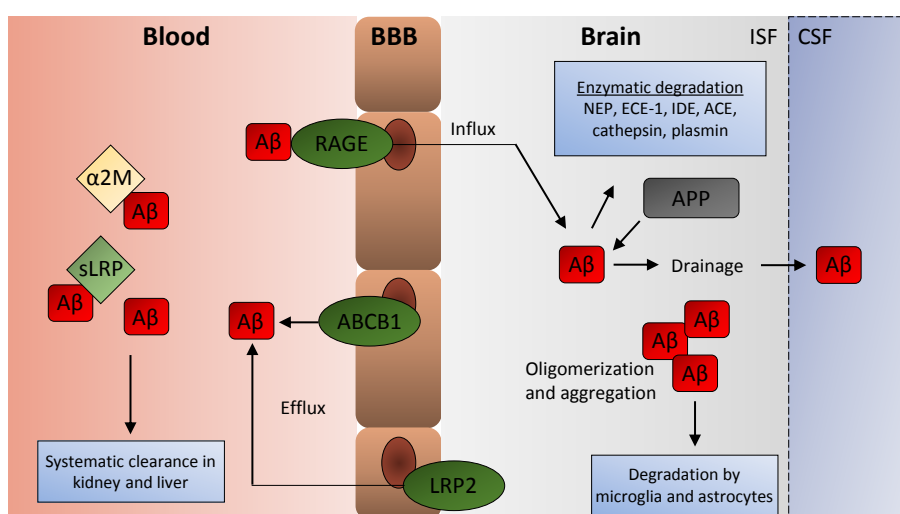


Figure 6: $A\beta$ clearance pathways. $A\beta$ can be eliminated from the brain by enzymatic degradation, transport through the BBB, degradation through activated astrocytes and microglia or by the ISF drainage pathway. LRP2 and ABCB1 mediate the efflux of the peptide while RAGE promotes its re-entry into the brain. In the plasma, unbound or bound $A\beta$ is transported to kidneys or liver and systematically cleared. Figure generated after (Tarasoff-Conway et al., 2015; Vandal et al., 2015).

1.7 Mouse models of Alzheimer's disease

Upon the discovery of mutations in *APP* and *PSEN* genes in familial AD patients, a variety of transgenic murine mouse models have been developed. These models carry

transgenes with mutated forms of human APP and/or PSEN1/2 and mimic various pathological features of AD such as amyloid plaque deposition, accumulation of phosphorylated tau, inflammation and behavioural deficits (Elder et al., 2010). The first APP-based transgenic AD model was the PDAPP model harbouring the Indiana mutation reported by Games et al. (Games et al., 1995). Subsequently, numerous other mouse lines with promoters driving the expression of APP transgenes with one or more FAD mutations were developed (e.g. Tg2576 (Hsiao et al., 1996), APP23 (Calhoun et al., 1999) and TgCRND8 (Chishti et al., 2001)).

Overexpression of human mutant PSENs alone does not cause amyloid plaque deposition but leads to elevated levels of $A\beta_{X-42}$. However, crossing of PSEN lines with APP-based transgenic mice causes early onset pathology and an extensive $A\beta$ plaque load (Holcomb et al., 1998). Examples for well-characterized APP/PS1 bigenic lines are APP/PS1KI (Casas et al., 2004), APP/PS1 Δ E9 (Borchelt et al., 1997) and 5XFAD mice (Oakley et al., 2006).

As rodents do not develop $A\beta$ plaque pathology spontaneously (Sarasa and Pesini, 2009), the relevance of APP/PSEN mouse models is undisputed. However, due to the use of mutations, they only reflect the minor fraction of approximately 1% of familial AD cases. Thus, the generation of genetically modified mice that represent a better model for sporadic AD has gained particular attention in recent years. A model showing features of the sporadic form of AD has been developed by intracerebroventricular (icv) injection of streptozotocin (STZ) leading to insulin-resistance in the brain. This icv-STZ model is therefore based on the AD environmental risk factor diabetes mellitus type II and reflects important pathological characteristics of the disease such as memory impairment (Salkovic-Petrisic et al., 2006). Another mutation-independent model is the previously generated Tg4-42 model, which exclusively expresses an N-truncated version of $A\beta$ without APP overexpression and therefore represents the sporadic form of AD better than APP/PSEN-based models (Bouter et al., 2013).

1.7.1 The Tg4-42 mouse model

The Tg4-42 mouse model exclusively expresses the $A\beta_{4-42}$ peptide, which is one of the most abundant $A\beta$ species found in human AD brain (Portelius et al., 2010). The $A\beta_{4-42}$ sequence is fused to the murine thyrotropin-releasing hormone (TRH) signal peptide, ensuring secretion through the secretory pathway, under the control of the Thy1-

promoter (Figure 7). A β accumulation correlates with the expression pattern of the neuron-specific promoter and occurs in a region-specific manner. Intraneuronal A β becomes apparent starting at 2 months of age in heterozygous Tg4-42 mice (Tg4-42^{het}) and is predominantly present in the CA1 region of the hippocampus, but also in the occipital cortex, piriform cortex, striatum, superior colliculus and spinal cord. A β immunoreactivity in the CA1 layer is accompanied by an inflammatory response as shown by reactive micro- and astroglia. Intraneuronal CA1 A β immunoreactivity declines during aging due to a massive neuron loss, leaving mainly larger extracellular A β aggregates. The CA1 neuron loss in Tg4-42 mice happens in an age- and dose-dependent manner. At 8 months of age, Tg4-42^{het} animals display a 38% neuron loss that is even more pronounced in homozygous Tg4-42 mice (Tg4-42^{hom}) with a 66% decline compared to WT controls. With 12 months of age, neurodegeneration is proceeded up to a loss of 50% in Tg4-42^{het} mice. The profound neuron death in Tg4-42 mice is accompanied by spatial reference memory deficits as assessed by the Morris water maze (MWM), starting with 12 months of age in heterozygous and 6 months of age in homozygous animals (Bouter et al., 2013). Additionally, 12-month-old Tg4-42^{het} mice display an impaired contextual learning, as demonstrated in the fear conditioning task (Bouter et al., 2014). Despite the massive neuron loss and the subsequent memory decline that develops in Tg4-42 mice, this model still responds to therapeutic interventions. A passive immunization study using an antibody directed against A β _{4-x} effectively decreased hippocampal neurodegeneration and rescued spatial reference memory deficits in Tg4-42^{hom} mice (Antonios et al., 2015). As the Tg4-42 model neither expresses human APP nor possesses any mutations, it rather represents the sporadic form of AD and therefore demonstrates a physiologically relevant model suitable to study new preventative and therapeutic approaches.

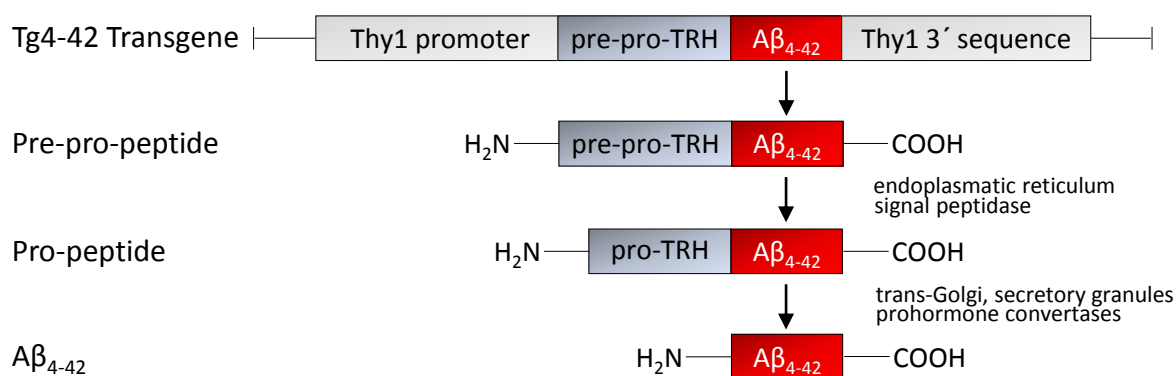


Figure 7: Schematic diagram of Tg4-42 transgene. The Aβ₄₋₄₂ sequence is fused to the pre-pro-TRH peptide. The Thy1 promoter induces the neuronal expression of the pre-pro-TRH-Aβ₄₋₄₂ fusion peptide. The fusion peptide is directed into the ER by an N-terminal signal sequence. In the ER, signal peptidases liberate the pro-TRH-Aβ₄₋₄₂ peptide. In the trans-Golgi network and secretory granules, prohormone convertases subsequently cleave off the remaining pro-TRH sequence and liberate the Aβ₄₋₄₂ peptide (Alexandru et al., 2011). Figure generated after (Wittnam, 2012).

1.7.2 The 5XFAD mouse model

The conventional 5XFAD mouse model co-expresses the two human mutant transgenes APP and PS1 under the control of the neuron-specific Thy1 promoter (Figure 8). The hAPP695 transgene contains the Swedish (KM670/671NL), Florida (I716V) and London (V717I) mutations and PS1 harbours the mutations M146L and L286V (Oakley et al., 2006). These mutations are known to cause familial AD in humans and promote the overproduction of Aβ_{x-42}, leading to an accelerated amyloid plaque formation as early as 2 months of age. While the Swedish mutation promotes elevated levels of total Aβ, the Florida, London and PS1 mutations specifically enhance the formation of Aβ₄₂. The amyloid pathology in 5XFAD mice starts with the accumulation of intraneuronal Aβ₄₂ in the 5th cortical layer, rapidly followed by plaque deposition in cortex and subiculum. With age, Aβ plaques become detectable throughout the hippocampus and cortex and amyloid pathology is paralleled with massive astro- and microgliosis (Oakley et al., 2006; Jawhar et al., 2012). In addition to the 5th cortical layer, 5XFAD mice display intraneuronal Aβ accumulation in the subiculum, which correlates well with a significant neuron loss in these regions (Eimer and Vassar, 2013). 5XFAD mice display a reduced body weight compared to healthy WT animals starting with 9 months of age, which further aggravates over time (Jawhar et al., 2012). Concomitantly, the model shows a premature death phenotype, probably caused by the heavy amyloid deposition and subsequent cerebral vascular damage (Heraud et al., 2014). 5XFAD mice develop

working memory deficits with 4 to 5 months of age in the Y-Maze test (Oakley et al., 2006) and display reduced anxiety levels starting with 6 months. Furthermore, this strain shows an age-dependent decline in motor function starting with 9 months of age (Jawhar et al., 2012; Shukla et al., 2013) and significant spatial reference memory as well as contextual and tone memory deficits with 12 months of age (Bouter et al., 2014). The 5XFAD model develops a rapid pathology and recapitulates the main features of AD. Therefore, the model is a useful tool to investigate the molecular mechanisms of neurodegeneration in AD (Ou-Yang and Van Nostrand, 2013; Bouter et al., 2014; Guzman et al., 2014; Landel et al., 2014; Anderson et al., 2015) as well as possible therapeutic strategies (Wirths et al., 2010; Hillmann et al., 2012; Cho et al., 2014; Zhang et al., 2014; Devi and Ohno, 2015).

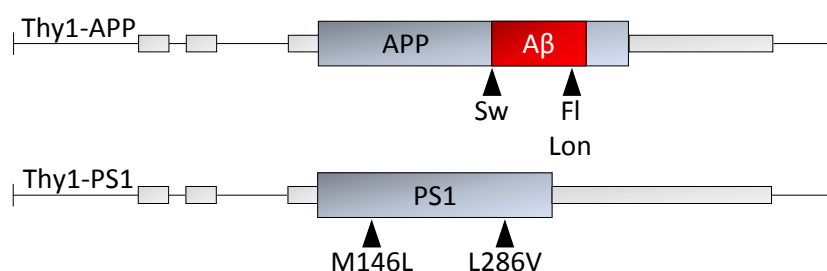


Figure 8: Schematic diagram of 5XFAD transgenes. 5XFAD mice co-express the human APP695 and PS1 transgenes under the control of the neuron-specific Thy1 promoter. Mutations in Thy1-APP and Thy1-PS1 transgenes are indicated by arrow heads. Sw, Swedish mutation; Lon, London mutation; Fl, Florida mutation. Figure generated after (Oakley et al., 2006).

1.8 Risk factors for Alzheimer's disease

1.8.1 Genetic risk factors

Besides advanced age, family history is one of the major risk factors of AD (Sperling et al., 2011). Twin and family studies have shown that up to 80% of all AD cases involve the inheritance of genetic factors (Gatz et al., 2006). AD is classified into early-onset AD (EO-FAD) and late-onset AD (LOAD). EO-FAD develops before the age of 65 years and accounts for only 2-5% of all AD cases (Campion et al., 1999). This rare form of AD is characterized by a rapid disease progression and a Mendelian pattern of inheritance. So far, more than 200 different mutations in the genes encoding APP, PSEN1 and PSEN2 have been identified to cause EO-FAD (Tanzi, 2012). Most of these mutations are

inherited in a penetrant, autosomal-dominant manner and lead to elevated levels of $A\beta_{42}$. The increase of extracellular $A\beta_{42}$ promotes its aggregation and fosters cerebral deposition of amyloid plaques (Scheuner et al., 1996).

Being clinically indistinguishable from EO-FAD, LOAD develops above the age of 65 and has no consistent mode of transmission (Bertram and Tanzi, 2005). Instead, LOAD is believed to be a multifactorial disease, with a combination of genetic and environmental factors influencing its onset. The greatest genetic risk factor linked to the sporadic form of AD is the $\epsilon 4$ allele of the lipid/cholesterol carrier apolipoprotein E (ApoE) on chromosome 19q3 (Strittmatter et al., 1993). In humans, three major polymorphisms in the ApoE gene have been described: $\epsilon 2$, $\epsilon 3$ and $\epsilon 4$. The ApoE $\epsilon 4$ allele is found in about 15% of the general population, while its frequency in AD patients is 40% (Farrer et al., 1997). The mechanism how ApoE $\epsilon 4$ predisposes to AD is still unclear, however, ApoE $\epsilon 4$ has been shown to codeposit and interact with $A\beta$ (Namba et al., 1991). Furthermore, it has been described that ApoE $\epsilon 4$ modulates $A\beta$ accumulation and clearance in the brain (Castellano et al., 2011). Additionally, ApoE $\epsilon 4$ is supposed to impair synaptic and mitochondrial function, representing an early event in the onset of sporadic AD (Ji et al., 2003;Valla et al., 2010). Next to ApoE $\epsilon 4$, recent genome-wide association studies (GWAS) have found new susceptibility genes linked to LOAD, such as *TREM2* (triggering receptor expressed on myeloid cells2) (Boutajangout and Wisniewski, 2013), *CLU* (clusterin) and *PICALM* (phosphatidylinositol-binding clathrin assembly protein) (Harold et al., 2009).

1.8.2 Environmental risk factors

The probability of developing LOAD is influenced by numerous environmental risk factors, including metabolic and cardiovascular (e.g. diabetes, midlife hypertension and midlife obesity) (Beydoun et al., 2008;Kennelly et al., 2009;Lu et al., 2009), psychological (e.g. depression) (Ownby et al., 2006) and health risk factors (e.g. smoking) (Cataldo et al., 2010). In addition, several studies showed that traumatic brain injuries in early adulthood increase the risk of developing AD in later life (Plassman et al., 2000). Population-based data analysis disclosed that such potentially modifiable risk factors cause about one third of all LOAD cases worldwide (Norton et al., 2014). On the other hand, several retrospective epidemiological studies suggested that a physically active lifestyle as well as cognitively stimulating activities result in a

significantly reduced risk of dementia (Valenzuela, 2008; Scarmeas et al., 2009; Scarmeas et al., 2011). For example, a study with 1449 participants showed that regular leisure-time physical activity at midlife lowers or delays the risk of developing dementia in later life (Rovio et al., 2005). In addition, a recent long-term follow-up study with a Finnish twin cohort revealed that vigorous physical activity protects from dementia and hence led to a lower mortality rate (Iso-Markku et al., 2015). Accordingly, a meta-analysis of 16 prospective studies led to the suggestion that 13% of all AD cases worldwide can be attributed to physical inactivity. A 10% reduction of physical inactivity could hence lead to the prevention of 380000 AD cases worldwide (Barnes and Yaffe, 2011). Intriguingly, beneficial effects of physical activity have also been proven in individuals already suffering from mild cognitive impairment and dementia (Heyn et al., 2004; Nagamatsu et al., 2013). There are ample mechanisms proposed how physical activity reduces the risk of AD and dementia (Barnes et al., 2007). First, physical activity lowers the risk of developing cardiovascular diseases such as diabetes or hypertension, which are, as previously mentioned, associated with LOAD (Profenno et al., 2010). Second, numerous studies in humans and animals have shown that physical activity has a direct beneficial effect on the structure and function of the brain (Cotman et al., 2007; Voss et al., 2010). As already stated, besides exercise, high education and cognitive stimulation throughout life are associated with a lower risk of AD. There is strong evidence that enhanced educational opportunities help to build up a cognitive reserve (CR) which enables individuals to stay asymptomatic despite ongoing neurodegenerative changes in the brain (Stern, 2002).

1.9 The cognitive reserve hypothesis

As mentioned earlier, AD is characterized by severe anatomical changes of the brain. Massive neuron loss leads to shrinkage of several brain areas with the hippocampus and cortex being primarily affected. Interestingly, a study in 1988 showed that there is a discrepancy between the degree of brain atrophy and the extent of clinical manifestation. The post mortem analysis revealed that individuals with no signs for cognitive decline during lifetime displayed a strong brain AD pathology (Katzman et al., 1988). This finding supported the idea of individual differences regarding the ability to compensate a certain degree of neurodegeneration and established the concept of a

“cognitive reserve”. The cognitive reserve hypothesis postulates that a stimulating environment consisting of complex mental activities, high education, occupational attainment and diverse leisure activities provides a brain reserve capacity that tolerates brain damage to a greater extent before becoming clinically present (Stern, 2002). Numerous following studies supported the cognitive reserve hypothesis and substantiated the idea that one can influence cognitive outcomes through lifestyle choices. For instance, individuals with high educational levels showed a 5-year delay in dementia onset when compared to lower educated persons (Katzman, 1993). Furthermore, a study with nuns revealed that a high extent of ideation and creativity throughout life correlates with well-preserved cognitive capacities in older age (Tyas et al., 2007a; Tyas et al., 2007b). In addition, a 9-year follow-up study by Paillard-Borg and colleagues showed that mental, social and physical activity delays the onset of cognitive decline. Intriguingly, a combination of all three types of activities clearly entailed an even stronger delay of disease onset (Paillard-Borg et al., 2012). However, it has to be considered that different genetically determined endowments in terms of brain structure and circuitry can influence the capacity to compensate certain disruptions as well (Stern, 2009). Therefore, it is suggestive that cognitive reserve is based on an interaction between genetic and environmental elements (Sale et al., 2014). The underlying neurobiological mechanisms contributing to cognitive reserve might include positive effects on synaptic plasticity, synaptic connectivity, hippocampal neurogenesis, neuronal density, as well as cortical thickness (Stern, 2009; Sale et al., 2014). These effects in humans have been tried to be explained by data obtained in animal models. Therefore, rodents are exposed to enriched environment (EE) paradigms, which mimic an intellectually and physically enriched lifestyle and will be addressed in the following paragraph.

1.10 The environmental enrichment paradigm

The beneficial effects of an enriched environment have first been described in 1940, when D.O. Hebb took a group of rats from the laboratory and let them run and play freely with his kids at home. When he compared these rats with the ones that remained under standard laboratory conditions, he observed positive effects on learning and memory of the animals (Redolat and Mesa-Gresa, 2012). Rosenzweig and colleagues

later introduced the EE as a scientific paradigm (Rosenzweig et al., 1962). Ever since, extensive studies have revealed that rodents kept in an EE display behavioural, physiological and anatomical alterations. The environmental enrichment is defined as “a housing condition that facilitates enhanced sensory, cognitive and motor stimulation relative to standard housing conditions” (Nithianantharajah and Hannan, 2006) (Figure 9). In this experimental setting, sensory and cognitive stimulation are provided by numerous enrichment objects including colourful toys, climbing apparatuses, ladders, nesting material, houses and tunnels. The regular re-arrangement and exchange of EE objects (daily or weekly) provides novelty and complexity in the system and therefore challenges cognitive modalities such as learning and memory. In order to model a physically active lifestyle, EE cages can be equipped with running wheels, providing the continuous possibility to exercise voluntarily. In addition, the larger size of cages used for EE, but also the EE objects itself, encourage the animals to be more active and support exploration. To increase social interaction, higher numbers of conspecifics are maintained together in EE cages. Enriched environment protocols can vary substantially amongst studies, depending on the number and complexity of EE objects, the duration of the paradigm, the number of animals per cage and the age at which the protocol starts (Nithianantharajah and Hannan, 2006). However, rodents display highly motivated behaviours in such enriched environments. In order to handle these environmental demands, the brain undergoes a variety of changes (Leggio et al., 2005; Mandolesi et al., 2008).

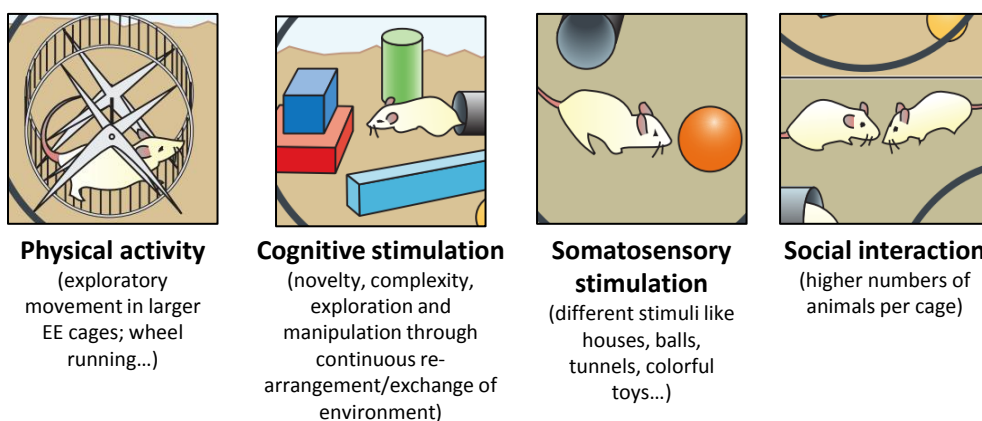


Figure 9: The environmental enrichment paradigm. EE promotes physical activity, cognitive stimulation, somatosensory stimulation and social interaction. Figure generated after (Nithianantharajah and Hannan, 2006)

1.10.1 Benefits of environmental enrichment in rodents

In rodents, enriched housing has been shown to have numerous positive effects on a cellular, molecular and behavioural level. Next to an altered cortical weight and thickness (Diamond et al., 1976), studies described increased branching and length of dendrites, increases in the number of dendritic spines and the size of synapses (Greenough and Volkmar, 1973; Connor et al., 1982; Turner and Greenough, 1985). Furthermore, EE stimulates hippocampal neurogenesis and the integration of newborn neurons into existing neuronal circuits (Kempermann et al., 1997; 1998; van Praag et al., 2000). It also promotes an increase in levels of neurotransmitter receptors as well as an elevation of neurotrophic and growth factors in the brain (Kempermann et al., 2010). Additionally, in brain regions that are susceptible for neurodegenerative changes such as hippocampus or striatum, EE has been described to induce long-term changes in terms of altered gene expression profiles (Li et al., 2007; Thiriet et al., 2008). At the behavioural level, EE has been shown to decrease anxiety and increase exploratory behaviour (Chapillon et al., 1999; Roy et al., 2001). Moreover, enriched housing diminishes memory decline in aged animals and improves cognitive function and sensory-motor performance (Bennett et al., 2006; Nithianantharajah and Hannan, 2006).

1.10.2 Benefits of environmental enrichment in AD mouse models

As EE is thought to represent a preventative therapeutic intervention, the paradigm has been evaluated in numerous mouse models of AD. Regarding cognitive outcomes, the majority of results indicate that living in an EE has beneficial effects on AD mice. After long-term exposure to EE, APP23 mice displayed an improved spatial memory performance (Polito et al., 2014). Verret et al. found that an exposure of Tg2576 mice to EE prior to the onset of amyloidosis protects against cognitive impairment during AD pathology (Verret et al., 2013). In addition, lifelong EE counteracted age-related cognitive decline in both male and female PS1/PDAPP mice (Costa et al., 2007). However, other studies have not confirmed positive effects of EE on the cognitive performance of AD mouse models. For example, Cotel et al. found that after 4 months of continuous EE, no improvement in working memory performance was present in APP/PS1KI mice (Cotel et al., 2012). Levi and colleagues also observed that EE did not

counteract memory decline in APOE ϵ 4 mice after exposure to EE (Levi and Michaelson, 2007). Furthermore, conflicting results regarding A β deposition upon EE living conditions have been reported. For example, some studies found a decrease in A β deposition (Yuede et al., 2009; Ke et al., 2011; Liu et al., 2013), some constant A β plaque loads (Parachikova et al., 2008; Richter et al., 2008; Cotel et al., 2012; Marlatt et al., 2013) or even enhanced A β abundance (Jankowsky et al., 2003) following enriched housing.

1.11 Project objectives

1.11.1 Project I: The effect of long-term environmental enrichment and physical activity on the pathology of Tg4-42 and 5XFAD mice

To date, no efficacious therapeutic approach against Alzheimer's disease has been developed. Hence, preventative strategies and non-pharmacological interventions to delay age-related cognitive changes and AD have moved into focus. Numerous epidemiological studies revealed that a physically and cognitively active lifestyle reduces the risk of developing AD (Rovio et al., 2005;Valenzuela, 2008;Scarmeas et al., 2009). The experimental work carried out in the present doctoral thesis aims to extend and broaden investigations of a challenging lifestyle in combination with regular exercise as a potential preventative strategy for AD. To this end, the effect of long-term housing in an enriched environment (EE) on the newly-developed Tg4-42 as well as the widely-used 5XFAD mouse model will be tested. Tg4-42 mice reflect the key features of sporadic AD as this model overexpresses $A\beta_{4-42}$ without APP mutations. Hence, special emphasize will lay on the effect of EE on hippocampal neuron loss and associated behavioural impairments. Therefore, the following questions will be addressed:

- Does living in an enriched environment prevent the severe memory decline of Tg4-42 mice?
- Can the CA1 neuron loss in Tg4-42 mice be delayed or rescued due to prolonged enriched living conditions?
- Does mental and physical activity influence neurogenesis in aged WT and Tg4-42 mice?
- Are $A\beta$ brain levels changed upon lifelong living in a physically and cognitively enriched environment?
- Are gene expression profiles changed in WT and Tg4-42 mice maintained under enriched conditions?
- How does physical activity alone affect neurodegenerative processes in Tg4-42 mice?

To date, the well characterized 5XFAD model has not been tested in a physically and mentally demanding environment. The aim of this project is to investigate, whether the strong behavioural and neuropathological phenotype of 5XFAD mice can be modified by a rather mild intervention like EE. Therefore, the aims of this part of the study can be summarized in main questions as follows:

- Can the severe motor phenotype of 5XFAD mice be ameliorated due to lifelong EE?
- Does cognitive and physical activity influence the behavioural changes in the 5XFAD mouse model?
- Are A β levels in 5XFAD mice modifiable through enriched living conditions?

1.11.2 Project II: Neprilysin deficiency alters the neuropathological and behavioural phenotype in the 5XFAD mouse model of Alzheimer's disease

The 5XFAD mouse model represents a widely used, conventional model that develops major neuropathological AD hallmarks such as extracellular amyloid deposition, memory impairment, motor deficits and selective neuron loss (Jawhar et al., 2012). Neprilysin has been described to be the major A β -degrading enzyme in the brain and its role in AD pathology has been proposed in a variety of studies. The aim of this part of the thesis will be the analysis of the effects of neprilysin depletion in 5XFAD mice. Therefore, the following inquiries will be investigated:

- Does neprilysin deficiency have an effect on the working memory performance of 5XFAD mice?
- Does the lack of a neprilysin allele aggravate extracellular plaque pathology?
- Is the inflammatory response in 5XFAD mice increased upon depletion of neprilysin?
- How does the neprilysin loss influence the expression levels of other ADEs?

2 MATERIALS AND METHODS

2.1 Chemicals, Reagents and Kits

The chemicals and reagents used in the present study are listed in Table 1, kits used are listed in Table 2.

Table 1: Chemicals and Reagents

Reagent	Manufacturer
3,3 -diaminobenzidine-tetrahydrochloride (DAB)	Roth, Karlsruhe, Germany
Agarose	Lonza, Basel, Switzerland
Acetic acid	Merck, Darmstadt, Germany
Amersham Hybond-ECL Membrane	GE Healthcare, Chalfont St. Giles, GB
Benzonase	Merck, Darmstadt, Germany
Boric acid	Sigma-Aldrich, St. Louis, USA
Bovine serum albumin (BSA)	Roth, Karlsruhe, Germany
Citric acid	Roth, Karlsruhe, Germany
Complete Mini-Protease Inhibitor Tablets	Roche, Basel, Switzerland
Complete Mini-Phosphatase Inhibitor Tablets	Roche, Basel, Switzerland
Cresyl violet	Merck, Darmstadt, Germany
Dimethyl sulfoxide	Roth, Karlsruhe, Germany
DNA ladder 100 bp	Bioron, Ludwigshafen, Germany
DNase 10X reaction buffer with MgCl ₂	Thermo Fisher Scientific, Waltham, USA
DNase	Thermo Fisher Scientific, Waltham, USA
dNTPs	Invitrogen, Carlsbad, CA, USA
Dulbecco's Phosphate Buffered Salt Solution (DPBS)	Pan Biotech, Aidenbach, Germany
Ethanol, absolute	Merck, Darmstadt, Germany
Ethidium bromide	Roth, Karlsruhe, Germany
Ethylendiaminetetraacetic acid (EDTA)	AppliChem, Darmstadt, Germany
Fetal Calf Serum (FCS)	Biochrom, Berlin, Germany
Formic Acid, 98%	Roth, Karlsruhe, Germany
Hematoxylin Solution	Roth, Karlsruhe, Germany
Histofix solution containing 4% formalin	Roth, Karlsruhe, Germany
Hydrochloric acid (HCl), 37%	Roth, Karlsruhe, Germany

Hydrogen peroxide (H ₂ O ₂)	Roth, Karlsruhe, Germany
Isopropanol	Roth, Karlsruhe, Germany
Ketamine	Medistar, Ascheberg, Germany
Methanol	AppliChem, Darmstadt, Germany
MgCl ₂ (25 mM)	Axon, Kaiserslautern, Germany
Molecular-grade water	Braun, Melsungen, Germany
Natrium acetate trihydrate	Roth, Karlsruhe, Germany
Non-fat Dry Milk Powder	Roth, Karlsruhe, Germany
Paraffin	Roth, Karlsruhe, Germany
Paraformaldehyde (PFA)	Roth, Karlsruhe, Germany
PCR 10X reaction buffer	Axon, Kaiserslautern, Germany
Ponceau S	Roth, Karlsruhe, Germany
Proteinase K	Peqlab, Erlangen, Germany
Roti-Histokitt	Roth, Karlsruhe, Germany
Sodium chloride (NaCl)	Roth, Karlsruhe, Germany
Sodium dodecyl sulfate (SDS)	Roth, Karlsruhe, Germany
Sodium hydroxide (NaOH)	AppliChem, Darmstadt, Germany
Sucrose	Roth, Karlsruhe, Germany
Taq polymerase	Axon, Kaiserslautern, Germany
Thioflavin S	Sigma-Aldrich, St. Louis, USA
Trifast®	Peqlab, Erlangen, Germany
Tris(hydroxymethyl)aminomethane (Tris)	Roth, Karlsruhe, Germany
Triton X-100	Roth, Karlsruhe, Germany
Tween 20	Roth, Karlsruhe, Germany
Xylazine (Xylarium)	Ecuphar, N.V. Oostkamp, Belgium
Xylene	Roth, Karlsruhe, Germany

Table 2: Kits

Kit	Manufacturer
Human (6E10) Abeta Peptide Ultra-Sensitive Kit	Meso Scale Discovery, Rockville, USA
RevertAid First Strand cDNA Synthesis Kit	Thermo Fisher Scientific, Waltham, USA
FastStart Universal SYBR Green Master (Rox) qRT-PCR Kit	Roche, Basel, Switzerland
RotiQuant Universal Protein Assay	Roth, Karlsruhe, Germany
Vectastain ABC Kit	Vector Laboratories, Burlingame, USA

2.2 Laboratory Animals

2.2.1 Animal care and general conditions

All animals used for these studies were of the species *Mus musculus* and were housed under specific-pathogen-free (SPF) conditions in the central animal facility of the University Medicine Göttingen (UMG). Mice were kept on a 12 hour/12 hour inverted dark/light cycle (light from 8.00 p.m. to 8.00 a.m.), while handling and behavioural testing were performed during the dark phase. Access to food and water was provided *ad libitum*. Only female mice were used in the current study. All animal experiments were conducted in accordance with the guidelines of the 'Federation of European Laboratory Animals Science' (GV-SOLAS) and the guidelines of the 'Federation of European Laboratory Animal Science Association' (FELASA). All animal experiments were approved by the 'Lower Saxony State Office for Consumer Protection and Food Safety' (LAVES). All effort was made to minimize the number and the suffering of animals used in the present study.

2.2.2 Housing conditions

2.2.2.1 Standard housing

Mice kept under standard housing (SH) conditions were maintained in standardized individually ventilated cages (33 cm x 18 cm x 14 cm) in groups of 4-5 animals until the age of 12 months. The cages were equipped with sawdust bedding and nesting material.

2.2.2.2 Environmental enrichment housing

Mice that were assigned to environmental enrichment (EE) living conditions were transferred to rat cages (55 cm x 34 cm x 20 cm) after weaning until the age of 12 months. EE cages were equipped with sawdust bedding, nesting material, tunnels, houses, climbing apparatuses and toys, which were cleaned, changed and re-arranged weekly to maintain the concept of novelty and complexity in the system (Nithianantharajah and Hannan, 2006). Additionally, the cages were equipped with

three different running wheels to promote physical activity on a voluntary basis. Mice were kept in groups of 4-5 animals.

2.2.2.3 Individual cage housing

Individual cage housing experiments were performed in collaboration with the group of Prof. David Liebetanz in Göttingen. For running wheel recording experiments, 2-month-old Tg4-42^{hom} mice were assigned to individual cages (22 cm x 16 cm x 14 cm), which were equipped with sawdust bedding and a running wheel (diameter of 11.3 cm) until the age of 6 months. The running wheels of one group were freely movable and a rotation sensor connected to the running wheel axis transmitted the running activity with a resolution of 1/16 revolution and a sampling rate of 1/0.48 s to a customized recording device (Boenig und Kallenbach oHG). The average weekly running distance (km) was calculated and visualized using a custom-designed Matlab (The MathWorks, Inc.) program. The running wheels of the control group were blocked to prevent the mice from running activity while providing the same level of environmental enrichment.

2.2.3 Tg4-42 transgenic mice

The generation of Tg4-42^{het} mice has been described previously (Bouter et al., 2013). In brief, Tg4-42 mice express the human A β ₄₋₄₂ sequence combined with the signal peptide sequence of the thyrotropin-releasing hormone (TRH), ensuring secretion through the secretory pathway, under the control of the neuronal Thy1 promoter. Tg4-42 mice were generated and maintained on a C57Bl/6J background. In addition to heterozygous Tg4-42 mice, a homozygous Tg4-42 line (Tg4-42^{hom}) was generated in our group and used in the present study.

2.2.4 5XFAD transgenic mice

The generation of 5XFAD mice (Tg6799) has previously been described by Oakley and colleagues (Oakley et al., 2006). Briefly, 5XFAD mice overexpress the 695 amino acids isoform of the human amyloid precursor protein (APP695) carrying the Swedish, Florida and London mutations under the control of the murine Thy1 promoter. Additionally, human presenilin-1 (PSEN1), carrying the mutations M146L and L286V,

is expressed under the control of the murine Thy1 promoter. 5XFAD mice used in the current study were backcrossed for more than 10 generations to C57Bl/6J wild-type mice (WT) (Jackson Laboratories) to obtain an incipient congenic line on a C57Bl/6J genetic background (Jawhar et al., 2012).

2.2.5 Neprilysin gene-disrupted mice

The neprilysin gene-disrupted mouse model has been initially generated and described by Lu and colleagues (Lu et al., 1995) and was a generous gift of Dr. Takaomi Saido (RIKEN Brain Institute, Japan). The mice were kept as a homozygous line (NEP^{-/-}) and bred with hemizygous 5XFAD mice resulting in the genotypes 5XFAD/NEP^{+/-} and NEP^{+/-}.

2.2.6 Tissue collection and preservation

Brain tissue was collected and preserved in different ways depending on the subsequent analysis:

For RNA and protein extractions, directly frozen tissue is needed. Therefore, mice were sacrificed via CO₂ anesthetization followed by cervical dislocation. Brains were rapidly dissected on ice, cerebellum and olfactory bulb were removed and hemispheres were separately frozen on dry ice. The tissue was kept at -80°C until further processing.

For immunohistochemical stainings, mice were sacrificed and brains were dissected as described above. Hemispheres were placed into embedding cassettes (Simport) and stored in 4% formalin histofix solution at 4°C for at least 72 h under light protection until being embedded in paraffin (Section 2.6.1).

Another way to obtain brain tissue for immunohistochemical stainings and/or stereological analysis is the perfusion via the vascular system through the heart. Therefore, mice were deeply anesthetized with a mixture of ketamine (10% stock solution) and xylazine (23.3 mg/ml) diluted in molecular-grade water. The anaesthetic was administered intraperitoneally at a dosage of 100 mg/kg ketamine and 10 mg/kg xylazine body weight, respectively. Once mice were no longer responsive to pain stimuli, they were pinned by their limbs on a perfusion board. The abdominal wall was opened, the diaphragm was cut and the rib cage was split to reveal the beating heart. The right atrium was supplied with an incision to allow blood to drain from the

circulatory system. A sterile needle, which was attached to a tubing system of a peristaltic pump, was inserted into the left ventricle and the mouse was perfused with 20 ml of ice-cold 0.01 M PBS to clear the circulatory system from blood. Then, the perfusion tubing was transferred to a cylinder containing ice-cold 4% PFA in 0.01 M PBS and perfusion was continued until an amount of approximately 40 ml PFA solution was administered. After perfusion, brain tissue was carefully collected. The right hemisphere was placed in 4% formalin histofix solution for post-fixation before being embedded in paraffin as described above. The left hemisphere was post-fixed for additional 24 h in 4% PFA in 0.01 M PBS before being transferred in 10 ml of 30% sucrose solution prepared in 0.01 M PBS. The brain tissue was incubated in sucrose until it sunk to the bottom of its container, subsequently frozen on dry ice and stored at -80°C until further use.

2.3 Behavioural Analysis

2.3.1 Motor phenotype assessment

2.3.1.1 Balance Beam

To analyse balance and fine motor coordination, the balance beam test was conducted (Luong et al., 2011). A 1 cm wide wooden beam was attached to two wooden support columns at a height of 44 cm. The surface was padded to protect against fall injuries. At either end of the 50 cm long beam, a 9 x 15 cm escape platform was attached. Mice were gently placed on the centre of the beam facing one of the platforms and released. The latency to fall from the beam or to reach one of the platforms was recorded. The test consisted of 60-seconds trials with 3 consecutive trials on a single testing day. If a mouse remained on the beam for the whole 60-seconds trial or escaped to one of the platforms, the maximum time of 60 seconds was recorded. Between each trial, the apparatus was cleaned with 70% ethanol to remove any olfactory cues.

2.3.1.2 String suspension

To test agility and grip strength, the string suspension task was performed (Arendash et al., 2001). The string suspension apparatus was comprised of a 50 cm long cotton string fixed between two wooden support beams at a height of 35 cm. The surface was

padding to protect against fall injuries. Mice were allowed to grasp the 3 mm thick cotton string only by their forepaws. During a single 60-second trial, the performance of each animal was assessed using a 0 to 5 rating system (Moran et al., 1995): 0 = unable to remain on the string; 1 = hangs only by fore- or hind paws; 2 = as for 1, but with attempt to climb onto string; 3 = sits on string and holds balance; 4 = four paws and tail around string with lateral movement; 5 = escape to one of the platforms. Between each trial, the apparatus was cleaned with 70% ethanol to diminish odour cues.

2.3.1.3 Rotarod

Motor performance and motor learning were tested using the rotarod task. Testing consisted of four trials per day for 2 consecutive days with inter-trial intervals of 2–3 min using a computer-controlled Rotarod system (TSE, Technical and Scientific Equipment). Each mouse was placed on the rod, which accelerated from 1 to 45 rpm over a maximum trial time of 300 seconds. Trials were terminated when animals fell off (or the maximum time was reached) and latency to descent (in sec) served as an indicator of motor coordination. Between each trial, the rotarod was cleaned with 70% ethanol to diminish odour cues.

2.3.2 Y-Maze

Working memory performance was assessed using a triangular Y-maze apparatus. The maze consisted of three arms (30 cm length x 8 cm width x 15 cm height), which extended from a triangular central region. During a 10-minute test session, each mouse was randomly placed at the end of one arm and was allowed to explore the Y-maze freely while it was tracked by the ANY-maze™ video tracking system. Alternation was defined as successive arm entries into all three arms in overlapping triplet sets (e.g. 1, 3, 2 or 3, 1, 2 but not 1, 2, 1). The percentage alternation was calculated as the ratio of actual alternations to possible alternations. Between each trial, the maze was cleaned with 70% ethanol to diminish odour cues.

2.3.3 Cross Maze

Spontaneous alternation rates were determined using the cross maze test (Jawhar et al., 2012). The cross maze apparatus was constructed of black plastic material and

consisted of four arms arranged in a 90° position extending from a central space of 8 x 8 cm. Each arm was 30 cm in length, 8 cm in width and 15 cm in height. During a single 10-minute test session, each mouse was randomly placed in 1 arm and allowed to move freely through the maze, while it was tracked using the ANY-maze™ video tracking system. The sequence of the arm entries, the average speed as well as the total distance travelled was recorded. An alternation was defined as successive entries into the four arms in overlapping quadruple sets (e.g. 2, 3, 1, 4 or 4, 2, 1, 3 but not 2, 3, 4, 2) (Arendash et al., 2001). The alternation percentage was calculated as the percentage of actual alternations to the possible number of arm entries (n (arm entries) - 3) (Wietrzych et al., 2005). To standardize odours, the maze was cleaned with 70% ethanol after each mouse.

2.3.4 Elevated plus maze

The elevated plus maze tests anxiety-related behaviours in rodents (Karl et al., 2003). The test is based on the conflict of the animals desire to explore a novel environment and the avoidance of elevated open spaces due to the anxiety to fall. Therefore, the time spent in the open arms is an indication of the intensity of anxiety of the animal. The 75 cm raised maze was shaped like a “+” with two open and two closed arms (15 cm length x 5 cm width) extending from a central platform (5 cm length x 5 cm width). Mice were placed individually into the centre field facing one of the closed arms and allowed to explore the maze freely for a single, 5 min trial. The percentage of time spent in the open arms as well as the ratio of open arm entries to total arm entries were measured using the ANY-maze™ video tracking system. After each mouse, the maze was cleaned with 70% ethanol to standardize odours.

2.3.5 Morris water maze

Spatial reference memory abilities were evaluated using the Morris water maze (Morris, 1984). In this task, mice learn to locate a hidden circular platform (10 cm diameter) in a circular pool (110 cm diameter) filled with tap water using spatial cues. By adding a non-toxic white paint, the water was made opaque and maintained at 20°C for the whole test duration. By the use of the ANY-Maze video tracking software, the pool was divided into four virtual quadrants that were defined based on their spatial

relationship to the platform: left (L), right (R), opposite (O), and target quadrant (T), which contained the goal platform. Escape latency, swimming speed, swimming path and quadrant preference were recorded.

Before animals were obliged to locate the submerged platform, a three-day cued training, in which the platform was marked with a triangular flag, was performed. Mice were introduced into the water at the edge of the pool facing the wall. They were given a maximum time of 1 min to find the platform. If mice were not able to find the platform in 60 sec, they were gently guided to it and allowed to sit on the platform for a few seconds before being removed to their cages. Between the cued training trials, both the location of the visible platform and the position from where mice were introduced into the pool, changed each time. The cued training served to evaluate the general health condition and intact vision of the animal. Each mouse received four cued training trials per day with an inter-trial interval of at least 10 minutes.

Twenty-four hours after the last cued training trial, mice performed five days of acquisition training. In this part of the test, the platform was submerged and invisible for the animals. In addition to distal cues attached to curtains surrounding the pool, proximal cues were placed to the outside of the pool. Between the acquisition training trials, the position of the platform remained stationary while the position from where mice were introduced into the pool changed each time (Vorhees and Williams, 2006). Again, each mouse received four trials per day.

Twenty-four hours after the last trial of the acquisition training, the probe trial was performed to assess spatial reference memory. The platform was removed from the pool and mice were placed into the water from a novel position. Mice were allowed to swim freely for 1 minute and the time spent in each of the virtual quadrants as well as the swimming speed was recorded. During the whole testing period, mice were kept in front of a heat lamp between the different trials to prevent hypothermia.

2.3.6 Novel object recognition

The novel object recognition (NOR) test was performed in an open field box made of grey plastic (50 cm x 50 cm). On the first day, each mouse was given 5 min to explore the testing environment and become habituated. 24 h later, the 5 min exploration phase was performed in which the arena contained two identical objects (two red bricks). Again 24 h later, mice were placed in the apparatus for the 5 min test trial, now

with a familiar and a novel object (a red brick and a glass cylinder). The time mice spent with each object was recorded. The objects were cleaned with 70% ethanol between each animal to remove any lingering scents.

2.4 Molecular Biology

2.4.1 Isolation of genomic DNA and genotyping of transgenic mice

Genomic DNA was isolated from tail biopsies. 500 μ l lysis buffer (100 mM Tris/HCl [pH 8.5], 5 mM EDTA, 0.2% dodecyl sulfate [SDS] and 200 mM NaCl) supplemented with 5 μ l Proteinase K was added to the tail biopsy and incubated at 55°C for 20 h under shaking conditions in a Thermomixer Compact (450 rpm). Samples were then centrifuged at 17,000 rpm for 20 min at 4°C (Heraeus Biofuge Stratos). The supernatant was transferred to a fresh 1.5 ml reaction tube containing 500 μ l ice-cold isopropanol and inverted in order to precipitate the DNA. The sample was centrifuged again at 13,000 rpm for 10 min at room temperature (RT). The supernatant was discarded and the remaining pellet was washed with 500 μ l ice-cold 70% absolute ethanol. After another centrifugation step at 13,000 rpm for 10 min at RT, the supernatant was removed and the DNA pellet was dried at 37°C in a Thermomixer Compact for 45 min. Genomic DNA was resuspended in 30 μ l molecular-grade water and dissolved at 55°C overnight in a Thermomixer Compact before being stored at 4°C until further usage. Genomic DNA samples were diluted to a concentration of 20 ng/ μ l and used for genotyping by conventional Polymerase-chain-reaction (PCR) as follows: Reagents for the reaction mixtures and cycling conditions are in Table 3, Table 4, Table 5 and Table 6, respectively. Primer details are listed in Table 9.

PCR products were analysed using agarose gel electrophoresis. Therefore, 100 ml of 1xTBE buffer was mixed with 2.0 g agarose to prepare a 2 % agarose gel and boiled in a microwave at 560 W until the agarose was dissolved. 3 μ l ethidiumbromide (10 mg/ml) was added before the agarose solution was transferred into a casting tray with a 20-pocket sample comb. After solidification, the comb was removed and the gel was placed in an electrophoresis chamber (Biorad) containing 1xTBE buffer. 10 μ l PCR product was mixed with 2 μ l of 10x agarose gel sample buffer and loaded into the wells. The first well was filled with 5 μ l of 100 bp DNA ladder for size indication of the PCR products. The gel was run for 30 – 60 min at 120 V and then visualized under UV light

using the Gel Doc 2000 (Biorad). Gels were analysed with the Quantity One software program (Version 4.30; Biorad).

10XTBE buffer: 108 g Tris and 55 g boric acid were dissolved in 900 ml ddH₂O. 40 ml 0.5 M Na₂EDTA (pH 8.0) was added and the volume was adjusted to 1 l with ddH₂O. Before use, the solution was diluted 1:10 in ddH₂O to obtain 1XTBE buffer.

Table 3: Reaction mix for Tg4-42 genotyping PCR

Reagent	Volume (µl)
DNA (20 ng/µl)	2.0
Aβ3-42 for2 primer	1.0
Aβ3-42 rev2 primer	1.0
dNTPs (2 mM)	2.0
MgCl ₂ (25 mM)	1.6
10X Reaction buffer	2.0
ddH ₂ O	10.2
Tag polymerase (5 U/µl)	0.2
Total volume per sample	20

Table 4: Reaction mixture for 5XFAD genotyping PCR

Reagent	Volume (µl)
DNA (20 ng/µl)	2.0
hAPP for primer	0.5
hAPP rev primer	0.5
dNTPs (2 mM)	2.0
MgCl ₂ (25 mM)	2.0
10X Reaction buffer	2.0
ddH ₂ O	10.8
Tag polymerase (5 U/µl)	0.2
Total volume per sample	20

Table 5: Reaction mixture for NEP knockout genotyping PCR

Reagent	Volume (μl)
DNA (20 ng/ μ l)	1
5'-ex12 primer	0.4
3'-ex13 primer	0.2
3'-neo(3) primer	0.5
dNTPs (2 mM)	2.5
MgCl ₂ (25 mM)	2.5
10X Reaction buffer	2.5
ddH ₂ O	15.2
Tag polymerase (5 U/ μ l)	0.2
Total volume per sample	24

Table 6: Cycling program for genotyping PCR

Step	Temperature	Duration
1	94°C	180 sec
2	94°C	45 sec
3	58°C	60 sec
4	72°C	60 sec
5	Repetition of steps 2-4 for 35 cycles	
6	72°C	300 sec
7	4°C	∞

2.4.2 RNA isolation from mouse brain

Deep frozen brain hemispheres were weighed and supplied with 1 ml Trifast[®] reagent per 100 mg brain tissue. Samples were homogenized using a glass-teflon homogenizer (15 strokes, 800 rpm) and incubated at RT for 5 min for dissociation of nucleoprotein complexes. 0.2 ml chloroform per 1 ml Trifast[®] was added to each sample and the mixture was vigorously shaken for 15 sec and then incubated for 10 min at RT. To separate the RNA from other cellular components, samples were centrifuged at 12,000 x g for 15 min at 4°C. The upper RNA-containing aqueous phase was carefully transferred to a sterile 2 ml microcentrifuge tube containing 0.5 ml isopropanol per 1 ml Trifast[®]. The samples were gently mixed and incubated on ice for 20 min for RNA

precipitation. After centrifugation at 12,000 x g for 10 min at 4°C, the supernatant was discarded and RNA pellets were washed twice with a volume of 75% absolute ethanol equivalent to that of isopropanol and centrifuged at 7,500 x g for 10 min at 4°C. After the last centrifugation step, the residual ethanol was carefully removed and RNA pellets were air-dried at RT. The RNA was redissolved with 30 µl of molecular grade water and incubated on ice for 1 h. RNA was stored at -80°C until further use.

2.4.3 Determination of nucleic acid concentration

DNA and RNA concentrations were determined using a Biophotometer (Eppendorf). 80 µl of molecular grade water was used as a blank for the photometry reading prior to sample measurements. For each sample, 2 µl DNA or RNA were diluted with 78 µl molecular grade water in an Uvette® 220-1600 nm cuvette (Eppendorf). For each DNA and RNA sample, the 260/230 and 260/280 absorbance ratios were measured, respectively. Concentration measurements were considered accurate if the 260/230 and 260/280 absorbance ratios were between 1.6 and 2.0.

2.4.4 Reverse transcription

Before total RNA isolated from mouse brain was used as a template for reverse transcription, RNA was subjected to digestion by DNase I. Therefore, 1 µg of RNA was mixed with 1 µl of 10x DNase reaction buffer (+MgCl₂) and 1 µl DNase I (1 u/µl). The reaction mixtures were brought to a total volume of 10 µl using molecular grade water and then incubated for 30 min at 37°C in a LabCycle (SensoQuest). 1 µl of 25 mM EDTA was added to each reaction mixture to inactivate the DNase I and samples were incubated for further 10 min at 65°C. The entire volume (11 µl) of the DNase digested RNA sample was used as a template for cDNA synthesis.

Reverse transcription was conducted using the RevertAid First Strand cDNA Synthesis Kit (Thermo Fisher Scientific) according to the manufacturer's instructions. Therefore, the 11 µl of DNase digested RNA sample were mixed with 1 µl of random hexamer primer, 4 µl 5x reaction buffer, 1 µl RiboLock® RNase inhibitor (20 u/µl), 2 µl of 10 mM dNTP mix and 2 µl M-MuLV reverse transcriptase (20 u/µl). The total reaction volume of 21 µl was incubated for 5 min at 25°C, 1 h at 37°C and 5 min at 70°C in a LabCycle (SensoQuest). The cDNA was stored at -20°C until further use.

2.4.5 Quantitative real-time polymerase chain reaction (qRT-PCR)

Gene expression analysis were performed using the FastStart Universal SYBR Green Master qRT-PCR Kit containing SYBR green as the intercalating fluorescent dye and ROX as an internal reference dye. cDNA was diluted 1:10 in molecular grade water to serve as a sample qPCR template. The reaction mix and the cycling program are given in Table 7 and Table 8, respectively. Every reaction was performed in duplicates. cDNA dilutions were pipetted into 200 μ l qRT-PCR tubes (Biozym Scientific) followed by the qRT-PCR reaction mix. Using a Spectrafuge Mini (Labnet Inc.), the tubes were briefly centrifuged before starting the qRT-PCR reactions in the Mx3000P cycler (Stratagene). Raw data were collected using the MxPro Mx3000P software (Stratagene). Average C_t values were determined from duplicates and relative quantification was performed using murine β -Actin as a reference gene for normalization. The transgene levels of the respective genes of interest (GOIs) were normalized to those of murine β -Actin and calibrated to a selected control animal using the $\Delta\Delta C_t$ method (Schmittgen and Livak, 2008):

$$Amount_{gene} = 2^{-\Delta\Delta C_t}$$

For an animal (q), the level of the gene of interest (GOI) gene expression normalized to the expression of murine β -Actin as a reference gene and calibrated to a control animal (cb), $\Delta\Delta C_t$ is calculated as follows:

$$\begin{aligned}\Delta C_t &= C_{t,GOI} - C_{t,\beta-Actin} \\ -\Delta\Delta C_t &= -(\Delta C_{t,q} - \Delta C_{t,cb})\end{aligned}$$

Table 7: qRT-PCR reaction mixture

Reagent	Volume (μ l)
1:10 cDNA dilution	2.0
SYBR Green Master Mix (Rox)	10
Primer for	0.5
Primer rev	0.5
ddH ₂ O	7
Total volume per sample	20

Table 8: qRT-PCR cycling program

Step	Temperature	Duration
1	95°C	10 min
2	95°C	15 sec
3	58°C	30 sec
4	72°C	30 sec
5	Repetition of steps 1-4 for 39 cycles	
6	95°C	1 min
7	55°C	30 sec
8	95°C	30 sec

2.4.6 Primers

All primers were purchased from Eurofins (Ebersberg) and used at a final concentration of 10 pmol/ μ l (1:10 dilution of the 100 pmol/ μ l primer stock prepared in ddH₂O). The primers are listed in order of the appearance in the results part.

Table 9: List of primers used for genotyping and qRT-PCR

Name	Sequence (5' - 3')	Usage
A β 3-42 for	GTGACTCCTGACCTTCCAG	Genotyping
A β 3-42 rev	GTTACGCTATGACAACACCC	Genotyping
hAPP for	GTAGCAGAGGAAGAAGTG	Genotyping
hAPP rev	CATGACCTGGGACATTCTC	Genotyping
5'-ex12	GCCTATTCTTACCAAATATTCTCCCAG	Genotyping
3'-ex12	TTGCGGAAAGCATTTTCTGGACTCCTTG	Genotyping
3'-neo	CTATCGCCTTCTTGACGAGTTCTTCT	Genotyping
Actb for	ATGGAGGGGAATACAGCCC	qRT-PCR
Actb rev	TTCTTTGCAGCTCCTTCGTT	qRT-PCR
BDNF for	GCCTTCATGCAACCGAAGTA	qRT-PCR
BDNF rev	TGAGTCTCCAGGACAGCAAA	qRT-PCR
Nr4a1 for	ATTGAGCTTGAATACAGGGCA	qRT-PCR
Nr4a1 rev	GCTAGAAGGACTGCGGAGC	qRT-PCR
Nfil3 for	CATCCATCAATGGGTCCTTC	qRT-PCR
Nfil3 rev	CTTTCTTTTCCCCCTCAGC	qRT-PCR
Grin2b for	AGCTTGCTGTTCAATGGATG	qRT-PCR
Grin2b rev	TCTGCTCAGACTCTCACCCC	qRT-PCR

Hspa1b for	ATGACCTCCTGGCACTTGTC	qRT-PCR
Hspa1b rev	GCTCGAATCCTATGCCTTCA	qRT-PCR
Cyrab for	GATCCGGTACTTCCTGTGGA	qRT-PCR
Cryab rev	TCTCTCCGGAGGAACTCAA	qRT-PCR
Gabra2 for	CTTTCCATTTTTGCCGAAAG	qRT-PCR
Gabra2 rev	TGATAATCGGCTTAGACCAGG	qRT-PCR
Gabrb2 for	TCTCCAGGCTTGCTGAAAAT	qRT-PCR
Gabrb2 rev	GACCAGATTTTTGGAGGTCCC	qRT-PCR
Ptgds for	ACTGACACGGAGTGGATGCT	qRT-PCR
Ptgds rev	CGGCCTCAATCTCACCTCTA	qRT-PCR
Dnaja4 for	ATTGCCTGTTCTCCACCTTG	qRT-PCR
Dnaja4 rev	CAAGTACCACCCGGACAAGA	qRT-PCR
Hsp105 for	GGCTTCTACAGGCAGCTCAA	qRT-PCR
Hsp105 rev	CAGAAGAAAGCAAACCCCA	qRT-PCR
Ociad2 for	GATTTGGGGCAAACAACAG	qRT-PCR
Ociad2 rev	ACGGCAATAGAAGAAAACGC	qRT-PCR
Stip1 for	AGCACTGTAAGGCATCATCAA	qRT-PCR
Stip1 rev	GAATTCGATTCAACGGGGT	qRT-PCR
Hsp90ab1 for	ACGGACCTTCTAAGTTGGAC	qRT-PCR
Hsp90ab1 rev	TCAGCCRRGRCATGCCAATG	qRT-PCR
Bfsp2 for	GCGTTTTCTAGGACAGCCTC	qRT-PCR
Bfsp2 rev	GAACTGGAAACACAACCTGCG	qRT-PCR
Ndn for	GTGTGGAGATTGGTCAGCCT	qRT-PCR
Ndn rev	AAAGAGGTCATGGGCAGCTA	qRT-PCR
Nep for	CCTCAGCCGAAACTACAAGG	qRT-PCR
Nep rev	TTGCTCTCTCCAGCAAAGC	qRT-PCR
Gfap for	CCTTCTGACACGGATTTGGT	qRT-PCR
Gfap rev	ACATCGAGATCGCCACCTAC	qRT-PCR
Ide for	CAGGCATCGTTCATCACATT	qRT-PCR
Ide rev	ACAGGTTTGCGCAGTTTTTC	qRT-PCR
Bace1 for	TGGTAGTAGCGATGCAGGAA	qRT-PCR
Bace1 rev	ATGTGGAGATGACCGTAGGC	qRT-PCR
Ece1 for	ATTTGTGTTACCTGGTGGG	qRT-PCR
Ece1 rev	ACTTGGAGCTGGAGCCTTAG	qRT-PCR
Ece2 for	CCCAGCTCCACCATGTAGTC	qRT-PCR
Ece2 rev	TCATCCAGGTGGACCAGTCT	qRT-PCR
Ace for	CACTGCTTGATCCTGAAGTCC	qRT-PCR

Ace rev

CGATGTTAGAGAAGCCCACC

qRT-PCR

2.4.7 Protein isolation from mouse brain

Frozen hemispheres were weighed and homogenized in 700 μ l TBS buffer (120 mM NaCl, 50 mM Tris, pH 8.0 incl. complete protease inhibitor cocktail) per 100 mg tissue using a R50D homogenizer at 800 rpm. The resulting solution was centrifuged at 17,000 \times g for 20 min at 4°C (Heraeus Biofuge Stratos). The TBS-soluble protein containing supernatant was stored at -80°C. The remaining pellet was dissolved in 800 μ l of 2 % SDS with complete protease inhibitor and sonicated with a Branson Sonifier 100 at intensity 2 (G. Heinemann Ultraschall und Labortechnik) followed by a centrifugation step of 17,000 \times g for 20 min at 4°C. The supernatant, which contained SDS-soluble proteins, was transferred to a new tube containing 1 μ l of Benzonase and was rotated at RT for 10 min followed by storage at -80°C.

2.4.8 Protein concentration determination

Protein concentrations were determined using the Roti®-Quant universal colorimetric protein concentration analysis kit according to the manufacturer's protocol. Briefly, a stock solution of 2 mg/ml albumin fraction V in 0.01 M PBS was diluted (2, 1.5, 1.0, 0.75, 0.5, 0.25, 0.125 mg/ml and ddH₂O) for the generation of a standard curve. 50 μ l of 1:10 dilutions of protein samples as well as albumin dilutions were applied in triplicates into a 96-well plate. Reagent 1 and Reagent 2 were mixed in a ratio of 15:1 and added to each well in a total volume of 100 μ l. The samples were gently mixed on a 96-well plate mixer and incubated at 37°C for 30 min in the dark. Protein concentrations were measured at 490 nm using a μ Quant plate reader (BioTek Instruments, Inc.) combined with the MikroWin 2000 software (v4.04, Mikrotek).

2.4.9 Enzyme-linked immunosorbent assay (ELISA) analysis

ELISA measurements were performed in collaboration with the group of Sascha Weggen in Düsseldorf, Germany. Protein samples were isolated as described in section 2.4.7. Monoclonal antibody IC16 (1:250 in PBS, pH 7.2), raised against amino acids 1-15 of the A β sequence, served as a capture antibody. To generate standard curves,

synthetic A β ₄₀ and A β ₄₂ peptides (JPT Peptide Technologies) were used. These A β peptides were solubilized in DMSO at 10 μ g/mL and aliquots were stored at -80°C . 96-well high-binding microtiter plates were incubated overnight at 4°C with the capture antibody. After the capture antibody was removed, freshly diluted brain samples and freshly diluted A β peptide standards (125-6000 pg/ml in PBS containing 0.05 % Tween-20, 1 % BSA) were added. Subsequently, C-terminal detection antibodies specific for A β ₄₀ and A β ₄₂ labeled with horseradish peroxidase (HRP) using the Pierce EZ-Link™ Plus Activated Peroxidase kit (Thermo Fisher Scientific) were diluted in PBS containing 0.05 % Tween-20, 1 % BSA, added to each well, and incubated overnight at 4°C . Plates were washed 3 times with PBS containing 0.05 % Tween-20 and once with PBS. Then 50 μ l of TMB ELISA Peroxidase Substrate (Interchim) was added and incubated for 1-10 min at RT in the dark. The reaction was stopped by adding 50 μ l of 2 M H₂SO₄ and the absorbance was measured using a Paradigm microplate reader (Beckman Coulter) at 450 nm.

2.4.10 Electrochemiluminescence A β assay

For determination of A β levels in whole brain hemispheres, an electrochemiluminescence total A β assay obtained from Meso Scale Discovery was used. The A β assay is based on the Human (6E10) A β ₄₀ Ultra-Sensitive kit. Here, the A β ₄₀ detection antibody is replaced by anti-A β 4G8 monoclonal antibody. Therefore, the total A β assay employs monoclonal antibody 6E10 (directed against an amino terminal epitope of A β) for capture and the monoclonal antibody 4G8 (directed against A β ₁₇₋₂₆) for detection.

The assay was performed according to the protocol of the manufacturer and readout on a MSD QuickPlex SQ 120. In brief, a 96-well plate pre-coated with an A β antibody (6E10) was blocked with 3% BSA under shaking conditions at room temperature for 1 h. After 3 washing steps with 150 μ l/well of 1 X Tris Wash Buffer, 25 μ l of 2 mg/ml protein lysates or calibrator was added per well and incubated under shaking conditions at room temperature for 1 h. After 3 additional washing steps, 25 μ l of detection antibody solution (4G8) was added and again incubated with shaking for 1 h at room temperature in the dark. Upon 3 more washing steps, 150 μ l of 1X Read Buffer T was added to each well and plate was read on MSD instrument.

2.5 Deep sequencing analysis

Deep sequencing analysis were performed in collaboration with the Microarray and Deep-Sequencing Core Facility of the University Medicine Göttingen (UMG). Total RNA was extracted from WT and Tg4-42^{het} SH/EE mouse brain hemispheres (n = 6 per group) as described in section 2.4.2. 0.5 µg of total RNA was used as start material for the library preparation. The libraries were generated according to the TruSeq mRNA Sample Preparation Kits v2 Kit from Illumina (Cat. N°RS-122-2002). For accurate quantitation of cDNA libraries a fluorometric based system, the QuantiFluor™ dsDNA System from Promega (Mannheim, Germany) was used. The size of final cDNA libraries was determined by using the Fragment Analyser from Advanced Bioanalytical. The average of libraries was 320 bp. cDNA libraries were amplified and sequenced by using the cBot and HiSeq2000 from Illumina (SR; 1x50 bp; ca. 30 Mio reads per sample). Sequence images were transformed with Illumina software BaseCaller to bcl files, which were demultiplexed to fastq files with CASAVA v1.8.2. Quality check was done via fastqc. Read alignment was performed using STAR v2.3.0 to the hg19 reference genome. Data were converted and sorted by samtools 0.1.19 and reads per gene were counted via htseq version 0.6.1. Data analysis was performed using R/Bioconductor (3.0.2/2.12) with DESeq2 and gplots packages. Candidate genes were filtered to a minimum of FDR-corrected p-value < 0.05. For functional analysis, gene ontology enrichment was tested via R-package goseq. Protein-protein interactions of differentially expressed genes were assessed using the Search Tool for the Retrieval of Interacting Genes/Proteins database (STRING v10).

2.6 Immunohistochemistry

2.6.1 Paraffin embedding of mouse brain

Following tissue fixation (section 2.2.6), brains were transferred in the TP Automatic Tissue Processor (Leica) for dehydration and paraffin immersion. Table 10 displays the dehydration protocol:

Table 10: Brain tissue dehydration protocol

Reagent	Time
4% histofix	5 min
Tap water	30 min
50%, 60%, 70%, 80%, 90% EtOH	1 h, respectively
100% EtOH	2 x 1 h
Xylol	1h
Melted paraffin	2 x 1 h

The tissue was embedded in paraffin blocks after processing using an EG1140 H Embedding Station (Leica). Embedded brains were cut in 4 μm sagittal sections using a HM 335E microtome (Thermo Fisher Scientific). Sections were transferred to a ddH₂O water bath and mounted onto Superfrost® slides (Thermo Fisher Scientific). In a 55°C water bath (Medax), sections were defolded and fixed onto slides before a 30 min incubation at RT followed by an overnight incubation at 37°C before being used for immunohistochemistry.

2.6.2 3, 3'-Diaminobenzidine (DAB) immunohistochemistry

For DAB staining, sections were deparaffinized in xylol (2 x 5 min) and rehydrated in a series of ethanol (10 min 100% EtOH; 5 min 95% EtOH; 3 min 70% EtOH) followed by a 1 min incubation in ddH₂O. After treatment with 0.3% H₂O₂ in 0.01 M PBS to block endogenous peroxidases, antigen retrieval was achieved by boiling sections in 0.01 M citrate buffer pH 6.0 (2 min at 800 W, 8 min at 80 W). After a 10 min cool down, sections were dipped in ddH₂O for 1 min and permeabilized for 15 min in 0.1% Triton X-100 in 0.01 M PBS. A washing step in 0.01 M PBS for 1 min was followed by 3 min incubation in 88% formic acid to reveal intracellular A β . Non-specific binding sites were blocked for 1 h by treatment with 10% skim milk and 4% fetal calf serum (FCS) in 0.01 M PBS prior to the addition of the primary antibodies. The primary antibodies were diluted to the desired concentrations in 10% FCS in 0.01 M PBS (Table 11). After incubation overnight in a humid chamber at RT, sections were washed with 0.1% Triton X-100 in 0.01 M PBS for 15 min followed by a brief rinse in 0.01 M PBS. Then, sections were incubated with the respective biotinylated secondary antibodies (Table 12), which were diluted in 0.01 M PBS containing 10% FCS, for 1 h. At least 30 min before use, the

Avidin-biotin complex (ABC) solution was prepared using the Vectastain Elite ABC Kit according to the instructions of the manufacturer and stored at 4°C. Following a 15 min washing step in 0.01 M PBS, sections were incubated with 100 µl of ABC solution per section for 1.5 h at 37°C. After removal of the ABC solution by washing in 0.01 M PBS for additional 15 min, the staining was visualized using DAB as a chromogen. The DAB developing solution was prepared by mixing 100 µl DAB stock solution (25 mg/ml DAB in 50 mM Tris/HCl) with 5 ml 50 mM Tris/HCl and 2.5 µl 30% H₂O₂. Sections were incubated with the DAB developing solution until the desired staining pattern was seen. Then, sections were washed in 0.01 M PBS for 15 min and counterstained with hematoxylin for 40 seconds. Sections were dipped in tap water and washed under running tap water for 5 min before getting dehydrated using the following incubations: 1 min 70% EtOH; 5 min 95% EtOH, 10 min 100% EtOH, 2 x 5 min xylol. Each section received 3 drops of Roti®-Histokitt mounting medium and a cover slip was applied to the slide.

2.6.3 Free-floating immunohistochemistry

As DAB immunohistochemistry in paraffin sections is not applicable for the detection of antigens with sensitive epitopes, they can be visualized by immunostaining in free-floating frozen sections. Therefore, one series of frozen sections was carefully transferred to a 12-well net system (Costar) providing constant floating of the sections. First, sections were hydrated for 15 min in ice-cold 0.01 M PBS before being transferred to 0.3% H₂O₂ in 0.01 M PBS for blocking endogenous peroxidase activity. Sections were subsequently washed 3 x 10 min in 0.01 M PBS containing 0.1% Triton X-100 for membrane permeabilization. Unspecific binding of antibodies was blocked by treatment with 0.01 M PBS containing 10% FCS and 4% skim milk powder for 1 h at RT prior to overnight incubation in primary antibody diluted in 0.01 M PBS with 10% FCS. On the next day, sections were washed 3 x 10 min in 0.01 M PBS containing 0.1% Triton X-100 followed by one washing step in 0.01 M PBS for 1 min. Then, sections were incubated with the secondary antibody in 0.01 M PBS containing 10% FCS for 2 h at RT followed by three additional washing steps in 0.01 M PBS for 10 min each. As a next step, sections were incubated in Avidin-Biotin complex (ABC) solution for 1.5 h at RT. After washing, staining was visualized using DAB as described in section 2.6.2. Sections were incubated in DAB staining solution for 4 min followed by 3 x 10

min washing in 0.01 M PBS. After washing, sections were mounted in PBS onto Superfrost slides and left to dry overnight. The next day, sections were incubated in 0.01 M PBS for hydration before being counterstained with filtered hematoxylin for 40 sec. After shortly being dipped in ddH₂O, sections were put under running water for 5 min. Thereafter, sections were dehydrated in baths of the following EtOH concentrations: 1 min 70% EtOH; 5 min 95% EtOH; 10 min 100% EtOH followed by 2 x 5 min in xylol. As a final step, sections were embedded using Roti® Histokitt mounting medium.

2.6.4 Thioflavin S staining of paraffin sections

Thioflavin S stains aggregated forms of A β , but no monomers or dimers. Paraffin embedded sections were deparaffinized and rehydrated as described in section 2.6.2. Then, sections were washed 2 x 1 min in distilled water and stained with 1% Thioflavin S solution in distilled water for 8 min. Sections were then washed 2 x 1 min in distilled water and again immersed for 4 min in the Thioflavin S solution. Followed by 2 x 1 min washes in 80% ethanol and 3 x 1 min washes in distilled water, sections were counterstained with DAPI and embedded in aqueous fluorescent protecting mounting medium.

2.6.5 Quantification of A β plaque load, Thioflavin S and GFAP immunoreactivity

Extracellular A β plaque load and Thioflavin S signal was evaluated in cortex (Ctx), dentate gyrus (DG), subiculum (Subic) and thalamus (Thal) using an Olympus BX-51 microscope equipped with a Moticam Pro 282A camera (Motic) and the ImageJ software package. Serial images of 100x magnification were captured on three sections per mouse which were at least 30 μ m apart from each other. Using ImageJ the pictures were binarized to 8-bit black and white images and a fixed intensity threshold was applied defining the DAB signal or Thioflavin S signal. Measurements were performed for a percentaged area covered by DAB or Thioflavin S staining.

Accordingly, for GFAP staining quantification, images of 200x magnification were captured and the astrocyte-covered areas were analysed as described before. The relative A β plaque load or GFAP immunoreactivity is expressed with 5XFAD-SH mice as the reference parameter.

2.6.6 Primary Antibodies

Table 11: Primary Antibodies

Antibody	Host	Epitope	Working dilution	Manufacturer	Usage
4G8	mouse	A β ₁₈₋₂₂	1:10000	Covance	IH
4G8-SULFO-TAG	mouse	A β ₁₈₋₂₂	1:50	Mesoscale Discovery	MSD
IC16	mouse	A β ₁₋₁₅	1:250	Generous gift of Sascha Weggen	ELISA
BAP-24	mouse	A β ₄₀	1:500	Roche	ELISA
BAP-15	mouse	A β ₄₂	1:500	Roche	ELISA
DCX	goat	Doublecortin, expressed by migrating neurons	1:500	Santa Cruz	IH
GFAP	mouse	Glial fibrillary acidic protein	1:500	Synaptic Systems	IH
NEP	mouse	Nepriylsin	1:250	Santa Cruz	IH

2.6.7 Secondary Antibodies

Table 12: Secondary Antibodies

Antibody	Host	Conjugate	Working dilution	Manufacturer	Usage
anti-mouse	rabbit	biotinylated	1:250	Dako	IH
anti-goat	rabbit	biotinylated	1:250	Dako	IH

2.7 Quantification of neuron numbers

2.7.1 Sample preparation

For neuronal stereology, fixed frozen left brain hemispheres were cut into 10 series of 30 μ m thick coronal sections using a CM1850 UV cryostat (Leica). Every 10th section was systematically sampled and stored at -80°C until further use. One brain series was transferred into ice-cold 0.01M PBS, carefully mounted onto Superfrost® slides and dried overnight at RT. Sections were stained with cresyl violet and used for stereological analysis.

2.7.2 Cresyl violet staining

Sections were treated 2 x 10 min in work solution A followed by 20 min in work solution B and again 2 x 10 min in work solution A for delipidation. As a next step, sections were stained twice for 8 min in filtered cresyl violet staining solution. After washing, sections were dehydrated by incubating them 3 x 10 min in 100% EtOH, 10 min in isopropanol and 2 x 5 min in xylol. Slides were mounted with 5 drops of Roti®-Histokitt mounting medium and a cover slip was applied to the slide.

Work solution A: 13.61 g Natrium Acetate Trihydrate was diluted in 100 ml ddH₂O to produce a 1 M Natrium Acetate solution. 40 ml of 1 M Natrium Acetate solution was mixed with 9.6 ml 100% Acetic acid and the volume was adjusted to 1 l with ddH₂O

Work solution B: 2 ml Triton X-100 was dissolved in 10 ml ddH₂O. 2.5 ml of this solution was mixed with 50 ml ddH₂O and 150 ml 100% EtOH.

Cresyl violet staining solution: 0.1 g cresyl violet was added to 1 l work solution A and stirred overnight under light protection.

2.7.3 Stereological analysis

2.7.3.1 Quantification of total neuron numbers in CA1 area and dentate gyrus of the hippocampus

Design-based stereological analysis were performed on cresyl violet stained brain sections to quantify the neuron numbers in the CA1 pyramidal cell layer and the subgranular cell layer of the dentate gyrus in an unbiased manner. Therefore, a BX51 stereology work station (Olympus) with a motorized specimen stage for automatic sampling and the Stereo Investigator 7 software (MBF Bioscience) were used. The parameters used for stereological analysis of neurons in the CA1 and dentate gyrus are listed in Table 13.

Table 13: Parameters for stereological analysis of CA1 and dentate gyrus neuron numbers

Parameter	CA1	Dentate gyrus
Sampling Grid (x) (μm)	49	133
Sampling Grid (y) (μm)	105	75
Sampling Grid Area (xy) (μm^2)	5145	9975
Counting Frame Width (X) (μm)	14	14
Counting Frame Height (Y) (μm)	14	14
Counting Frame Area (XY) (μm^2)	196	196
asf	26.25	50.9
ssf	10	10
Z (μm)	5	5

The CA1 area of the hippocampus or the granular cell layer of the dentate gyrus were delineated at a low magnification (40x), respectively (CA1: Bregma -1.22 to -3.80 mm; DG: Bregma -1.34 to -3.80 mm (Franklin and Paxinos, 2012) (Figure 10). Neuronal nuclei were sampled randomly at a high magnification (100x) using optical dissector probes, and the total number of neurons was subsequently estimated by the optical fractionator method using a 2 μm top guard zone. On every grid site, the section thickness was measured with a 5 μm dissector height (Z). The number of neurons was estimated using the following formulas:

- $P = asf \times ssf \times tsf$
- $N = \sum_{i=1}^n (P \times Q)_i$

Where:

asf = area sampling fraction (xy/XY)

ssf = section sampling fraction

tsf = thickness sampling fraction (T/Z)

P = number of neurons

Q = total markers counted

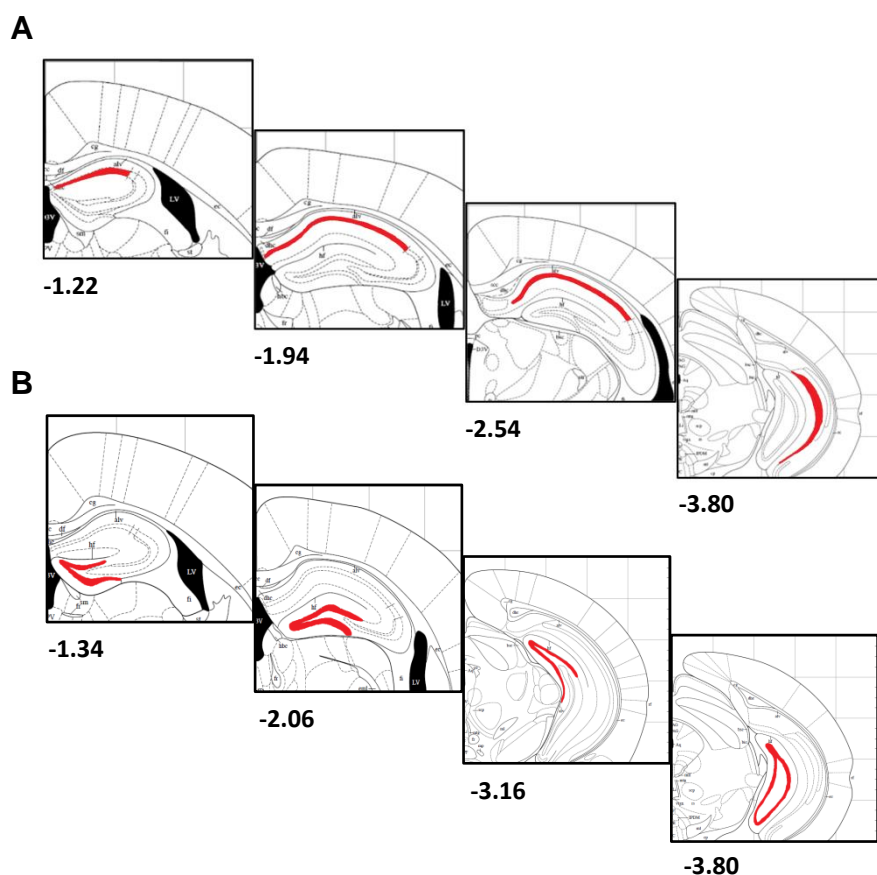


Figure 10: Schematic representation of hippocampal counting areas. (A) The CA1 region (outlined in red) was counted from Bregma -1.22 mm to -3.80 mm. (B) The granule cell layer of the dentate gyrus was counted from Bregma 1.34 mm to -3.80 mm. The pictures are modified from (Franklin and Paxinos, 2012).

The number of doublecortin (DCX)-positive neurons within the subgranular zone (SGZ) of the dentate gyrus was counted using the Meander Scan platform of the Stereo Investigator 7 software. Sections were obtained by systematically collecting every 10th 30 μ m thick coronal frozen section. Therefore, the adult neurogenesis rate was obtained by multiplying the counted number of DCX-positive neurons by a factor 10.

2.7.3.2 Estimation of volume of CA1 area and dentate gyrus of the hippocampus

To estimate the volume of the CA1 pyramidal cell layer and the granular cell layer of the dentate gyrus, the Cavalieri principle was used (Rosen and Harry, 1990). The formula used to calculate the volume is the following:

$$V = d \left(\sum_{i=1}^n (y_i) \right) - (t) y_{max}$$

Where:

V = Cavalieri's estimator of volume

d = distance between analysed sections ($d = 300 \mu\text{m}$)

y_i = cross-sectional area of the i -th section

n = total number of sections

y_{max} = maximal value of y (maximum area)

t = thickness of y_{max} section

2.8 Statistical analysis

Details of statistical analysis are given in the respective results section and in the figure legends. Differences between groups were tested with unpaired t-test, paired t-test, one-way analysis of variance (ANOVA) followed by Bonferroni multiple comparison/unpaired t-test or two-way ANOVA followed by Bonferroni multiple comparison. Survival data were analysed using the log-rank test. Significance levels were given as follows: *** $p < 0.001$; ** $p < 0.01$; * $p < 0.05$. The number of animals used for behavioural experiments as well as sample sizes used for biochemical or stereological analysis are given in the figure legends (n). All data were given as means \pm standard error of the mean (SEM). All statistics were performed using GraphPad Prism version 5.04 for Windows (GraphPad Software, San Diego, CA, USA).

3 RESULTS

3.1 PROJECT I: The effect of long-term environmental enrichment and physical activity on the pathology of Tg4-42 and 5XFAD mice

Wild-type (WT), Tg4-42^{het} and 5XFAD mice were randomly assigned to either standard housing (SH) or environmental enriched (EE) housing conditions at an age of 1 month for a duration of 11 months. At the end of either housing paradigm, mice were subjected to behavioural testing and sacrificed for further biochemical and/or stereological analysis (Figure 11).

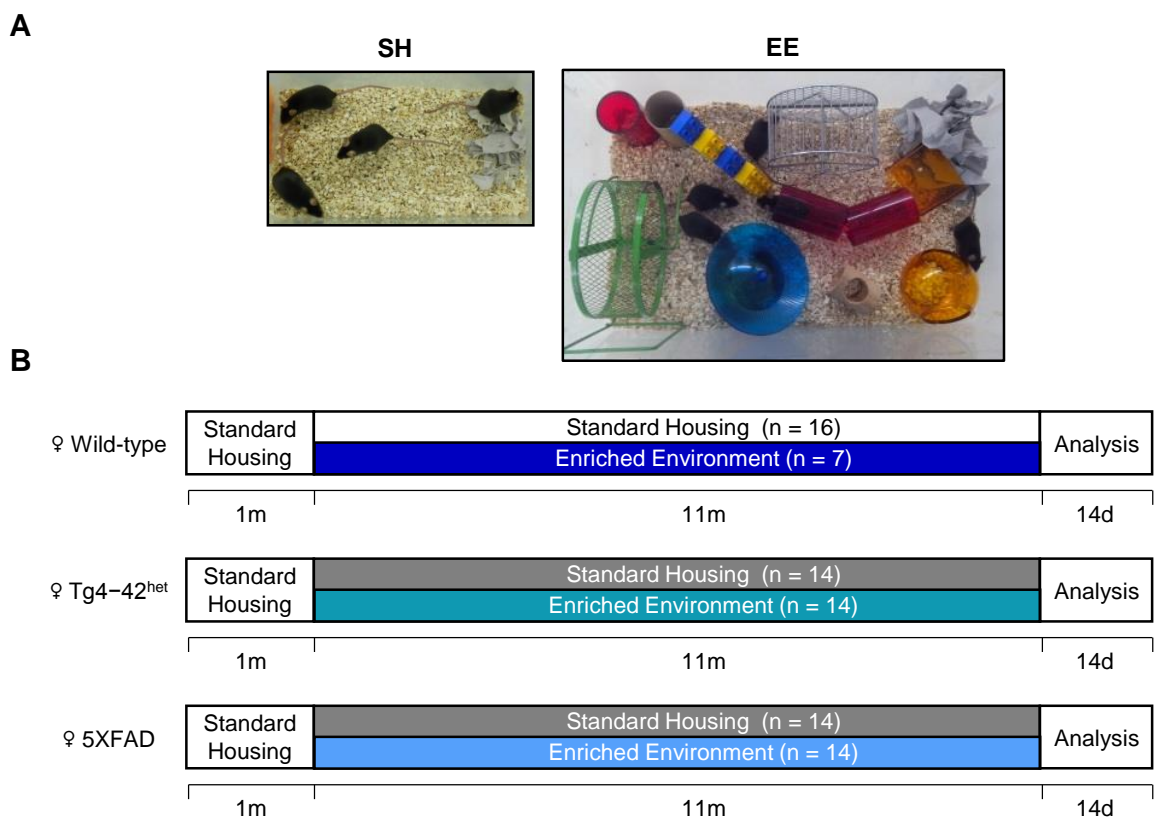


Figure 11: Housing conditions and experimental design. (A) Exemplary pictures of standard housing (SH) and environmental enrichment (EE) cages used for the study. Mice were housed in groups of 4-5. EE cages were equipped with colourful toys, tunnels, climbing apparatuses and three different running wheels. The environment was modified and rearranged completely once a week. (B) After weaning, female wild-type, Tg4-42^{het} and 5XFAD mice were randomly assigned to either SH or EE housing conditions for 11 months. With 12 months of age, mice were behaviourally analysed followed by sacrifice and tissue collection.

3.1.1 Part I: Enriched living conditions and physical activity delays hippocampal neurodegeneration and rescues memory deficits in the Tg4-42 mouse model of Alzheimer's disease

3.1.1.1 The impact of environmental enrichment and voluntary exercise on the sensory-motor performance of Tg4-42^{het} mice

In order to examine the effect of enriched housing combined with voluntary exercise on the sensory-motor performance of Tg4-42^{het} mice, animals were subjected to different motor tasks. In the balance beam test, no significant difference was detected between WT SH and Tg4-42^{het} SH mice. However, Tg4-42^{het} EE mice performed significantly better than Tg4-42^{het} SH mice (One-way ANOVA, $p < 0.01$). No difference in the proportion of mice remaining on the beam or reaching the escape platform was noticed between WT SH and WT EE mice (Figure 12A).

In the string suspension task, standard housed Tg4-42^{het} displayed significant impairments when compared to WT SH controls (One-way ANOVA, $p < 0.05$). This phenotype was completely rescued after 11 months of enriched housing as Tg4-42^{het} EE mice showed significantly higher scores compared to sedentary controls (One-way ANOVA, $p < 0.01$). Housing conditions did not affect the performance of WT animals in the string suspension task (Figure 12B).

Typical phases of motor skill learning as well as motor coordination and balance were assessed in the rotarod task. Over eight trials in two days, WT SH, Tg4-42^{het} SH and EE mice improved their ability to stay on the rotarod over each trial. No differences in the rotarod performance could be determined between WT SH and Tg4-42^{het} SH mice. However, enriched transgenic mice showed a significantly better performance on the rotarod compared to standard housed Tg4-42^{het} mice as demonstrated by overall higher latencies to fall (Two-way repeated measures ANOVA, $p < 0.05$, Figure 12C). No WT EE mice were tested in the rotarod task.

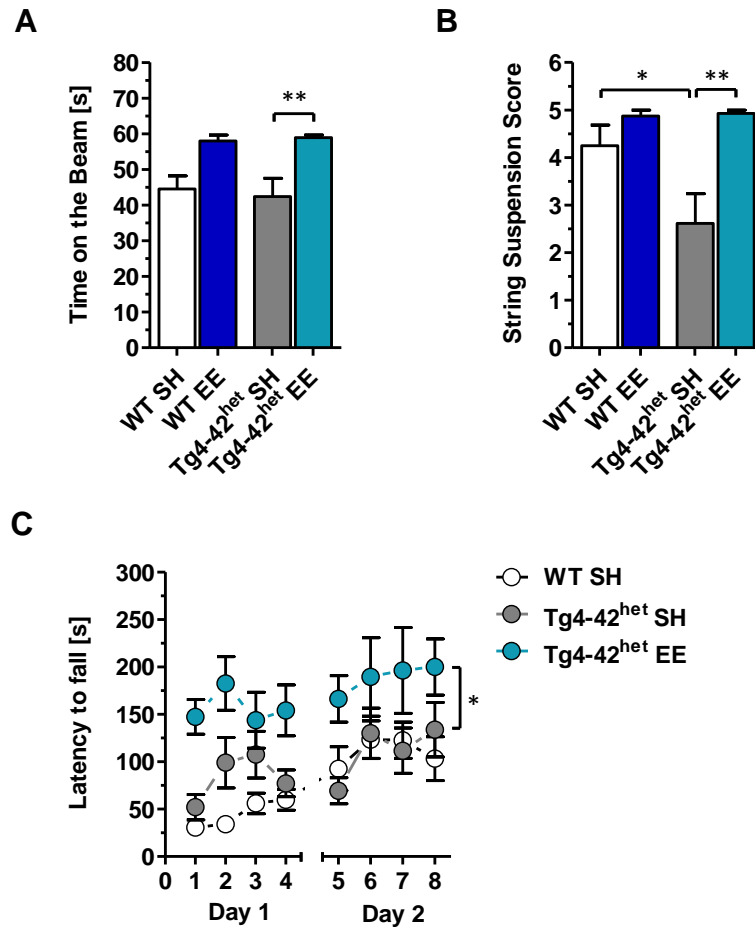


Figure 12: Effects of EE on sensory-motor performance of WT and Tg4-42^{het} mice. (A) Tg4-42^{het} SH mice and WT SH controls displayed a comparable performance in the balance beam test. However, Tg4-42^{het} EE mice stayed significantly longer on the beam when compared to Tg4-42^{het} SH mice. No such improvement could be detected in enriched housed WT mice compared to sedentary controls. (B) Tg4-42^{het} SH mice performed significantly worse than WT SH mice in the string suspension test. This phenotype could be completely rescued upon EE with Tg4-42^{het} EE animals performing at WT levels. No differences in string suspension performance were detected between WT SH and EE mice. (C) In the rotarod test, Tg4-42^{het} EE showed significantly higher latencies to fall compared to Tg4-42^{het} SH mice. No differences were seen between WT controls and Tg4-42^{het} SH animals. (A) and (B): One-way ANOVA followed by Bonferroni multiple comparisons. (C): Two-way repeated measures ANOVA. ** $p < 0.01$; * $p < 0.05$. All data were given as means \pm standard error of the mean (SEM). $n = 7-16$ per group.

3.1.1.2 Enriched environment and voluntary exercise prevent spatial reference memory deficits in Tg4-42^{het} mice

12-month-old Tg4-42^{het} mice display severe spatial reference memory deficits (Bouter et al., 2013). To analyse whether long-term environmental enrichment in combination with voluntary exercise leads to an amelioration of these behavioural deficits, the Morris water maze (MWM) test was performed. WT SH and EE as well as Tg4-42^{het} SH and EE mice showed progressively decreased escape latencies over three days of cued training, which serves as an initial control experiment to rule out that sensory or motor

deficits bias the interpretation of the MWM result. However, Tg4-42^{het} SH mice performed significantly worse than WT SH controls during the cued training as shown by overall higher escape latencies (Two-way repeated measures ANOVA, $p = 0.0475$, Figure 13A). All groups showed comparable swimming speeds during the whole cued training phase (Figure 13C).

In the following acquisition training phase, no difference in spatial learning could be detected between standard housed WT and Tg4-42^{het} mice. However, enriched housed WT and Tg4-42^{het} mice displayed significantly shorter escape latencies over the whole 5-day training period compared to their sedentary controls, respectively. This indicates improved spatial learning upon prolonged enrichment and physical activity (Two-way repeated measures ANOVA, $p < 0.0199$ (WT) and $p < 0.0208$ (Tg4-42^{het}), Figure 13B). Again, no differences in swimming speed were noted during the acquisition training period between all groups analysed (Figure 13D).

During the probe trial, WT SH and EE mice showed a clear, significant preference for the target quadrant. Standard housed Tg4-42^{het} mice displayed no significant preference for the target quadrant demonstrating severe spatial reference memory deficits. This phenotype could be completely rescued by long-term physical and cognitive stimulation as Tg4-42^{het} mice maintained under enriched conditions showed a clear preservation of spatial reference memory demonstrated by their target quadrant preference (Figure 13E). The swimming speed was comparable between WT and Tg4-42^{het} SH/EE mice in the probe trial, indicating that altered motor abilities could not account for the observed results (Figure 13F). Representative occupancy plots of all groups revealed that WT mice and enriched housed Tg4-42^{het} mice focused their search on the initial platform location during the probe trial while sedentary transgenic animals visited the quadrants randomly (Figure 13E).

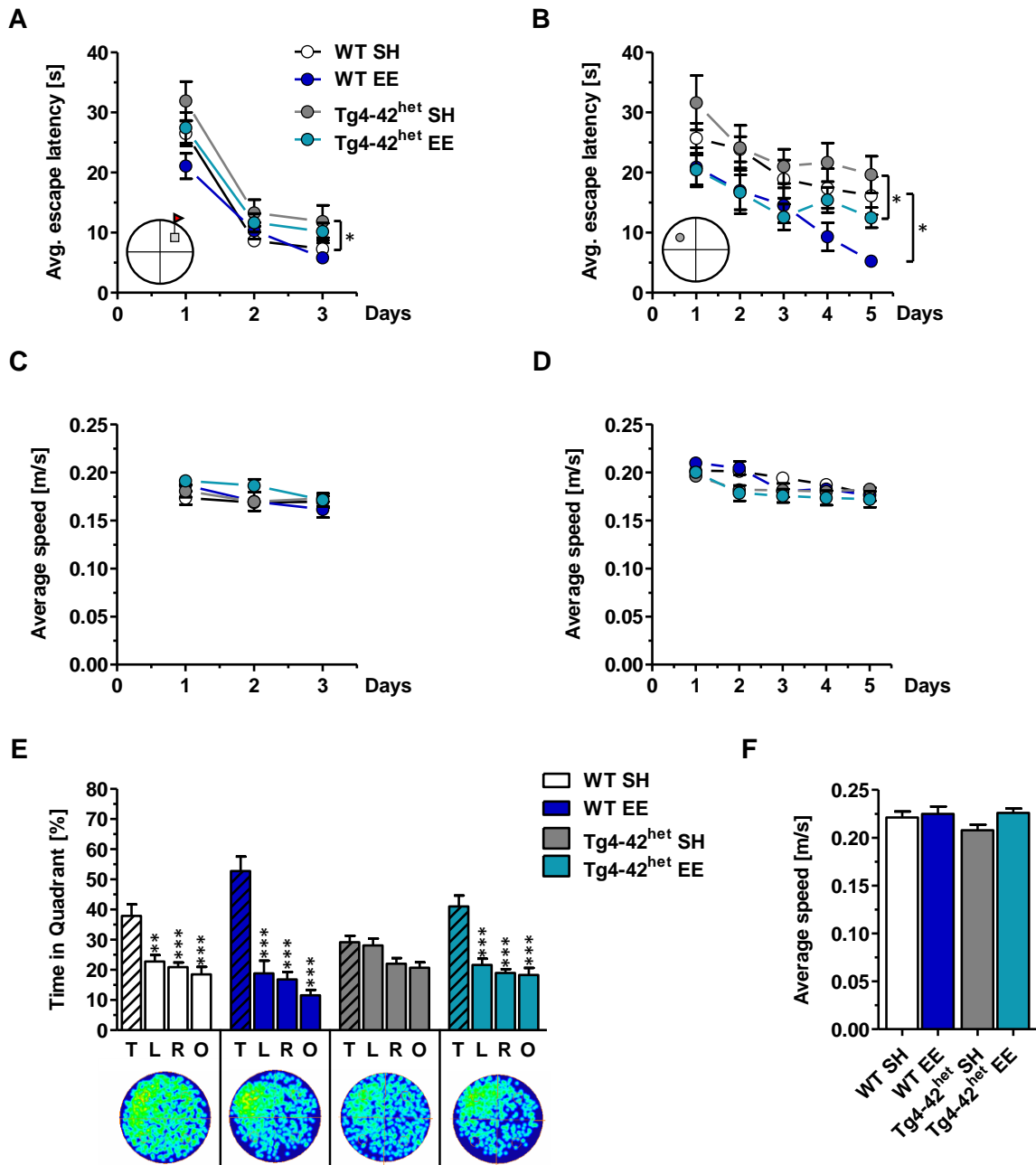


Figure 13: Impaired spatial reference memory in Tg4-42^{het} mice is restored upon EE housing. (A) WT SH and EE as well as Tg4-42^{het} SH and EE mice showed decreased escape latencies over the three days of cued training. However, Tg4-42^{het} SH mice displayed a significantly poorer performance than WT SH mice as shown by overall higher escape latencies during the entire duration of the cued training. (B) Similar to A, mice of all groups showed progressively reduced escape latencies over the five days of acquisition training. WT EE and Tg4-42^{het} EE mice displayed an improved spatial learning performance compared to their sedentary control groups, respectively, as seen by lower escape latencies over the whole training period. (C, D) No differences in swimming speed were observed between WT and Tg4-42^{het} SH/EE mice in both cued and acquisition training. (E) Tg4-42^{het} SH mice showed no preference for any of the quadrants during the probe trial. WT SH and EE as well as Tg4-42^{het} EE mice displayed an intact spatial reference memory as they spent significantly more time in the target quadrant (T) compared to all the other quadrants (L, R, O). The occupancy plots indicate exemplarily the averaged swimming traces of WT and Tg4-42^{het} SH/EE mice during the probe trial. (F) During the probe trial, all groups analysed showed comparable swimming speeds. (A-D): Two-way repeated measures ANOVA. (E, F): One-way ANOVA followed by Bonferroni multiple comparisons. *** $p < 0.001$; ** $p < 0.01$; * $p < 0.05$. All data were given as means \pm standard error of the mean (SEM). $n = 7-16$ per group. L = Left, R = Right, O = Opposite.

3.1.1.3 Enriched environment combined with physical activity restores recognition memory in Tg4-42^{het} mice

The novel object recognition (NOR) task was used to measure object recognition memory and preference for novelty in standard and enriched housed WT and Tg4-42^{het} mice (Silvers et al., 2007). On the exploration day, WT and Tg4-42^{het} SH/EE spent an equal amount of time with the two presented identical objects (Figure 14A). When tested for recognition memory 24 h later, standard housed WT as well as enriched housed WT and Tg4-42^{het} mice spent significantly more time with the novel object (N) compared to the familiar one (F), indicating intact object recognition memory (t-test, $p < 0.001$, respectively). Tg4-42^{het} SH mice did not show a preference for any of the objects, indicating recognition memory deficits (Figure 14B).

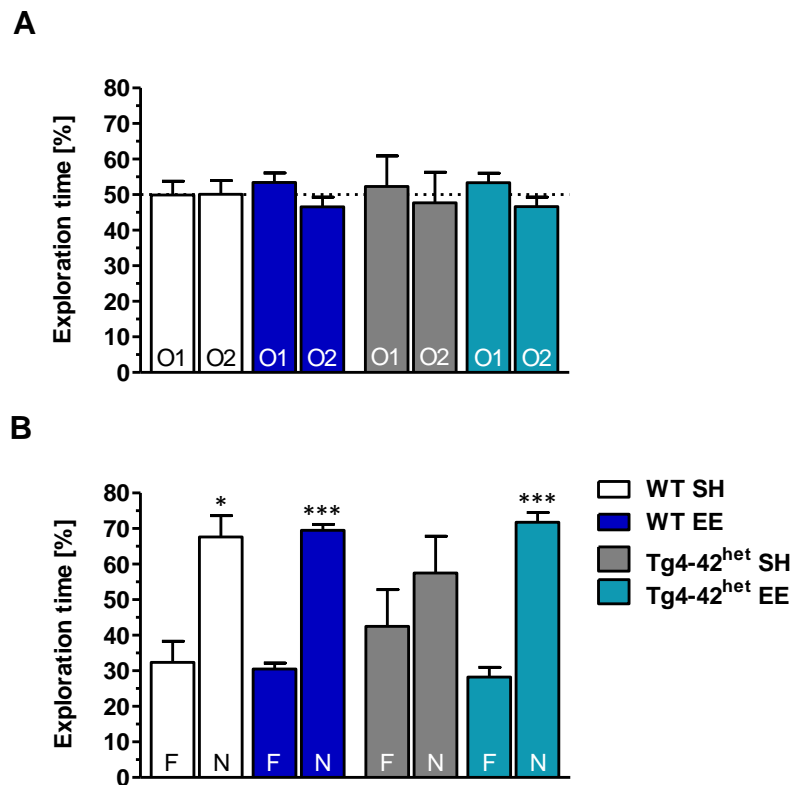


Figure 14: The impact of EE and physical activity on recognition memory performance. (A) The novel object recognition (NOR) task was used to test recognition memory. During the exploration phase on day one, SH and EE WT and Tg4-42^{het} mice spent an equal amount of time with each of the similar objects 1 and 2 (O1, O2). (B) During the test trial, WT SH as well as enriched housed WT and Tg4-42^{het} mice spent significantly more time with the novel object (N) while sedentary controls spent an equal amount of time with the familiar (F) and novel object. Paired t-test. * $p < 0.05$; *** $p < 0.001$. All data were given as means \pm standard error of the mean (SEM). $n = 7-16$ per group.

3.1.1.4 The effect of environmental enrichment and voluntary exercise on hippocampal neuron numbers and volume in Tg4-42^{het} mice

Heterozygous 12-month-old Tg4-42 mice display a massive neuron loss in the CA1 layer of the hippocampus compared to wild-type controls (Bouter et al., 2013). In order to analyse whether lifelong cognitive and physical stimulation positively impacts on CA1 neuron numbers of Tg4-42^{het} mice, unbiased design-based stereological analyses were conducted. Therefore, the hippocampal CA1 pyramidal cell layer was quantified from Bregma -1.22 to -3.80 mm. As previously shown, stereological analysis revealed a 51.1% loss in CA1 neuron numbers between WT SH controls (mean = 293319.88 ± 34662) and Tg4-42^{het} SH mice (mean = 146346.43 ± 4655) (One-way ANOVA, $p < 0.001$). However, Tg4-42^{het} mice maintained under enriched conditions with permanent access to running wheels showed a 12.8% higher number of CA1 pyramidal neurons (mean = 165123.88 ± 3332) compared to Tg4-42^{het} SH mice (t-test, $p < 0.01$), indicating reduced CA1 neuronal death upon EE. Housing condition did not affect the number of CA1 neurons in WT animals (WT EE: mean = 291750.77 ± 21897) (Figure 15A).

Analysis of the CA1 volume did not show significant differences related to housing conditions in Tg4-42^{het} mice (Tg4-42^{het} SH: mean = $2.412 \times 10^8 \pm 1.239 \times 10^7 \mu\text{m}^3$; Tg4-42^{het} EE: mean = $2.345 \times 10^8 \pm 1.189 \times 10^7 \mu\text{m}^3$). In contrast, enriched housed WT mice (mean = $3.274 \times 10^8 \pm 3.252 \times 10^7 \mu\text{m}^3$) showed a significantly higher CA1 volume compared to sedentary controls (mean = $2.541 \times 10^8 \pm 1.393 \times 10^7 \mu\text{m}^3$) (One-way ANOVA, $p < 0.001$). Despite the massive neuron loss in Tg4-42^{het} SH mice, no CA1 volume difference could be detected between WT SH and Tg4-42^{het} SH mice (Figure 15B).

In order to investigate whether long-term effects of an EE paradigm and voluntary exercise influence the total neuron number of the granular cell layer of the dentate gyrus (DG), stereological analysis were performed in this region from Bregma -1.34 to -3.88 mm. However, no changes in DG granule cells could be revealed between any of the analysed groups (WT SH: mean = 451001 ± 61864 ; WT EE: mean = 517112 ± 30443 ; Tg4-42^{het} SH: mean = 509158.86 ± 16460 ; Tg4-42^{het} EE mice: mean = 527183.84 ± 22760 , Figure 15C).

Analysis of the DG volume showed no difference between Tg4-42^{het} SH (mean = $5.376 \times 10^8 \pm 5.335 \times 10^7 \mu\text{m}^3$) and Tg4-42^{het} EE mice (mean = $5.780 \times 10^8 \pm 4.778 \times 10^7 \mu\text{m}^3$).

However, WT mice displayed a higher dentate gyrus volume upon EE (mean = $5.434 \times 10^8 \pm 5.161 \times 10^7 \mu\text{m}^3$) compared to standard housed controls (mean = $4.010 \times 10^8 \pm 6.742 \times 10^7$) (One-way ANOVA, $p < 0.001$). No dentate gyrus volume difference was seen between standard housed WT and Tg4-42^{het} mice (Figure 15D).

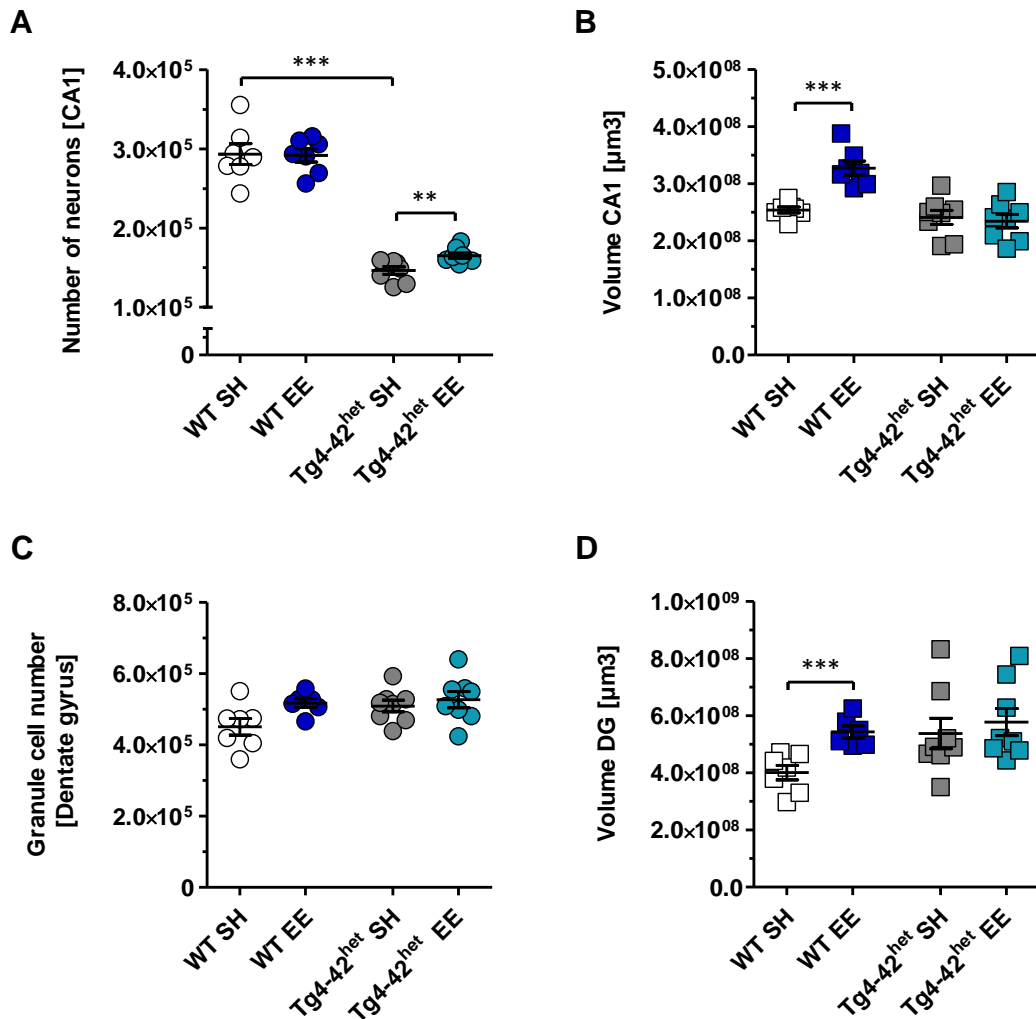


Figure 15: The effect of EE on hippocampal neuron numbers and volume. (A) Design-based stereological analysis revealed significantly reduced CA1 neuron numbers in Tg4-42^{het} SH mice compared to WT SH littermates (-51.1%). This massive neuron loss was reduced upon enriched housing as Tg4-42^{het} EE mice showed significantly higher CA1 neuron numbers (+12.8%) when compared to SH littermates. Housing condition had no effect on CA1 neuron numbers in WT mice. (B) No differences in CA1 volume could be discovered between SH and EE Tg4-42^{het} mice. In contrast, WT EE mice displayed a significantly higher CA1 volume than sedentary WT animals. (C) Stereological analysis revealed no differences in dentate gyrus (DG) granule cells between WT and Tg4-42^{het} SH/EE mice. (D) No differences in DG volume could be discovered between SH and EE Tg4-42^{het} mice. WT EE mice showed a significantly higher DG volume than WT SH mice. One-way ANOVA followed by Bonferroni multiple comparisons. (A) Tg4-42^{het} SH vs. Tg4-42^{het} EE: One-way ANOVA followed by unpaired t-test. ** $p < 0.01$; *** $p < 0.001$. All data were given as means \pm standard error of the mean (SEM). $n = 7-8$.

3.1.1.5 Enriched environment and physical activity do not affect subgranular adult neurogenesis in Tg4-42^{het} mice

Frozen brain sections were stained with an antibody directed against Doublecortin (DCX) (Figure 16A). DCX is a marker protein being expressed in new-born, immature neurons. The quantification of DCX⁺ neurons has been shown to accurately measure modulations in the rate of adult neurogenesis (Couillard-Despres et al., 2005). The number of new-born neurons in the subgranular zone (SGZ) of the DG was significantly reduced in 12-month-old Tg4-42^{het} SH mice in comparison to WT SH mice (-39.09%, WT SH: mean = 985 ± 195.4; Tg4-42^{het} SH: mean = 600 ± 148.4) (One-way ANOVA, $p < 0.01$). Despite higher levels of physical activity and environmental diversity, enriched housed Tg4-42^{het} mice still showed very low levels of adult neurogenesis, which were comparable to Tg4-42^{het} SH mice. Also WT mice did not show increased DCX⁺ neuron numbers upon enriched living conditions with 12 month of age (Figure 16B).

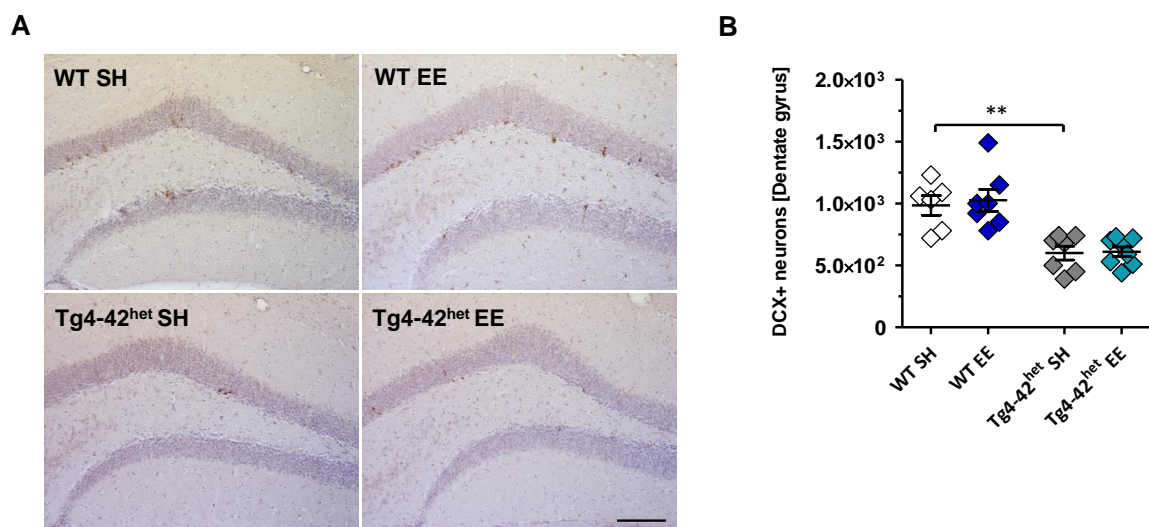


Figure 16: The impact of EE on adult neurogenesis in WT and Tg4-42^{het} mice. (A, B) New-born doublecortin (DCX)-positive neurons were stained and quantified in the subgranular zone (SGZ) of the DG. 12-month-old Tg4-42^{het} SH showed significantly reduced neurogenesis levels compared to standard housed WT mice. This marginal adult neurogenesis could not be restored upon enriched living conditions at that age in Tg4-42^{het} mice. Housing condition also had no effect on adult neurogenesis in WT animals. (B): One-way ANOVA followed by Bonferroni multiple comparisons. $**p < 0.01$. All data were given as means ± standard error of the mean (SEM). $n = 7-8$. Scale bar: 100 μm .

3.1.1.6 The effect of long-term cognitive and physical stimulation on A β brain levels in Tg4-42^{het} mice

Tg4-42 mice display strong intraneuronal A β immunoreactivity predominantly in the CA1 region of the hippocampus starting with 2 months of age. Due to massive neuron loss, CA1 A β immunoreactivity is declining during aging, showing mainly larger, extracellular aggregates by the age of 12 months (Wittnam, 2012). In order to evaluate if enriched living conditions combined with voluntary exercise are accompanied by decreased levels of A β_{4-42} in Tg4-42^{het} mice, immunohistochemical stainings using a pan-A β antibody (4G8) were performed in enriched and sedentary animals. Qualitatively, no differences in A β immunoreactivity could be determined between Tg4-42^{het} SH and EE mice (Figure 17A).

To further confirm this result quantitatively, brain A β levels of Tg4-42^{het} SH and EE mice were measured using an electrochemiluminescence A β assay. However, no significant differences in A β levels could be detected between both groups (Tg4-42^{het} SH: mean = 19.69 ± 0.69 pg/ml; Tg4-42^{het} EE: mean = 21.74 ± 1.05 pg/ml, Figure 17B).

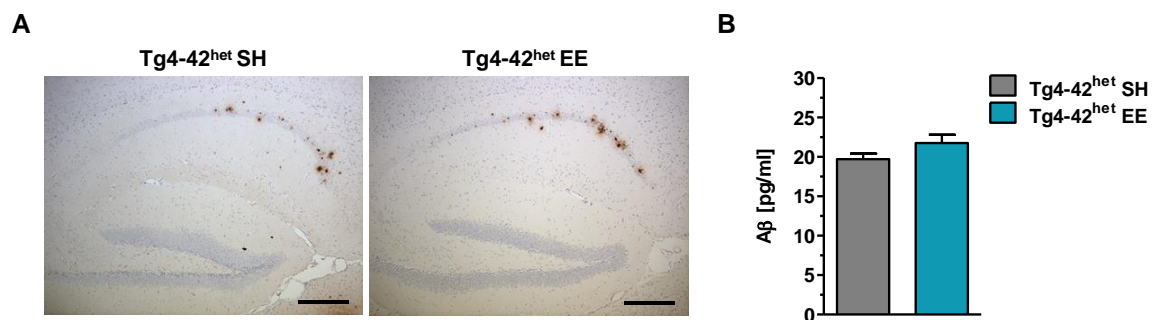


Figure 17: The effect of EE and physical activity on A β brain levels in Tg4-42^{het} mice. (A) Immunohistochemical stainings using a pan-A β antibody (4G8) revealed that Tg4-42^{het} SH and EE mice showed a comparable A β staining pattern in the CA1 region of the hippocampus. (B) Using an electrochemiluminescence assay, A β levels of whole brain hemispheres were quantified. Tg4-42^{het} SH and EE displayed equal amounts of the peptide. (B): Unpaired t-test. All data were given as means \pm standard error of the mean (SEM). n = 6 per group. Scale bar: 200 μ m.

3.1.1.7 Housing under enriched conditions and physical activity changes the gene expression profile of WT and Tg4-42^{het} mice

To assess whether long-term exposure to an enriched environment and voluntary exercise influences the gene expression profile of WT and Tg4-42^{het} brains, deep sequencing analysis on brain hemispheres were performed with both groups in

standard and enriched housed animals. In order to demonstrate gene expression changes, volcano plots were created for both WT and Tg4-42^{het} mice (Figure 18A, C). Each dot represents one gene that is significantly differentially regulated in WT or Tg4-42^{het} EE when compared to SH mice, respectively. In 12-month-old WT EE mice, 375 genes were significantly ($p < 0.05$) differentially expressed when compared to SH controls, with 296 genes being upregulated and 79 genes being downregulated (Figure 18A). In Tg4-42^{het} EE mice, 155 genes were found to be significantly differentially expressed in comparison to their sedentary counterparts, with 80 genes being upregulated and 75 genes being downregulated (Figure 18C). To validate deep sequencing results, several differentially expressed genes (DEGs) either up- or downregulated were randomly selected and verified by qRT-PCR analysis. For all selected genes, the qRT-PCR analysis confirmed the expression levels of the deep sequencing results in WT and Tg4-42^{het} mice (Figure 18B, D). A gene ontology (GO) analysis of the upregulated genes in WT EE mice using the String 10 software package revealed a significant association with several GO terms. Among those, the biological processes “cellular macromolecule metabolic process” ($p = 1.55E-5$), “gene expression” ($p = 3.40E-4$), “negative regulation of apoptotic process” ($p = 5.94E-3$) and “cellular response to stress” ($p = 4.70E-2$) were present. A GO analysis of the upregulated genes in Tg4-42^{het} EE animals indicated an association with the biological processes “protein folding” ($p = 7.750E-6$), “response to stress” ($p = 5.689E-3$) and “negative regulation of inclusion body assembly” ($p = 1.830E-2$). A KEGG pathway analysis of upregulated genes in WT EE mice showed a significant association with several pathways like “basal transcription factors” ($p = 9.48E-3$), “glutamatergic synapse” ($p = 2.04E-2$) and “protein processing in endoplasmic reticulum” ($p = 3.49E-2$). In Tg4-42^{het} EE mice, a KEGG pathway analysis revealed only one significant pathway association for “protein processing in endoplasmic reticulum” ($p = 3.15E-9$). Interestingly, 15 genes were identified to be upregulated upon EE in both WT and Tg4-42^{het} mice indicating a common pathway associated with long-term cognitive and physical stimulation (Figure 18E). A GO analysis of this common subset of genes exhibited a significant association with the biological process “protein folding” ($p = 4.73E-6$) and a significant pathway association with “protein processing in endoplasmic reticulum” ($p = 1.55E-5$, Figure 18F). GO analysis of downregulated genes in WT EE mice showed no significant association with any biological processes. A KEGG pathway analysis

revealed a significant association with the pathway “ECM-receptor interaction” ($p = 3.11E-3$). In Tg4-42^{het} EE mice, downregulated genes showed a significant association with the biological process “response to stimulus” ($p = 4.97E-3$). However, no pathway was significantly associated with the downregulated genes in Tg4-42^{het} mice upon enriched living conditions. 8 genes were found to be downregulated in both WT EE and Tg4-42^{het} EE mice. These genes however could not be assigned to any significant association with biological processes or pathways.

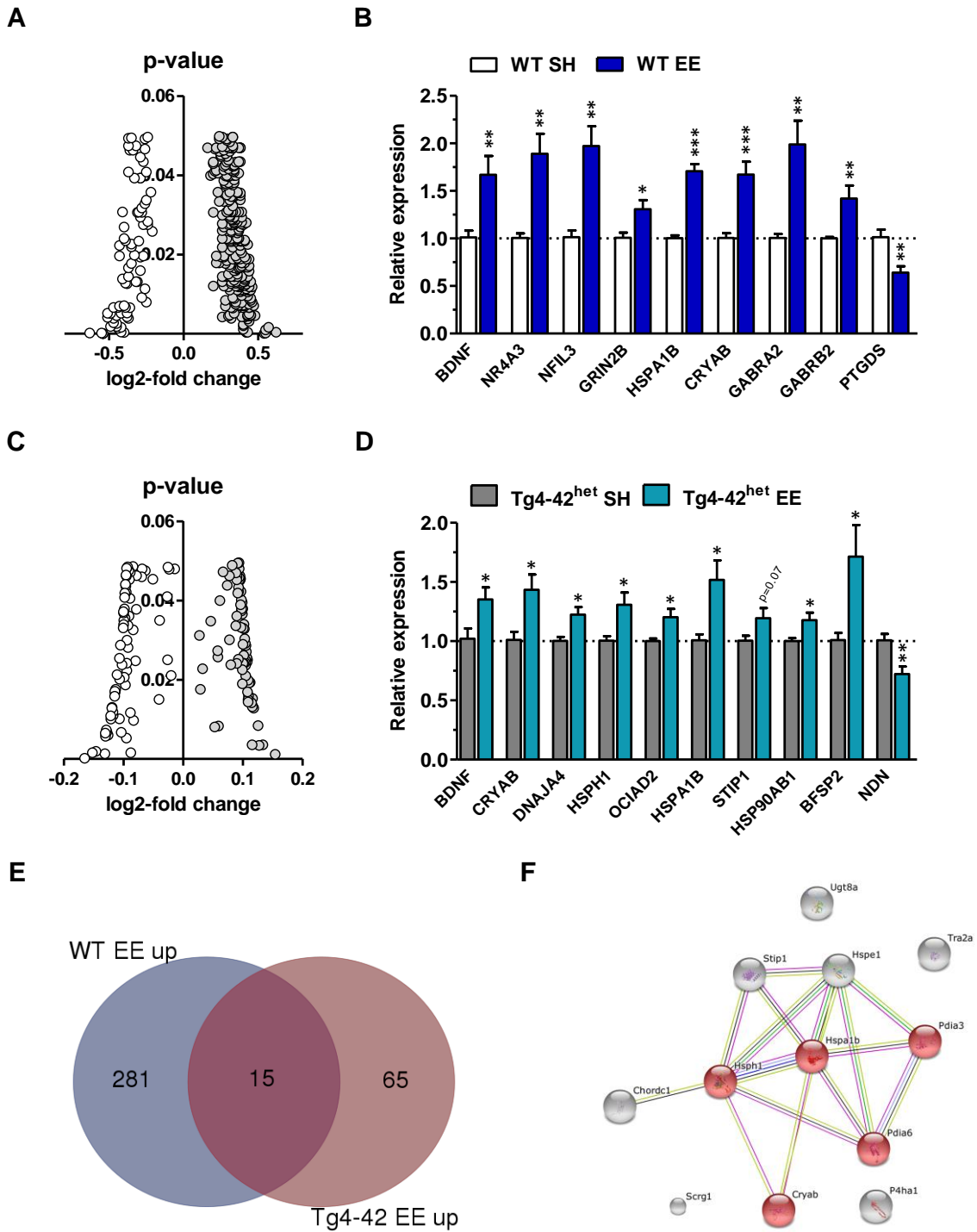


Figure 18: Gene expression profile changes upon long-term EE in WT and Tg4-42^{het} mice. (A, C) Volcano plots of significantly differentially expressed genes (DEGs) in 12-month-old WT (A) and Tg4-42^{het} mice (C) upon prolonged enriched living conditions. The x-axis represents the log₂-fold change, the y-axis the *p*-value. White dots indicate downregulated genes, grey dots indicate upregulated genes. (B, D) To validate deep sequencing data, qRT-PCRs were performed in WT and Tg4-42^{het} mice for randomly selected DEGs. Normalization was performed against the house-keeping gene actin. (E) Venn diagram analysis for genes that were significantly upregulated upon EE in both WT and Tg4-42^{het} mice. (F) Using the STRING10 software, a protein-protein interaction network of the 15 genes found to be induced upon EE in both WT and Tg4-42^{het} mice was created. A significant pathway association with “protein processing in endoplasmic reticulum” was found. The involved proteins are highlighted in red. (B, D): Unpaired t-test. ****p* < 0.001; ***p* < 0.01; **p* < 0.05. All data were given as means ± standard error of the mean (SEM). n = 6 per group.

The most strongly downregulated gene upon EE in Tg4-42^{het} mice was Necdin (*NDN*). In order to analyse whether *NDN* levels *per se* are changed under pathological conditions, qRT-PCR analyses were performed with WT SH/EE and Tg4-42^{het} SH/EE mice. *NDN* expression levels were significantly increased in Tg4-42^{het} mice when compared to healthy control animals (One-way ANOVA, $p < 0.001$). Upon enriched living conditions, however, *NDN* levels significantly decreased again in Tg4-42^{het} mice (One-way ANOVA, $p < 0.01$). In WT animals, housing condition had no influence on Necdin levels (Figure 19).

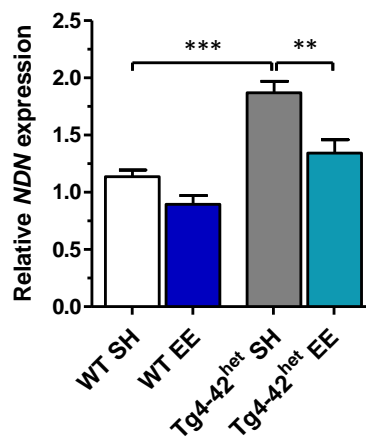


Figure 19: Necdin expression analysis. Tg4-42^{het} mice display significantly increased Necdin expression levels when compared to healthy WT controls. However, upon enriched living conditions, levels drop again to baseline. In WT mice, housing condition has no effect on Necdin expression. Normalization was performed against the house-keeping gene actin. One-way ANOVA followed by Bonferroni multiple comparisons. *** $p < 0.001$; ** $p < 0.01$. All data were given as means \pm standard error of the mean (SEM). $n = 6$ per group.

3.1.1.8 The effect of physical activity alone on the pathology of Tg4-42^{hom} mice

As the enriched environment paradigm in combination with voluntary exercise did not allow predictions about running wheel use of individual animals, an additional control experiment with homozygous Tg4-42 mice (Tg4-42^{hom}) housed in individual cages equipped with either a free or blocked running wheel was performed. Tg4-42^{hom} mice show a fast AD pathology progression. At 2 months of age, no difference in the number of neurons can be observed between Tg4-42^{hom} mice and wild-type littermates (Antonios et al., 2015). However, 6-month-old Tg4-42^{hom} mice display cognitive deficits and a CA1 neuronal loss comparable to 12-month-old Tg4-42^{het} mice (Antonios et al., 2015). Therefore, 2-month-old Tg4-42^{hom} mice were assigned to individual cages and

running wheel recordings were performed for 3.5 months. With 5.5 months of age, Tg4-42^{hom} mice were analysed (Figure 20A).

Tg4-42^{hom} mice with continuous access to running wheels showed increasing weekly running distances which reached a plateau from week seven on and corresponded to ~30 km/week at the end of the trial (Figure 20B).

In order to assess if physical activity alone is sufficient to ameliorate the neuronal cell death in Tg4-42 mice, stereological analysis of the CA1 pyramidal cell layer was performed. Single-housed Tg4-42^{hom} mice subjected to free wheel conditions revealed a 16.5% increase in CA1 neuron numbers (mean = 146867.857 ± 3202) compared to the blocked wheel group (mean = 126120.238 ± 3422) (t-test, $p < 0.001$, Figure 20C). However, no significant differences in CA1 volume could be detected between both groups (Blocked wheel: mean = $1.784 \times 10^8 \pm 6.128 \times 10^6 \mu\text{m}^3$; Free wheel: mean = $1.945 \times 10^8 \pm 5.742 \times 10^6 \mu\text{m}^3$) (Figure 20D).

Due to an unexpected tail hyperflexion phenotype, which broke experimenter's blindness and precluded MWM testing due to swimming incapability, the stereological data of this group could not be backed-up with behavioural data (Figure 20E).

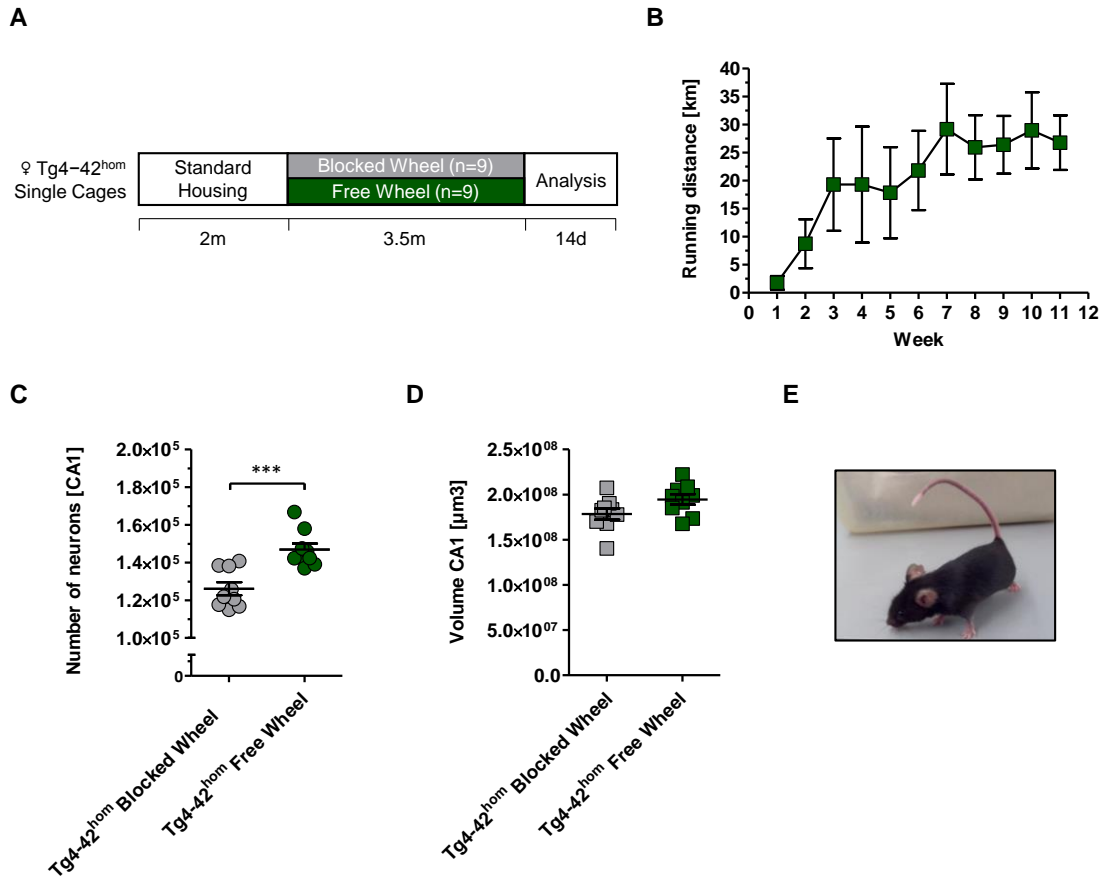


Figure 20: The effect of physical activity on hippocampal neurodegeneration of Tg4-42^{hom} mice. (A) Experimental design. 2-month-old Tg4-42^{hom} mice were randomly assigned to single cages equipped with either a blocked or a free running wheel, which was connected to a rotation sensor. With 5.5 months of age, mice were analysed. (B) Overview of average weekly running distance (km). (C) Tg4-42^{hom} mice with continuous access to a free running wheel displayed 16.5% increased CA1 pyramidal neuron numbers compared to mice housed in cages with a blocked wheel. (D) However, no significant CA1 volume difference could be detected between active and inactive mice. (E) Exemplary picture of tail hyperflexion due to excessive running wheel usage. (C, D): Unpaired t-test. *** $p < 0.001$. All data were given as means \pm standard error of the mean (SEM). $n = 9$ per group.

3.1.2 Part II: Lifelong environmental enrichment in combination with voluntary exercise has limited effects on the pathology of 5XFAD mice

3.1.2.1 The effect of environmental enrichment on the physiological status and the sensory-motor phenotype of 5XFAD mice

To examine if enriched housing conditions and voluntary exercise have an impact on the survival rate of WT and 5XFAD SH/EE mice, a survival analysis was performed. All WT SH and EE mice reached the 12-month time point. 5XFAD SH mice displayed a premature death phenotype compared to WT SH controls as only 70% survived the entire paradigm (Log-rank test, $p = 0.03$). However, housing condition had no significant effect on the survival rate of 5XFAD mice (Figure 21A).

To assess if the enriched environment has an impact on the physiological status of the animals, their body weight was determined at the end of each paradigm. As previously shown, 12-month-old 5XFAD SH mice exhibited a drastically reduced body weight when compared to WT SH littermates (One-way ANOVA, $p < 0.001$). The environmental enrichment in combination with long-term voluntary exercise had no influence on the body weight of WT or 5XFAD mice (Figure 21B).

12-month-old 5XFAD mice show significant impairments in sensory-motor abilities compared to WT controls (Jawhar et al., 2012). Therefore, after 11 months spent either in SH or EE living conditions, the motor performance of 5XFAD mice was analysed using different tasks. 5XFAD SH mice performed significantly worse than age-matched WT SH mice in the balance beam task (One-way ANOVA, $p < 0.001$). This phenotype could not be rescued upon prolonged enriched housing. However, a significantly higher proportion of mice remaining on the beam or reaching the escape platform was noticed in WT EE mice compared to their sedentary littermates (One-way ANOVA, $p < 0.01$, Figure 21C).

Housing conditions also had no effect on the performance of 5XFAD mice in the string suspension task. Both standard and enriched housed 5XFAD mice performed poorly in this task when compared to WT SH mice (One-way ANOVA, $p < 0.001$ respectively). EE had no effect on the string suspension performance of WT animals (Figure 21D).

In the rotarod test, the typical phases of motor skill learning and as well as motor coordination and balance are assessed. With 12 months of age, 5XFAD SH mice showed a worsened rotarod performance when compared to WT SH controls (two-way

repeated measures ANOVA, $p < 0.01$). This phenotype could be reversed upon enriched living conditions in 5XFAD EE mice as shown by overall higher latencies to fall over all trials (two-way ANOVA, $p < 0.01$, Figure 21E).

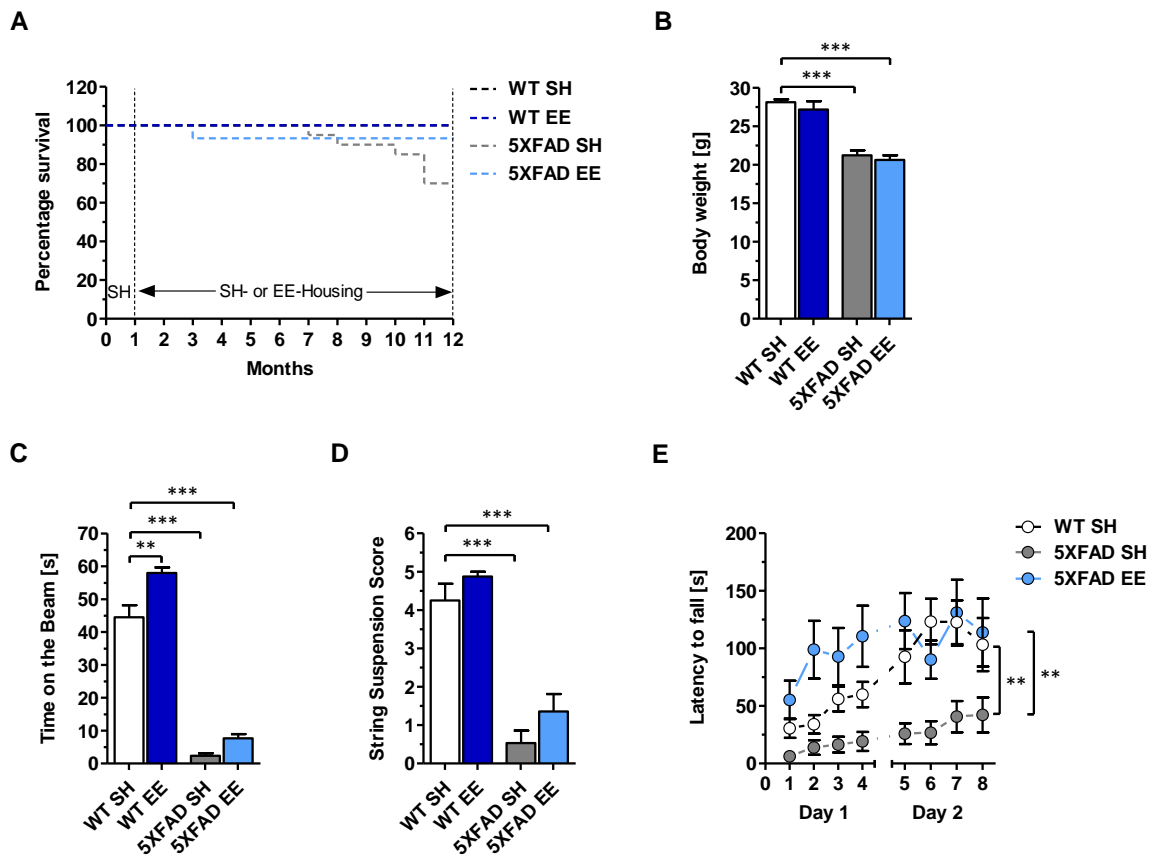


Figure 21: The effect of EE and physical activity on the survival, body weight and sensory-motor performance of 5XFAD mice. (A) Kaplan-Meier survival curve of WT and 5XFAD mice housed under standard or enriched living conditions. All WT SH and EE mice survived the entire paradigm. 5XFAD SH mice showed a premature death phenotype when compared to WT SH mice. Enriched housed 5XFAD displayed a tendency towards a better survival compared to 5XFAD SH mice which, however, did not reach statistical significance (B) Housing conditions had no effect on the significantly reduced body weight of 12-month-old 5XFAD mice. (C-E) The combination of EE and physical activity had limited effects on the sensory-motor performance of 5XFAD mice. The balance beam (C) and string suspension test (D) showed no improvement in enriched housed 5XFAD mice compared to sedentary controls. The rotarod test (E) revealed a rescue of the phenotype as 5XFAD EE mice stayed significantly longer on the rod when compared to 5XFAD SH mice. (A): Log-rank test. (B-D): One-way ANOVA followed by Bonferroni multiple comparisons. (E): Two-way repeated measures ANOVA. $**p < 0.01$; $***p < 0.001$. All data were given as means \pm standard error of the mean (SEM). $n = 7-16$ per group.

3.1.2.2 Environmental enrichment fails to restore decreased anxiety levels and spatial working memory deficits in 5XFAD mice

5XFAD mice show significantly reduced levels of anxiety in comparison to WT mice starting at the age of 6 months (Jawhar et al., 2012). To investigate whether this phenotype can be modulated by enriched living conditions, the elevated plus maze test

was performed. 12-month-old 5XFAD SH mice displayed abnormally low levels of anxiety as shown by a significantly higher time spent in open arms compared to WT SH mice, which was not influenced by prolonged enriched living conditions (One-way ANOVA, $p < 0.001$ respectively). Housing under enriched conditions did not affect the anxiety phenotype of WT animals (Figure 22A). The number of arm entries did not differ among the groups, leading to the suggestion that reduced anxiety levels in 5XFAD SH and EE mice could not be explained by an overall decreased explorative behaviour (Figure 22B).

To investigate whether the housing condition in combination with physical activity affects hippocampus-related spatial working memory, mice were tested in the cross maze task. As previously published, 12-month-old 5XFAD SH mice displayed a significantly impaired spatial working memory compared to age-matched wild-type controls (One-way ANOVA, $p < 0.05$). Enriched housed 5XFAD animals did not show an amelioration in spontaneous alternation behaviour when compared to sedentary controls as they still performed significantly worse than WT SH mice (One-way ANOVA, $p < 0.01$). Housing condition also had no effect on spatial working memory in WT animals (Figure 22C). Again, all analysed groups showed equal numbers of total arm entries indicating that the reduced alternation percentage of transgenic mice was not caused by a decrease in overall explorative behaviour (Figure 22D).

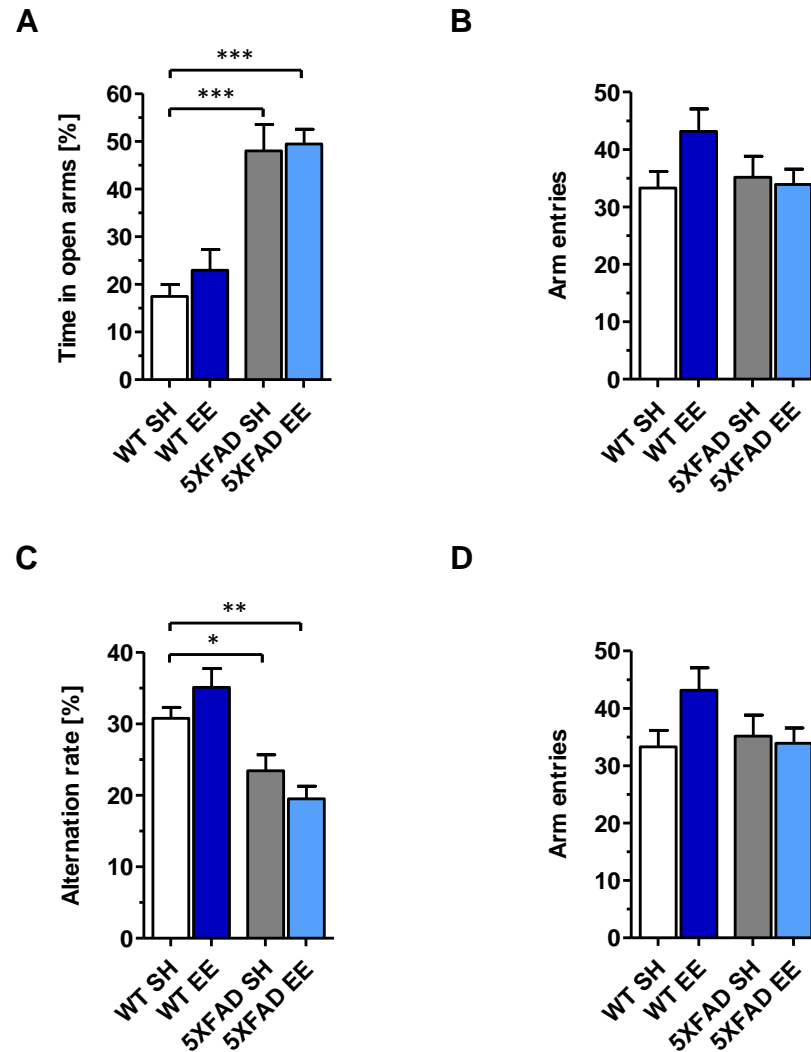


Figure 22: Anxiety-related behaviour and working memory performance in standard and enriched housed 5XFAD mice. (A) 5XFAD exhibited decreased levels of anxiety in the elevated plus maze task in both SH and EE housing conditions. Housing condition had no effect on anxiety levels of WT animals. (B) Decreased anxiety-related behaviour could not be explained by alterations in explorative behaviour, as all groups showed comparable numbers of arm entries. (C) Regarding hippocampus-related working memory, 5XFAD mice maintained under EE conditions for 11 months showed no improvement in spontaneous alternation behaviour measured in the cross maze task. (D) Again, no differences in arm entries could be detected between all analysed groups. One-way ANOVA followed by Bonferroni multiple comparisons. * $p < 0.05$; ** $p < 0.01$; *** $p < 0.001$. All data were given as means \pm standard error of the mean (SEM). $n = 7-16$ per group.

3.1.2.3 Long-term physical and cognitive stimulation does not influence amyloid plaque load and $A\beta_{1-42}$ levels in brains of 5XFAD mice

The 5XFAD model harbours a robust $A\beta$ plaque pathology in various brain areas at the age of 12 months (Oakley et al., 2006). In order to investigate if amyloid deposition is affected by enriched living conditions and physical exercise, a plaque load quantification was performed in cortex, dentate gyrus, subiculum and thalamus of

enriched and sedentary animals. Hence, immunohistochemical stainings using an anti $A\beta$ antibody to quantitatively examine $A\beta$ deposition were performed (Figure 23A). Brains of 5XFAD SH and EE mice showed a comparable $A\beta$ plaque load in all areas analysed (Figure 23B).

Using mass spectrometric analysis it has been shown that $A\beta_{1-42}$ is the most dominant $A\beta$ species in the brain of 5XFAD mice (Wittnam, 2012). To determine whether housing condition and voluntary exercise have an impact on $A\beta_{1-42}$ levels, ELISA experiments were conducted to measure $A\beta_{1-42}$ contents in TBS-soluble and insoluble (SDS soluble) brain fractions. No differences in $A\beta_{1-42}$ levels could be detected in either fraction between sedentary 5XFAD mice and enriched housed littermates (Figure 23C, D) (ELISA measurements were performed by Sandra Baches, Department of Neuropathology, Heinrich Heine University, Düsseldorf).

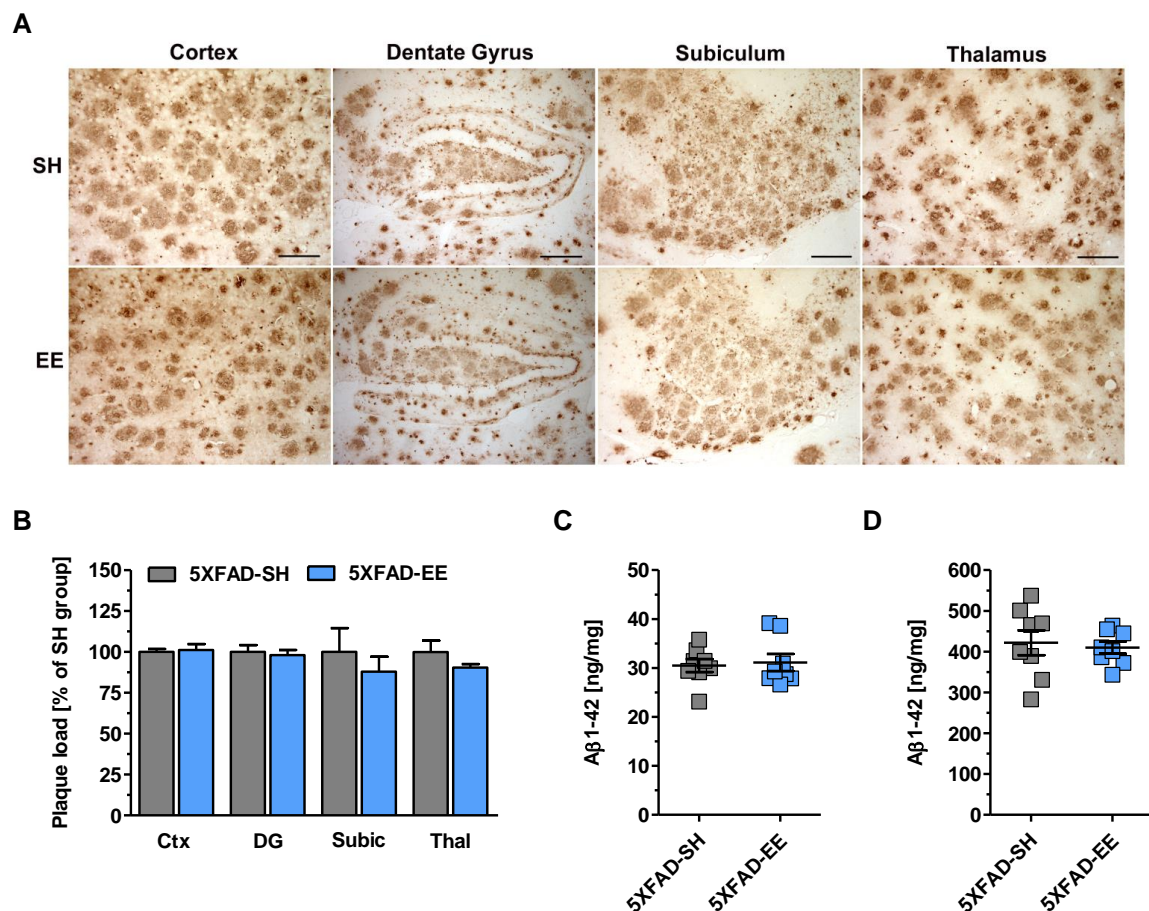


Figure 23: Housing condition has no effect on $A\beta$ plaque pathology and $A\beta_{1-42}$ levels of 5XFAD mice. (A, B) $A\beta$ plaque load in the cortex (Ctx), dentate gyrus (DG), subiculum (Subic) and thalamus (Thal) was unaffected by living conditions in 12-month-old 5XFAD mice. (C, D) Using ELISA, $A\beta_{1-42}$ levels were quantified in TBS- (C) and SDS-soluble (D) brain fractions of 5XFAD SH and EE mice. No differences could be detected in either fraction between the two groups. Unpaired t-test. All data were given as means \pm standard error of the mean (SEM). (B): n = 5 per group. (C, D): n = 8 per group.

3.1.2.4 Housing condition has no impact on the inflammatory phenotype of 5XFAD mice

5XFAD mice start to develop amyloid deposits and exhibit neuroinflammation as early as 2 months of age (Oakley et al., 2006). To determine whether long-term voluntary exercise prevents activation of inflammatory pathways, immunohistochemical stainings and subsequent quantifications with the reactive astrocyte marker GFAP were performed. No differences in GFAP signal could be detected in cortex, dentate gyrus and thalamus between standard and enriched housed 5XFAD mice with 12 months of age (Figure 24A, B).

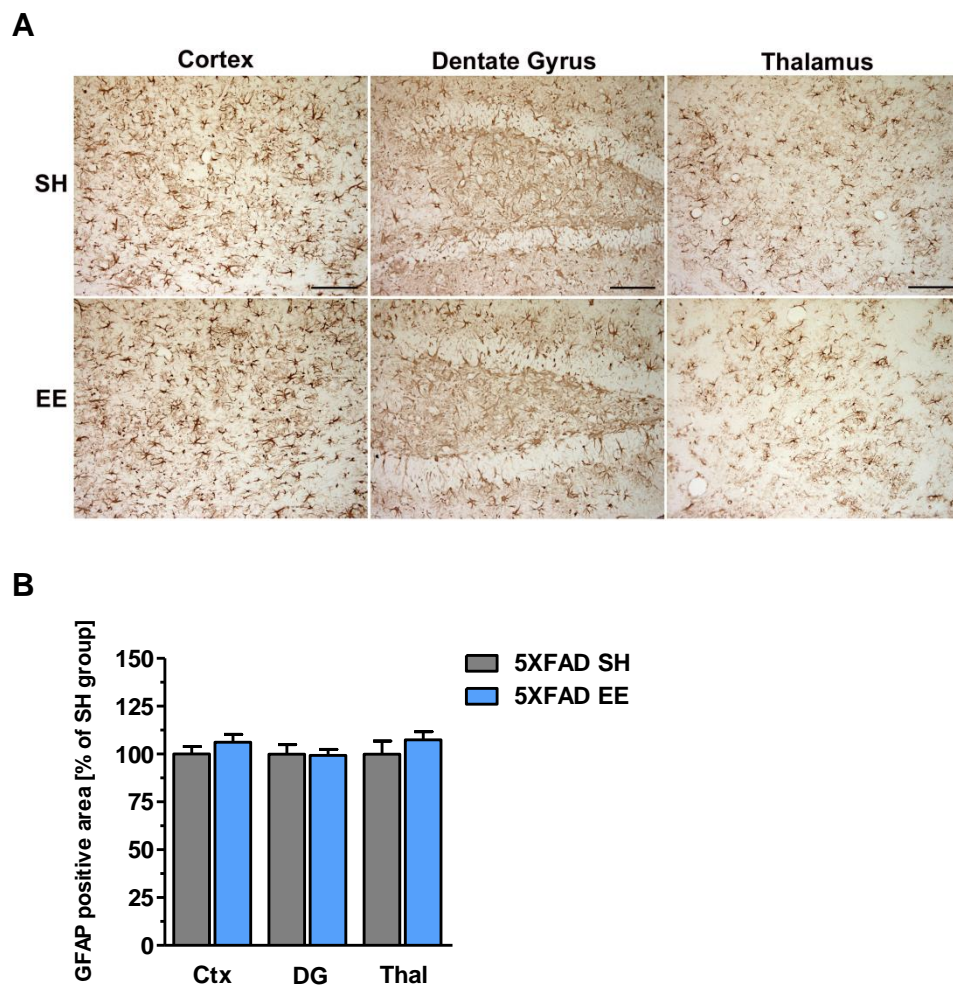


Figure 24: Housing condition has no influence on the inflammatory phenotype of 5XFAD mice. (A, B) The presence of reactive astrocytes was revealed by immunohistochemical stainings directed against the astrocytic marker GFAP and a quantification was performed in the cortex (Ctx), dentate gyrus (DG) and thalamus (Thal) of 12-month-old 5XFAD SH and EE mice. Equal levels of astrogliosis were detected between the two groups in all brain areas analysed. Unpaired t-test. All data were given as means \pm standard error of the mean (SEM). n = 5 per group. Scale bar 100 μ m.

3.1.2.5 The effect of voluntary exercise on gene expression in 5XFAD mice

To determine the effects of housing conditions on gene expression changes in 12-month-old 5XFAD mice, qRT-PCR analysis have been conducted (Figure 25). Numerous studies have shown that *BDNF* gene expression is upregulated upon EE, which could be confirmed in the present study as 5XFAD EE mice showed significantly higher levels of the neurotrophin when compared to sedentary controls (t-test, $p < 0.05$).

Proteases known to influence $A\beta$ levels in the brain like neprilysin (NEP), insulin-degrading enzyme (IDE) and BACE did not show expression level changes upon long-term environmental enrichment. However, mRNA levels of *CRYAB*, *STIP1*, *HSPA1B* and *HSP105*, which are members of the heat-shock protein family, were significantly upregulated in 5XFAD EE mice compared to 5XFAD SH animals (t-test, $p < 0.05$ and 0.01, respectively).

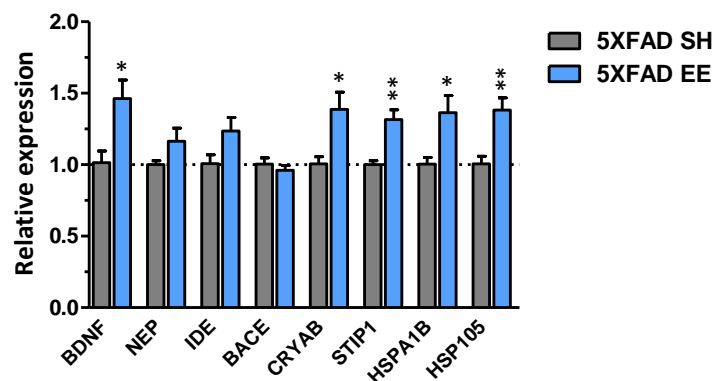


Figure 25: Gene expression changes in enriched housed 5XFAD mice. qRT-PCR analysis of RNA isolated from brain hemispheres revealed significant upregulated levels of *BDNF*, *CRYAB*, *STIP1*, *HSPA1B* and *HSP105* in enriched housed 5XFAD mice compared to sedentary controls. Expression levels of *NEP*, *IDE* and *BACE* were not changed by housing conditions. Normalization was performed against the house-keeping gene actin. Unpaired t-test. ** $p < 0.01$; * $p < 0.05$. All data were given as means \pm standard error of the mean (SEM). $n = 5$ per group.

3.2 Project II: Neprilysin deficiency alters the neuropathological and behavioural phenotype in the 5XFAD mouse model of Alzheimer's disease

3.2.1 Characterization of 5XFAD/NEP^{+/-} mice

In order to evaluate the effect of a reduction of the neprilysin (NEP) gene doses, NEP mRNA expression levels were analysed in 2.5- and 6-month-old WT, 5XFAD, 5XFAD/NEP^{+/-}, NEP^{+/-} and NEP^{-/-} animals using qRT-PCR. Interestingly, young 5XFAD mice showed significantly reduced NEP levels compared to WT mice (t-test, $p < 0.05$), which were further reduced in 5XFAD/NEP^{+/-} mice (t-test, $p < 0.001$ compared to WT and 5XFAD). NEP^{+/-} mice displayed levels comparable to 5XFAD mice at 2.5 month of age (Figure 26A). Neprilysin expression in 6-month-old 5XFAD mice was reduced when compared to WT mice, however, without reaching statistical significance. A hemizygous NEP knock-out led to a further significant reduction compared to 5XFAD mice (t-test, $p < 0.05$). Compared to WT mice, 5XFAD/NEP^{+/-} showed a drastically reduced NEP expression, reaching less than 10% of WT levels (t-test, $p < 0.001$, Figure 26B). In 2.5- as well as 6-month-old NEP^{-/-} animals, no neprilysin expression could be detected.

The successful NEP depletion was also confirmed using immunohistochemistry with an antibody against NEP. Compared to WT mice, 5XFAD and 5XFAD/NEP^{+/-} mice showed a strongly reduced immunoreactivity, which was most prominent in the area of the dentate gyrus, with an absent signal in NEP^{-/-} animals (Figure 26C).

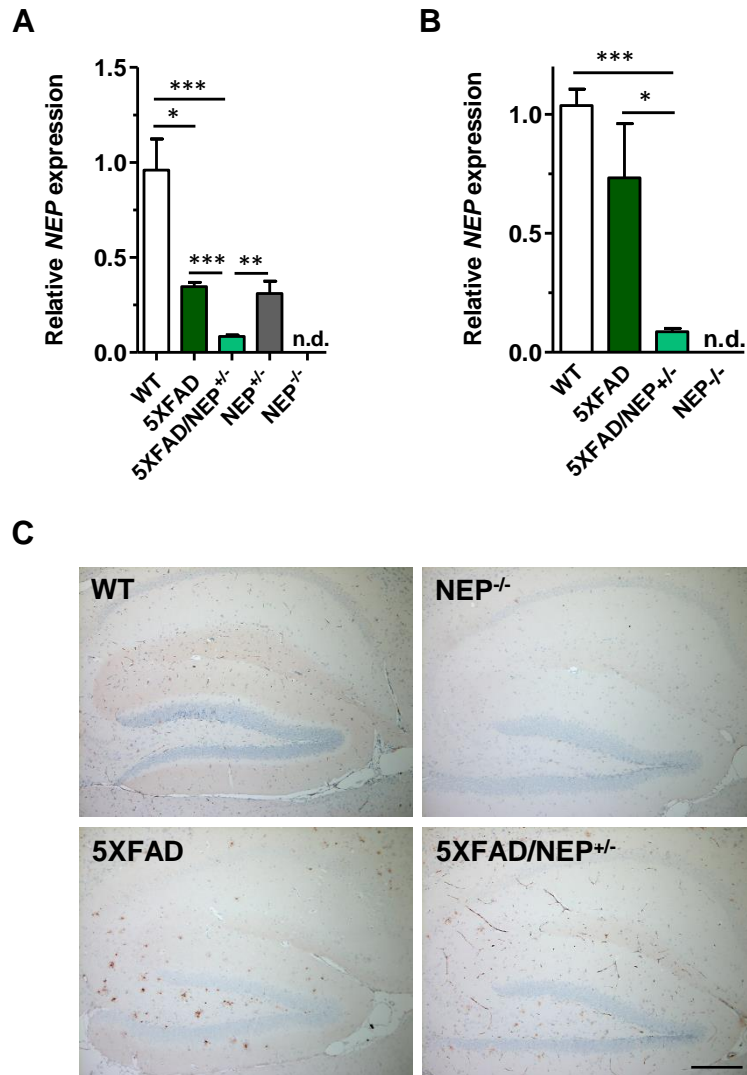


Figure 26: Neprilysin mRNA and protein levels. (A) qRT-PCR analysis revealed that 5XFAD mice displayed significantly reduced neprilysin (NEP) mRNA levels compared to WT mice at 2.5 months of age, which were even further decreased in 5XFAD/NEP^{+/-} mice. NEP^{+/-} mice showed comparable NEP levels like 5XFAD mice while in NEP^{-/-} animals, expression of the enzyme was not detectable. (B) In 6-month-old 5XFAD mice, NEP levels were still reduced when compared to WT mice without reaching statistical significance. 5XFAD/NEP^{+/-} mice showed drastically reduced NEP levels compared to WT and 5XFAD mice. Again, no detectable expression of NEP was seen in NEP^{-/-} mice. (C) Immunostaining in the hippocampus using an antibody against NEP (56C6, Santa Cruz) showed a clear NEP signal in WT mice, a strongly reduced immunoreactivity in 5XFAD and 5XFAD/NEP^{+/-} and an absent signal in NEP^{-/-} mice. One-way ANOVA followed by unpaired t-test. * $p < 0.05$; ** $p < 0.01$; *** $p < 0.001$. All data were given as means \pm standard error of the mean (SEM). $n = 3-5$. Scale bar: 200 μm

3.2.2 The effect of neprilysin deficiency on the spatial working memory performance of 5XFAD mice

To assess the effect of neprilysin knock-out on spatial working memory performance, Y-Maze and cross maze tasks were performed. No significant differences in alternation rates or arm visit frequencies were noted between the different genotypes in 2.5-

month-old animals in both tests (data not shown). In the Y-Maze, 6-month-old 5XFAD mice displayed alternation rates comparable to WT mice. However, age-matched 5XFAD/NEP^{+/-} mice performed significantly worse when compared to WT (t-test, $p < 0.01$), 5XFAD (t-test, $p < 0.001$), NEP^{+/-} (t-test, $p < 0.01$) and NEP^{-/-} (t-test, $p < 0.01$) animals (Figure 27A). The reduced alternation percentage of 5XFAD/NEP^{+/-} mice was not due to a decreased explorative behaviour as the number of arm entries did not differ among the groups (Figure 27B).

In the cross maze task, 6-month-old 5XFAD mice showed a tendency towards a reduced performance when compared to WT mice (t-test, $p < 0.0835$). 5XFAD/NEP^{+/-} mice displayed alternation rates only reaching chance level (dotted line) being significantly different from WT animals (t-test, $p < 0.01$) or NEP^{+/-} mice (t-test, $p < 0.05$). Compared to 5XFAD mice, 5XFAD/NEP^{+/-} animals showed a trend towards a reduced performance (t-test, $p < 0.082$, Figure 27C). Again, the number of total arm entries did not significantly differ among the analysed groups in this task (Figure 27D).

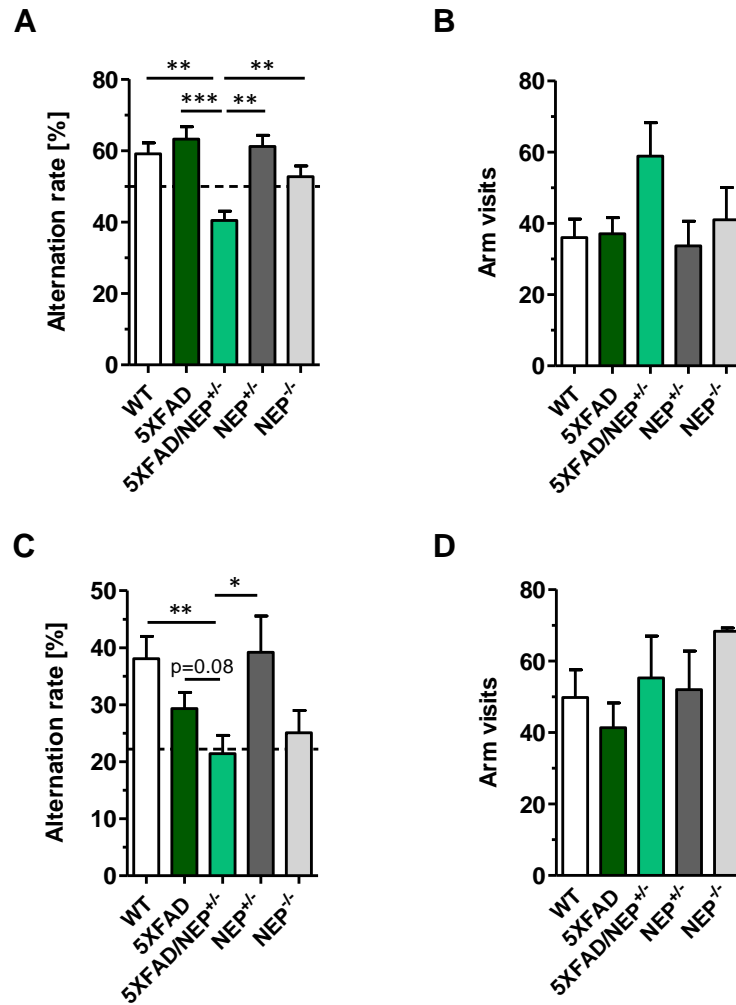


Figure 27: Spatial working memory performance of 5XFAD mice upon NEP depletion. (A) 5XFAD mice showed no impairment in spatial working memory performance at 6 months of age when compared to WT controls in the Y-Maze task. However, 5XFAD/NEP^{+/-} mice displayed a reduced working memory performance compared to WT, 5XFAD, NEP^{+/-} and NEP^{-/-} mice. (C) In the cross maze task, 5XFAD mice showed a tendency towards a reduced alternation rate compared to WT mice, which only reached significance upon hemizygous NEP depletion. (B, D) The observed impairments of 5XFAD/NEP^{+/-} mice in the Y- and cross maze task were not due to overall reduced exploratory behaviour as shown by equivalent number of arm entries in all groups in both tests. One-way ANOVA followed by unpaired t-test. * $p < 0.05$; ** $p < 0.01$; *** $p < 0.001$. All data were given as means \pm standard error of the mean (SEM). $n = 3-10$.

3.2.3 Region-specific increase in extracellular A β plaque load in aged 5XFAD/NEP^{+/-} mice

5XFAD mice display extracellular A β deposition in various brain areas starting with 2 months of age. To analyse whether neprilysin deficiency aggravates A β plaque pathology, plaque load was quantified in the cortex, dentate gyrus, subiculum, thalamus and spinal cord of 6-month-old 5XFAD and 5XFAD/NEP^{+/-} animals using the 4G8 antibody detecting a central A β epitope. In cortex and thalamus, no differences in

plaque load could be detected between the two groups. In contrast, 5XFAD/NEP^{+/-} mice displayed a significant increase in the overall plaque load in both dentate gyrus (+32%; t-test, $p < 0.05$) and subiculum (+40%; t-test, $p < 0.01$) when compared to 5XFAD mice (Figure 28A, B). Accordingly, plaque load quantification in the cervical spinal cord showed a related finding with significantly increased A β plaque deposition in 5XFAD/NEP^{+/-} compared to 5XFAD mice (+74%; t-test, $p < 0.05$, Figure 28D).

A fluorescent Thioflavin S staining was performed to analyse extracellular amyloid- β deposits with β -sheet structures. However, no statistical differences were detected in any of the analysed brain regions between 5XFAD and 5XFAD/NEP^{+/-} mice (Figure 28C).

Protein quantification of A β ₁₋₄₀ and A β ₁₋₄₂ levels in whole brain lysates of 6-month-old 5XFAD and 5XFAD/NEP^{+/-} mice revealed significantly increased A β ₁₋₄₂ levels in the TBS-soluble fraction of 5XFAD/NEP^{+/-} animals (t-test, $p < 0.05$), while A β ₁₋₄₀ levels were comparable between both groups (Figure 28E). Similar A β ₁₋₄₀ and A β ₁₋₄₂ levels were also detected in the SDS-soluble fraction of 5XFAD and age-matched 5XFAD/NEP^{+/-} brain lysates (Figure 28F) (ELISA measurements were performed by Sandra Baches, Department of Neuropathology, Heinrich Heine University, Düsseldorf).

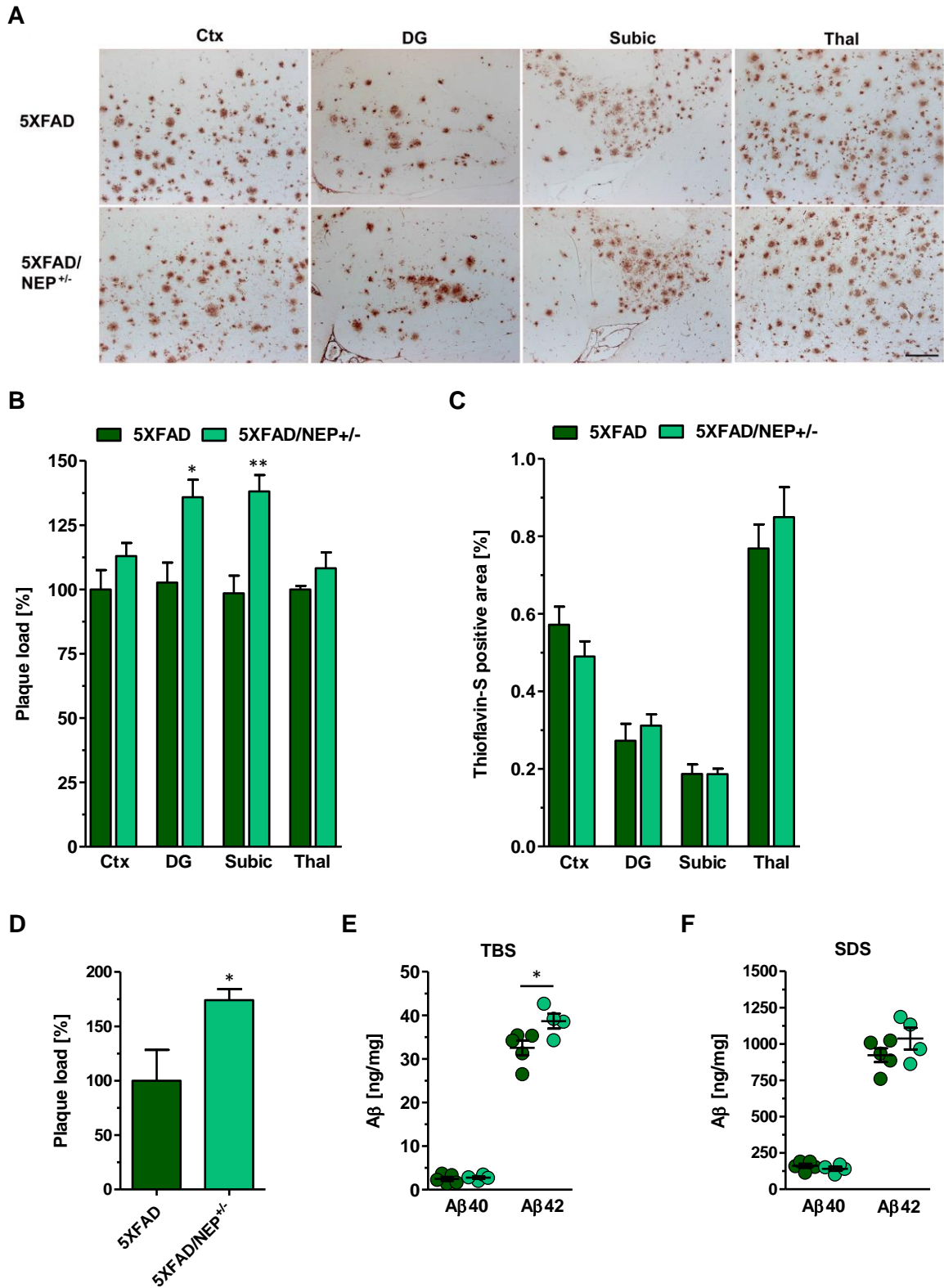


Figure 28: Aβ plaque deposition and Aβ₁₋₄₂ level in 6-month-old 5XFAD and 5XFAD/NEP^{+/-} mice. (A, B) Immunohistochemical staining against Aβ (A) using a pan-Aβ antibody (4G8, detecting Aβ₁₇₋₁₄) and quantification (B). An increased amyloid plaque pathology was detected in the dentate gyrus (DG) and subiculum (Subic) in 5XFAD/NEP^{+/-} mice compared to 5XFAD controls. No changes were seen in cortex (Ctx) and thalamus (Thal). (C) Quantification of Thioflavin-S-positive deposits showed no difference between the two groups in all brain areas analysed. (D) Staining with the 4G8 antibody against Aβ showed significantly increased plaque pathology in the cervical spinal cord of 6-month-old

5XFAD/NEP^{+/-} mice. **(E)** 6-month-old 5XFAD/NEP^{+/-} mice showed significantly increased soluble A β ₁₋₄₂ levels while A β ₁₋₄₀ levels were unchanged in the TBS fraction. **(F)** In SDS-soluble fractions, no changes in A β ₁₋₄₀ or A β ₁₋₄₂ levels were detected between 5XFAD and 5XFAD/NEP^{+/-} mice. Unpaired t-test. * $p < 0.05$; ** $p < 0.01$. All data were given as means \pm standard error of the mean (SEM). n = 4-5 per group. Scale bar: 100 μ m.

3.2.4 Increased astrocytosis in 5XFAD/NEP^{+/-} mice

To assess if the knock-out of neprilysin aggravates the inflammatory response in 5XFAD mice, immunohistochemical stainings and quantification of astrogliosis were carried out in different brain regions in 6-month-old 5XFAD and 5XFAD/NEP^{+/-} mice using an antibody against GFAP. 5XFAD mice lacking one NEP allele showed more abundant astrogliosis in the dentate gyrus (+39%; t-test, $p < 0.05$), cortex (+30%; t-test, $p < 0.05$) and thalamus (+23%; t-test, $p < 0.01$) (Figure 29A, B).

qRT-PCR analysis revealed 6- to 7-fold increased *GFAP* mRNA levels in 6-month-old 5XFAD and 5XFAD/NEP^{+/-} mice when compared to WT and NEP^{-/-} animals. However, no significant difference could be determined between 5XFAD and 5XFAD/NEP^{+/-} mice (Figure 29D). At the age of 2.5 months, only 5XFAD mice displayed significantly increased *GFAP* mRNA levels compared to WT (t-test, $p < 0.01$), 5XFAD/NEP^{+/-} (t-test, $p < 0.05$), NEP^{+/-} (t-test, $p < 0.05$) and NEP^{-/-} mice (t-test, $p < 0.01$) (Figure 29C).

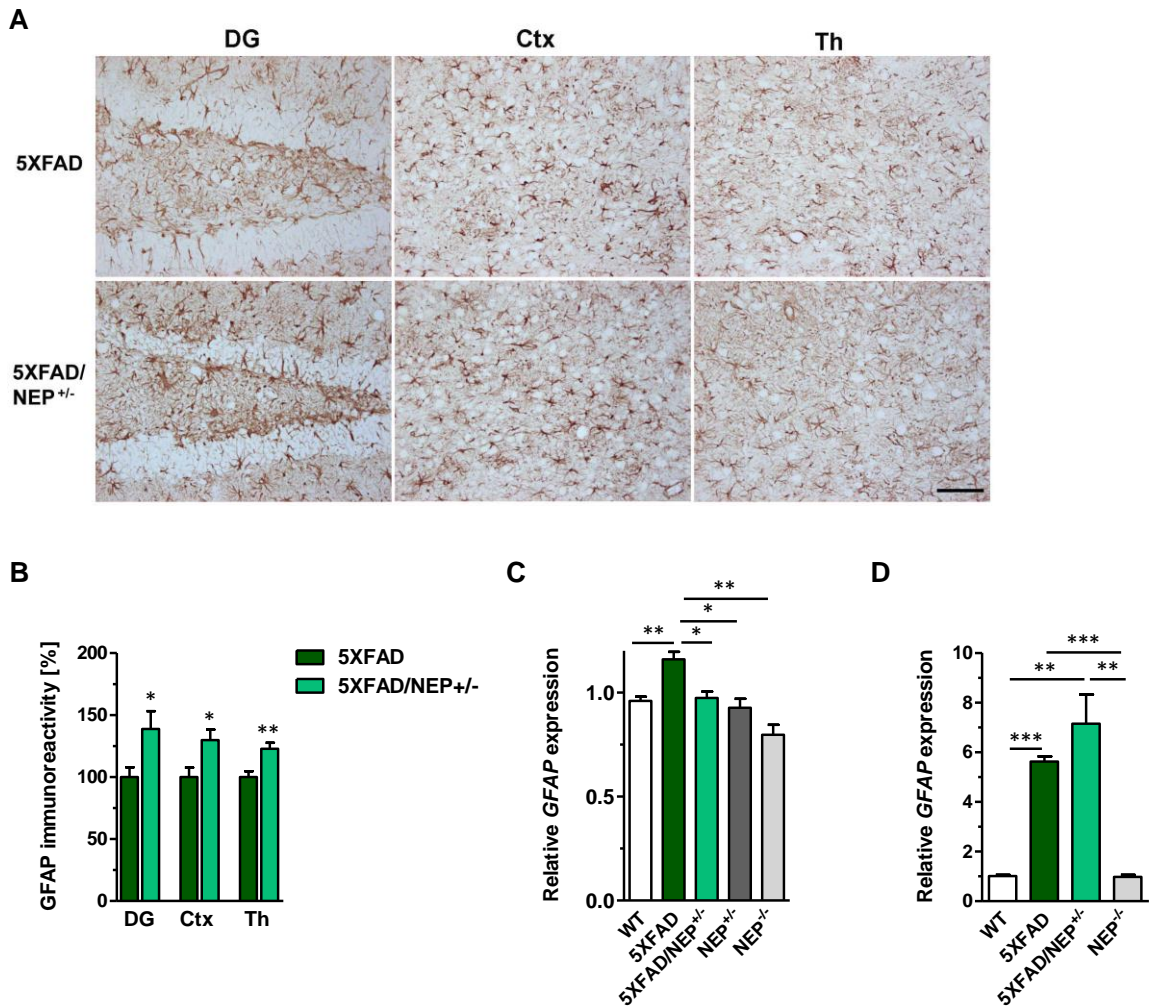


Figure 29: Inflammation status of 6-month-old 5XFAD and 5XFAD/NEP^{+/-} mice. (A, B) Using an antibody against the astrocytic marker GFAP, 5XFAD/NEP^{+/-} mice showed significantly elevated numbers of reactive astrocytes in the dentate gyrus (DG), cortex (Ctx) and thalamus (Th) compared to age-matched 5XFAD mice. (C) At 2.5 months of age, GFAP mRNA levels were significantly increased in 5XFAD mice compared to WT, 5XFAD/NEP^{+/-}, NEP^{+/-} and NEP^{-/-} mice. (D) GFAP levels strongly increased at 6 months of age in both 5XFAD and 5XFAD/NEP^{+/-} animals when compared to WT and NEP^{-/-} controls. (B): Unpaired t-test. (C, D): One-way ANOVA followed by unpaired t-test. * $p < 0.05$; ** $p < 0.01$; *** $p < 0.001$. All data were given as means \pm standard error of the mean (SEM). (B): $n = 5$ per group. (C, D): $n = 3$ per group. Scale bar: 50 μm .

3.2.5 Amyloid pathology in young 5XFAD/NEP^{+/-} mice

We were interested to assess whether an increased A β plaque pathology upon NEP depletion could be detected already at earlier time-points. Hence, young 5XFAD and 5XFAD/NEP^{+/-} mice at 2.5 months of age were analysed with regard to extracellular amyloid deposition. As expected, at an age of 2.5 months, the abundance of amyloid plaques was strongly decreased in both groups when compared to 6-month-old mice. Due to the brain-wide low abundance, plaque quantification was only possible in the cortex of young animals, where 5XFAD/NEP^{+/-} mice revealed a significantly reduced

amyloid deposition compared to age-matched 5XFAD mice (-69%; t-test, $p < 0.01$, Figure 30A-C).

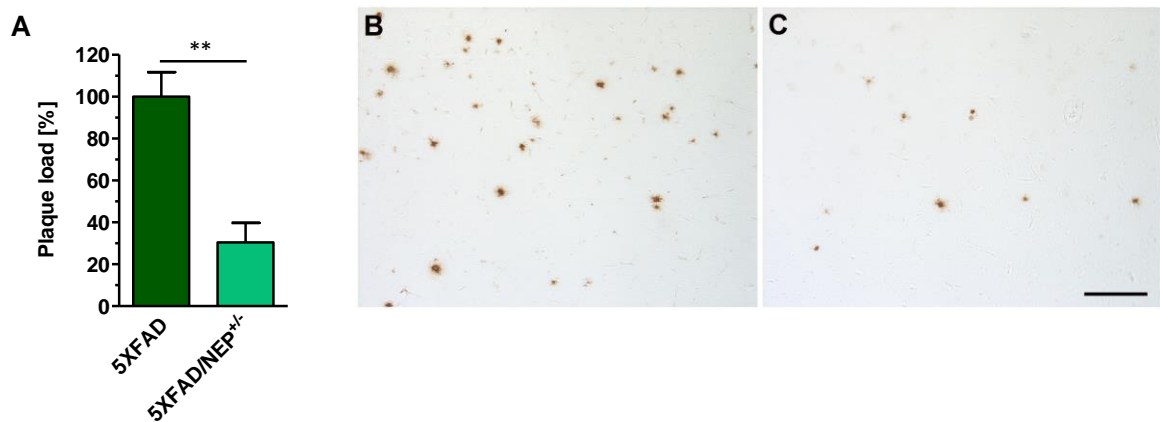


Figure 30: A β plaque load quantification in 2.5-month-old 5XFAD and 5XFAD/NEP^{+/-} mice. (A-C) Immunohistochemical stainings using a pan-A β antibody (4G8) revealed a strongly reduced plaque load in young 5XFAD/NEP^{+/-} mice (C) compared to age-matched 5XFAD mice (B). Unpaired t-test. ** $p < 0.01$. All data were given as means \pm standard error of the mean (SEM). $n = 4$ per group. Scale bar 50 μm .

3.2.6 A β -degrading enzyme expression in 5XFAD and 5XFAD/NEP^{+/-} mice

To explore the finding of a reduced plaque load in young 5XFAD/NEP^{+/-} mice in more detail, the expression levels of additional proteases known to be capable of A β degradation were measured in young and aged mice (Figure 31A, B). Young 5XFAD mice displayed significantly upregulated levels of insulin-degrading-enzyme (IDE) compared to both WT (t-test, $p < 0.05$) and 5XFAD/NEP^{+/-} mice (t-test, $p < 0.01$). No difference in IDE expression levels could be detected between 6-month-old 5XFAD and 5XFAD/NEP^{+/-} mice. Interestingly, the expression levels of endothelin-converting enzyme 1 (ECE1) were significantly increased in 5XFAD/NEP^{+/-}, NEP^{+/-} and NEP^{-/-} mice when compared to WT and 5XFAD mice at the 2.5-month-time point. However, no differences could be measured between the different genotypes at 6 months of age. Additional members of A β -degrading enzymes like angiotensin-converting enzyme (ACE) or endothelin-converting enzyme 2 (ECE2) did not show any differences in expression levels between groups of young or aged mice of either genotype.

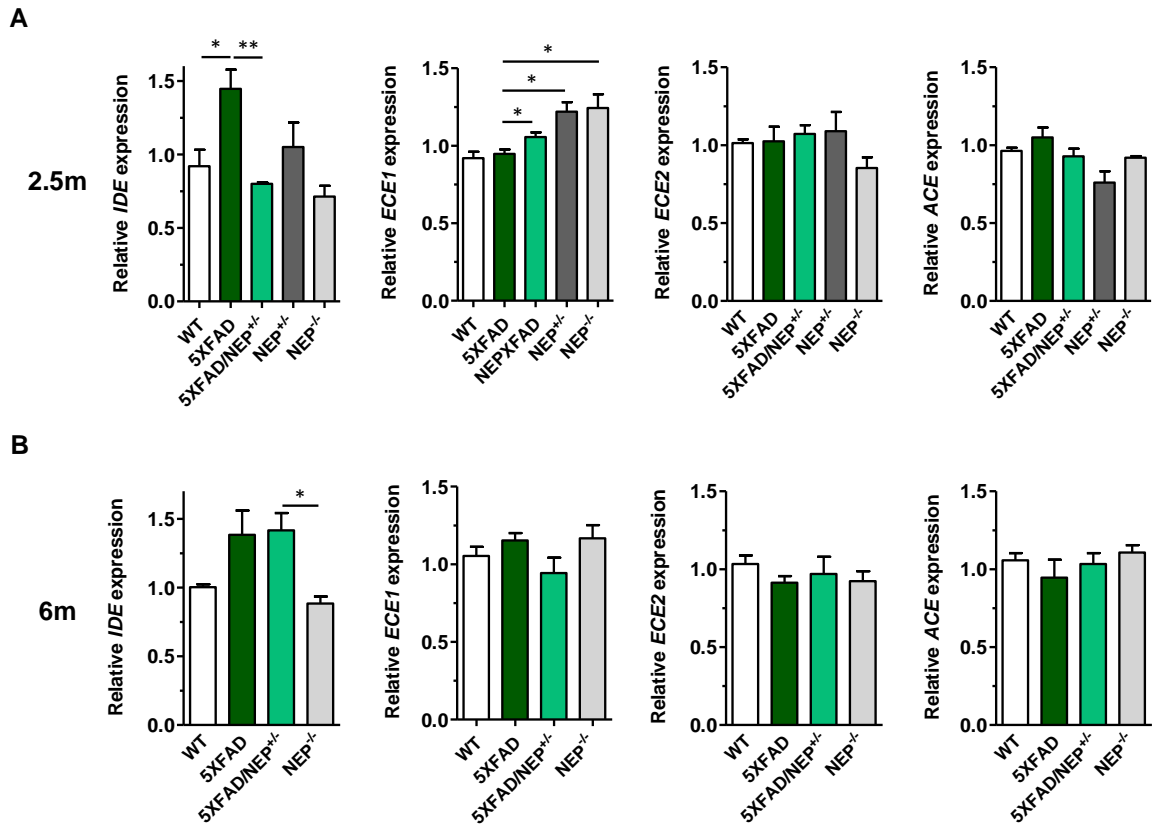


Figure 31: Expression analysis of A β -degrading enzymes. (A, B) IDE expression was significantly elevated in young 5XFAD mice, whereas 5XFAD and 5XFAD/NEP^{+/-} mice had similar levels at 6 months of age. Young 5XFAD/NEP^{+/-} mice showed significantly increased ECE1 levels compared to 5XFAD mice which did not differ at 6 months of age. Neither ECE2 nor ACE levels were significantly different among the analysed genotypes at 2.5 or 6 months of age. One-way ANOVA followed by unpaired t-test. * $p < 0.05$; ** $p < 0.01$. All data were given as means \pm standard error of the mean (SEM). $n = 3-5$ per group.

4 DISCUSSION

4.1 Project I: The effect of long-term environmental enrichment and physical activity on the pathology of Tg4-42 and 5XFAD mice

4.1.1 Part I: Enriched living conditions and physical activity delays hippocampal neurodegeneration and rescues memory deficits in the Tg4-42 mouse model of Alzheimer's disease

4.1.1.1 Improved sensory-motor performance in enriched housed Tg4-42^{het} mice

Next to cognitive symptoms like impaired memory or aphasia, an increasing number of reports have associated non-cognitive symptoms like loss of motor function with the progression of AD (Buchman and Bennett, 2011). Even though motor impairments are particularly present in late stages of AD, deficits have also been reported in early stage patients (Scarmeas et al., 2004). However, previous studies characterizing the novel Tg4-42 model have shown no alterations in measures of general motor activity when compared to WT mice, although A β pathology has been found in the spinal cord of 12-month-old animals (Wittnam, 2012). The absence of motor impairment could be largely validated in the present study as sedentary Tg4-42^{het} mice performed similar to WT controls in the balance beam and rotarod tests, which evaluate fine motor coordination and balance (Luong et al., 2011; Brooks et al., 2012) (Figure 12A, C). However, in the string suspension task, testing motor coordination as well as grip and muscle strength, Tg4-42^{het} mice showed an impaired performance compared to WT animals (Figure 12B). Intriguingly, Tg4-42^{het} mice exposed to an enriched environment exhibited a significant improved motor performance in all implemented tasks relative to standard housed controls (Hüttenrauch et al., 2016). Hence, the impaired performance of Tg4-42^{het} mice in the string suspension test could be completely rescued (Figure 12B). These observations are in accordance with recent studies in AD patients indicating beneficial effects of exercise on their physical performance and mobility (Pitkälä et al., 2013) as well as numerous analyses in rodents showing an improved general locomotor activity upon enriched living conditions (Cotel et al.,

2012;Ohia-Nwoko et al., 2014). Even though the increased motor performance of WT EE mice in comparison to standard housed controls did not reach statistical significance in the present study, an enhanced motor coordination has also been observed in physically active, healthy WT mice compared to their sedentary counterparts (Marlatt et al., 2012). Therefore, it is suggestive that this effect is independent of the genotype but rather a general consequence of the complex naturalistic motor stimulation induced through an environmental enrichment consisting of running, balancing and climbing. This is further corroborated by studies showing that enriched housing induces multiple morphological changes in brain areas coordinating motor function, such as an increased branching of dendritic trees in cortical pyramidal neurons, an enhanced size and arborisation of Purkinje cells as well as increased number of associated synapses (Uylings et al., 1978;Black et al., 1990). In conclusion, long-term enriched living conditions in combination with voluntary exercise led to an enhanced motor coordination of Tg4-42^{het} mice, corroborating an effective interaction with the environmental enrichment paradigm used in this study.

4.1.1.2 Voluntary exercise decelerates CA1 neuron loss in Tg4-42 mice

One of the major hallmarks of AD progression is severe hippocampal atrophy caused by neuron death (Carter and Lippa, 2001). To date, only a small number of AD mouse models display a reliable hippocampal neuron loss (Wirths and Bayer, 2010). Interestingly, Tg4-42 mice develop an age- and gene dose-dependent neuron loss in the CA1 layer of the hippocampus. The neuron loss strongly correlates with intraneuronal A β ₄₋₄₂ accumulation and reaches approximately 51% in hemizygous animals at the age of 12 months (Bouter et al., 2013). In comparison, homozygous Tg4-42 mice display a neuron loss of approximately 50% with 6 months of age (Antonios et al., 2015). The precise mechanisms by which A β , and specifically A β ₄₋₄₂, generates its toxicity are currently not known in detail. Former studies have shown that A β oligomers modulate pre- and postsynaptic structures and functions, thereby blocking long-term potentiation (LTP) (Haass and Selkoe, 2007). It has been further proposed that A β ₁₋₄₂ oligomers cause dysfunction of the metabotropic glutamate receptor 5 (mGluR5) by triggering cell surface receptor clustering near or within synapses (Renner et al., 2010). Glabe and Kaye have shown that A β oligomers lead to membrane permeabilization resulting in the initiation of a common group of

downstream pathological processes. These processes incorporate calcium dyshomeostasis, altered signaling pathways, production of reactive oxygen species (ROS) and mitochondrial dysfunction which ultimately lead to cellular dysfunction and neuron death (Glabe and Kaye, 2006). In the current thesis, stereological analyses revealed that long-term cognitive and physical stimulation significantly diminished the CA1 neuron loss in Tg4-42 mice (Hüttenrauch et al., 2016). Tg4-42^{het} mice maintained under enriched conditions with continuous access to running wheels showed a 12.8% higher number of CA1 pyramidal cells when compared to sedentary controls (Figure 15A). As one can not dissect whether the effect on neuron loss can be attributed to the EE paradigm, voluntary exercise or a combination of both, a control experiment using singly housed mice in cages equipped with blocked or free running wheels was performed employing homozygous Tg4-42 mice (Tg4-42^{hom}). Like Tg4-42^{het} mice, physically active Tg4-42^{hom} mice displayed significantly increased CA1 neuron numbers compared to mice housed in blocked wheel cages (Figure 20C). Therefore, it can be hypothesized that physical activity alone is sufficient to attenuate the pathological events triggering neuronal cell death (Hüttenrauch et al., 2016). Several studies support this hypothesis (Kobilo et al., 2011), however, without providing quantitative evidence using unbiased, design-based stereology. Um and colleagues showed that treadmill exercise for 12 weeks led to a decreased number of TUNEL-positive cells in the hippocampus of Tg-NSE/PS2m mice, concluding that neuronal cell death in the hippocampus could be markedly decreased due to physical activity (Um et al., 2011). Moreover, Tapia-Rojas and colleagues recently investigated the effect of 10 weeks of voluntary wheel running on hippocampal neuron numbers in the APP^{swe}/PS1 Δ E9 mouse model. The number of neurons was assessed by Nissl staining and subsequent manual counting of cells present in different hippocampal zones. Compared to WT mice, 7-month-old APP^{swe}/PS1 Δ E9 displayed significantly less neurons in the CA1-CA2, CA3 and dentate gyrus. After running, cell loss could be partially prevented in the CA3 and dentate gyrus, but not in the CA1 region (Tapia-Rojas et al., 2015). All of these studies indicate that physical activity can activate processes in the brain that lead to a better survival of neurons. The possible mechanistic links between exercise and its neuroprotective effect will be discussed in one of the next sections.

4.1.1.3 Prolonged physical activity prevents the cognitive decline in Tg4-42^{het} mice

The hippocampal expression of A β ₄₋₄₂ and the severe CA1 neuron loss correlate well with spatial reference memory deficits in Tg4-42 mice. Tg4-42^{het} mice display significant deficits with 12 months of age (Bouter et al., 2013), while homozygous animals develop comparable deficiencies with 6 months of age (Antonios et al., 2015). As mentioned earlier, both genotypes reveal a neuron loss of approximately 50% at that age. Former studies have assessed the cognitive decline in Tg4-42 mice using the Morris water maze (MWM) paradigm, a key method in the investigation of behavioural alterations due to changes in hippocampal circuitry (Morris, 1984). The MWM enables to distinguish between spatial learning, which is assessed by repeated trials in the acquisition training, and long-term spatial reference memory, evaluated by the preference for the platform quadrant when the platform is removed during the probe trial (Vorhees and Williams, 2006). Confirming previous studies, spatial memory was not impaired in the acquisition training in 12-month-old Tg4-42^{het} SH mice compared to WT controls in the present study. However, an improved spatial learning upon long-term physical activity was detected in both WT and Tg4-42^{het} mice when compared to their sedentary counterparts, respectively, indicating a general beneficial effect of the enriched environment independent from the genotype (Figure 13B). The lack of a quadrant preference in the probe trial validated the previously reported spatial reference memory deficits in 12-month-old Tg4-42^{het} SH mice (Figure 13E). Even though the MWM performance has been shown to be specifically sensitive to hippocampal function, lesions in other brain regions like entorhinal and perirhinal cortices, prefrontal cortex, cingulate cortex and neostriatum can influence the outcome of the test as well (D'Hooge and De Deyn, 2001). However, as Tg4-42 mice show A β ₄₋₄₂ immunoreactivity predominantly in the CA1 region of the hippocampus, it is suggestive that the toxic action of the N-truncated peptide and the accompanied neuron loss in this specific area mainly account for the observed memory impairment. Within the scope of this thesis, it could be demonstrated that in addition to a delayed CA1 neuron loss, spatial reference memory deficits in Tg4-42^{het} mice can be completely prevented by long-term physical and cognitive stimulation (Hüttenrauch et al., 2016). 12-month-old Tg4-42^{het} animals maintained under enriched living conditions displayed a preserved memory performance comparable to healthy wild-type mice (Figure 13E).

This finding is in line with recent clinical data claiming that aerobic fitness improves the memory performance of healthy individuals and patients with mild cognitive impairment (Etnier et al., 2007; Nagamatsu et al., 2013; Makizako et al., 2014). Moreover, beneficial effects of long-term exercise on memory task performance have been detected in other rodent AD models (Adlard et al., 2005; Verret et al., 2013; Rao et al., 2015). However, in the present study, the preserved memory capacity of active Tg4-42^{het} mice might be explained by the diminished hippocampal neurodegeneration and is in good agreement with data from Antonios and colleagues. They have shown that a 13% increase in CA1 neuron numbers upon immunization with an antibody targeting N-truncated A β was sufficient to rescue functional spatial reference memory in Tg4-42^{hom} mice at 6 months of age (Antonios et al., 2015). The fact that only moderate increases in CA1 neuron numbers, either due to physical activity as in the current study or a therapeutic approach by Antonios et al., can preserve memory in this mouse model, supports the findings of Broadbent and colleagues, who studied the relationship of hippocampal lesion size and spatial memory performance in rats (Broadbent et al., 2004). They claim that after bilateral dorsal hippocampal lesions that encompass 30-50% of the total volume, impairments in spatial memory start to be apparent. However, when lesion size increased from 50-100%, memory performance worsens dramatically. Therefore, it can be hypothesized that a certain percentage of hippocampal neuron loss can be compensated, while a loss of 50% and more seems to be critical for learning and memory performance. This is supported by the fact that 5-month-old homozygous Tg4-42 mice display a 43% loss of CA1 neurons and first but mild signs of cognitive decline. With 6 months of age, the spatial reference memory deficits become significant and the CA1 neuron number is reduced to 50% (Antonios et al., 2015).

Due to an unexpected tail hyperflexion phenotype of singly housed Tg4-42^{hom} mice, the stereological data of this group could not be backed-up with MWM data. The hyperflexion broke experimenter's blindness and caused a swimming incapability. There is not much literature existing on this phenomenon, however, it has been reported that such tail transformations can occur after extensive and regular running wheel usage for periods of at least 8 weeks (Richter et al., 2014). Therefore, it cannot be ruled out that the beneficial effects on spatial reference memory performance in Tg4-42^{het} mice are attributable to a combination of the enriched environment and

voluntary exercise and not to the physical activity *per se*. To address this point, future experiments using variations in the running wheel paradigm in order to prevent the formation of the tail hyperflexion phenotype are planned.

An alternative test to examine the neural basis of memory is the novel object recognition task (NOR) (Winters et al., 2008). In contrast to the MWM, the NOR task does not evaluate spatial learning and memory, but recognition memory, which is based on the ability to recognize a previously encountered object as familiar (Squire et al., 2007). For a long time, no consensus was apparent which areas of the brain are important for recognition memory performance. Many studies supported the assumption that recognition memory depends on the integrity of the medial temporal lobe (MTL) system, a brain structure including the hippocampus, entorhinal, perirhinal and parahippocampal cortices (Squire and Zola-Morgan, 1991). However, latest studies involving rodents, non-human primates and memory-impaired patients provided strong evidence that damage limited to the hippocampus is sufficient to cause recognition memory impairments (Squire et al., 2007; Broadbent et al., 2010). Consistent with these findings, an impaired recognition memory performance could be detected in 12-month-old Tg4-42^{het} mice. This phenotype was completely reversed by housing under enriched conditions (Figure 14) (Hüttenrauch et al., 2016). O'Callaghan and colleagues already reported an exercise-related improvement of recognition memory in rats after only 7 days of forced running (O'Callaghan et al., 2007). Moreover, it has been shown that 4 months of voluntary wheel running led to an improved memory in the object recognition test in 9-month-old Tg2576 mice (Yuede et al., 2009). In summary, the findings of an amelioration of spatial reference and recognition memory deficits in enriched housed Tg4-42^{het} mice indicate that enhanced physical and cognitive activity has an overall positive effect on hippocampus-dependent memory performances, which is not task-specific.

4.1.1.4 Adult hippocampal neurogenesis is unaffected in enriched housed WT and Tg4-42^{het} mice

Adult hippocampal neurogenesis drastically decreases in rodents in an age-dependent manner (Kuhn et al., 1996). Accordingly, 12-month-old WT mice displayed only marginal levels of new-born neurons in the present study. However, Tg4-42^{het} animals showed even lower levels of neurogenesis when compared to wildtypes (Figure 16),

which is consistent with numerous AD mouse models displaying abnormal low, or even absent neurogenesis levels (Feng et al., 2001; Donovan et al., 2006). It is currently not known which mechanisms lead to the diminished production of neurons in AD models, however, one hypothesis is the inflammatory environment in diseased brains. *In vivo* data have demonstrated that new-born neurons are highly vulnerable to inflammation insults, shown by a negative correlation between their survival rate and the number of activated microglia cells (Ekdahl et al., 2003). Hence, the low neurogenesis levels in 12-month-old Tg4-42^{het} mice might be explained by the strong gliosis present in the hippocampal area due to intraneuronal A β accumulation (Bouter et al., 2013).

There is vast literature reporting that environmental enriched living conditions, and specifically physical activity, increase hippocampal neurogenesis in rodent brains (Kempermann et al., 1997; van Praag et al., 1999). Surprisingly, no difference in the number of new-born cells could be detected between sedentary and enriched housed mice in both WT and Tg4-42^{het} animals in the current work (Figure 16). This observation is contradictory to numerous studies that have linked the cognitive protection provided by EE with increased levels of subgranular neurogenesis (Kempermann et al., 1998; van Praag et al., 2000; van Praag et al., 2005). Even under deleterious conditions like chronic stress or in advanced aged animals, hippocampal neurogenesis has been shown to be restored through exposure to enriched environment (Kempermann, 2002; Veena et al., 2009). On the contrary, a study employing healthy WT mice by Meshi and colleagues strongly supports the finding of the present study. They demonstrated that a blockade of neurogenesis by exposure to focal X-ray irradiation did not prevent the beneficial effects of EE on their cognitive performance (Meshi et al., 2006). Furthermore, another report from Catlow et al. could not find a difference in the number of new-born neurons between standard and enriched housed PS1/APP mice, despite overall cognitive-enhancing effects of the enriched environment (Catlow et al., 2009). Therefore, it is suggestive that neurogenesis does not necessarily contribute to the beneficial effects induced by a stimulating environment. Consequently, the cognitive protection seen in enriched housed Tg4-42^{het} mice is independent of changes in neurogenesis levels.

4.1.1.5 Tg4-42^{het} SH and EE mice display unaltered brain A β levels

N-truncated A β ₄₋₄₂ is one of the major species in the cortex and hippocampus of AD patients and its impact on AD pathology has long been neglected (Portelius et al., 2010). The Tg4-42 model exclusively expresses N-truncated A β ₄₋₄₂ fused to the TRH signal peptide under the control of the Thy1 promoter. The accumulation of A β ₄₋₄₂ therefore correlates with the expression pattern of the neuron-specific promoter and occurs in a region-specific manner (Caroni, 1997). Intraneuronal A β is detectable starting from 2 months of age and is predominantly present in the CA1 region of the hippocampus. However, due to the massive neuron loss, intracellular A β ₄₋₄₂ reactivity declines with age, leaving mainly larger extracellular A β aggregates as remnants of disintegrated neurons by the age of 12 months (Figure 17A). This phenomenon has also been observed in human AD patients. Brain regions with an excessive intracellular A β ₄₂ accumulation showed evidence of neuronal death, resulting in the release and dispersion of the peptides to the extracellular space where they contributed to the formation of plaques (D'Andrea et al., 2001).

Improved memory performance and a reduced neuron loss in Tg4-42^{het} mice upon enriched environment was not accompanied by decreased levels of A β ₄₋₄₂ in the present study (Figure 17B) (Hüttenrauch et al., 2016). Therefore, it can be speculated that the cognitive improvement and the neuroprotective effect induced by long-term environmental and physical stimulation is not dependent on a simple reduction in A β levels. This is in contrast to many other studies on enriched environment in AD mouse models showing reduced A β levels upon continuous exercise. Rao and colleagues recently reported that environmental enrichment lowered total, soluble and insoluble A β levels in both cortex and hippocampus of active APP/PSEN1 mice while they concurrently showed an improved cognition (Rao et al., 2015). In addition, Lazarov et al. reported decreased levels of A β upon enrichment in another AD model which they explained by enhanced levels of the A β -degrading enzyme neprilysin (NEP) through long-term exercise (Lazarov et al., 2005). However, it is worth noting that a study by Costa and colleagues revealed decreased levels of A β deposition upon enrichment in double transgenic PS1/PDAPP mice without being able to correlate their cognitive performance with the A β pathology (Costa et al., 2007). This supports the finding of the present study showing that the cognitive protection induced by exercise can occur

irrespective of brain A β levels. However, it cannot be ruled out that despite unchanged total A β levels, long-term exercise has an impact on conformational changes of the peptide resulting in reduced neurotoxicity. This hypothesis will be further discussed in the next section.

4.1.1.6 Gene expression changes underlying the beneficial effects of long-term enriched environment

BDNF – a notorious gene found to be induced upon EE

Multiple studies have linked beneficial effects of voluntary exercise and enriched environment with gene expression changes in specific brain areas (Tong et al., 2001; Barak et al., 2013; Hu et al., 2013). One candidate gene found to be upregulated upon enriched living conditions in both WT and Tg4-42^{het} mice in the present study is the brain derived neurotrophic factor (BDNF) (Figure 18D) (Hüttenrauch et al., 2016). BDNF belongs to a small family of secreted trophic proteins including nerve growth factor (NGF), neurotrophin 3 (NT-3) and neurotrophin 4 (NT-4) and regulates neural development, synaptogenesis and neuronal plasticity in the brain (McAllister et al., 1999; Huang and Reichardt, 2001; Poo, 2001). Consistent with the present study, numerous former reports have shown that both environmental enrichment and long-term physical activity increase BDNF expression levels (Neeper et al., 1996; Ickes et al., 2000; Rossi et al., 2006). As an induction of BDNF is often accompanied by an enhanced cognitive performance, it is suggestive that the beneficial effects of exercise on memory function depend on BDNF. Several lines of evidence link BDNF with improved learning and memory. For example, mutations or region-specific manipulations of BDNF and its receptors have been shown to cause deficits in spatial, as well as object recognition memory (Linnarsson et al., 1997; Mizuno et al., 2000; Saarelainen et al., 2000; Furini et al., 2010). In addition, BDNF appears to play a substantial role during the late phase of LTP in the CA1 region of the hippocampus (Pang and Lu, 2004) and its overexpression causes increased dendrite complexities in the CA1 region and dentate gyrus (Tolwani et al., 2002; Alonso et al., 2004). Hence, it is tempting to speculate that the exercise-induced cognitive improvement in WT and Tg4-42^{het} mice is at least partially dependent on BDNF function. Another factor supporting the notion of BDNF as a trigger for the beneficial effects of EE on Tg4-42 pathology is its neuroprotective function. Nagahara and colleagues recently reported an ameliorated neuron loss in an

AD model upon BDNF gene delivery to the entorhinal cortex (Nagahara et al., 2013). This neuroprotection was achieved without detectably altering A β deposition, which is in good agreement with the findings of the current thesis and demonstrates that BDNF-dependent neuronal survival is not *per se* dependent on changes in amyloid pathology.

Molecular chaperones and their attempt to protect neurons from damage

A striking number of transcripts found to be upregulated in physically active Tg4-42^{het} mice belong to the family of heat shock proteins (Hsps) (Figure 18D) (Hüttenrauch et al., 2016). It has been shown in numerous studies that the induction of Hsps can be triggered by environmental stress conditions such as exercise in both humans and rodents (Lancaster et al., 2004; Nickerson et al., 2005; Ding et al., 2006). The fundamental role of Hsps is to protect cells from damage by refolding or degrading misfolded proteins and therewith maintaining the functionality of the proteome (Wilhelmus et al., 2007). Due to the tendency of A β to misfold into toxic oligomers, the role of Hsps in AD and especially their interaction with A β , has gained particular interest. Magrané and colleagues have shown that an overexpression of Hsp70 protects primary neuronal cultures from toxic effects of intracellular A β ₄₂ accumulation (Magrane et al., 2004). Furthermore, Hsp70/40 and Hsp90 have been described to block A β self-assembly at substochioemetric concentrations *in vitro*, mainly by causing structural changes in A β oligomers (Evans et al., 2006). A similar function has been proposed for the HSP40-homolog DNAJB6, which modulated A β ₄₂ aggregation *in vitro* by binding to A β fibrils thereby inhibiting their elongation and growth (Mansson et al., 2014). The strongest upregulated gene in Tg4-42^{het} EE mice was α B-Crystallin, a small heat shock protein being predominantly localized in astrocytes and oligodendrocytes, as well as around neuron surrounding plaques (Shinohara et al., 1993; Renkawek et al., 1994). α B-Crystallin has been shown to co-localize with A β *in vivo* (Yoo et al., 2001). *In vitro*, the co-chaperone binds to A β ₄₂ fibrils along their entire length thereby inhibiting their elongation (Shammas et al., 2011). Moreover, α B-Crystallin has been described to have a protective effect on A β -induced cytotoxicity (Dehle et al., 2010). Taken together, it can be assumed that the chaperones found to be upregulated in Tg4-42^{het} mice in the current analysis interact with A β ₄₋₄₂ in a similar fashion. Thereby, they might induce conformational changes resulting in a reduced neurotoxicity, as shown by a diminished CA1 neuron loss, despite unchanged total A β levels.

A subset of Hsps found to be upregulated upon enriched environment in Tg4-42^{het} mice could also be observed in active WT animals (Figure 18E), indicating a common pathway associated with long-term cognitive and physical stimulation, which is independent of the genotype. This collective of genes, implying *CRYAB*, *HSPH1* and *HSPA1B*, can be collated to the “protein processing in the endoplasmic reticulum” pathway (Figure 18F). This pathway is involved in endoplasmic reticulum (ER) quality control leading to the disposal of misfolded proteins and their degradation through the proteasome and is part of a cellular stress response (Liu and Chang, 2008). The induction of growth factors like BDNF, as well as the upregulation of genes that encode cytoprotective proteins such as heat-shock proteins, is carried out by neurons as a consequence of mild stressors like exercise or caloric restriction. This might represent a synergistically acting “pre-conditioning” phenomenon needed to increase cellular abilities to resist more severe stress, including accumulation of misfolded amyloid peptides (Mattson et al., 2004).

Necdin – a new candidate gene implicated in the beneficial effects of EE?

The gene showing the strongest downregulation in Tg4-42^{het} mice upon lifelong exercise compared to standard housed animals was Necdin (*NDN*) (Figure 19), a protein implicated in Prader-Willi syndrome (Jay et al., 1997). *NDN* is expressed in postmitotic neurons and it was shown that *Ndn*^{-/-} mice display an improved spatial learning and memory performance in the MWM task (Muscatelli et al., 2000). As *NDN* expression levels increase in Tg4-42^{het} SH mice compared to wild-type controls and drop again to baseline upon enrichment (Figure 19), it is suggestive that *Ndn* plays a role in the improved phenotype of exercised Tg4-42^{het} mice. However, further studies are warranted to explore the precise mechanistic link between Necdin and memory performance.

In summary, EE training appears to upregulate genes involved in pathways yielding to neuroprotective events. As these genes control multiple cellular processes, their analysis at the system level would be the next suitable step to gain further knowledge about the molecular substantiation of EE. It is indisputable that the beneficial effects seen upon cognitive and physical enrichment in rodents are a product of multiple mechanisms either acting additive or overlapping.

4.1.1.7 Conclusions of Project I, Part I:

Based on the results of the current work:

- Long-term physical activity exerts a preventive effect on CA1 neuron loss induced by intraneuronal A β ₄₋₄₂ expression in the Tg4-42 AD mouse model.
- The diminished neuronal cell death is accompanied by an improved motor performance and a complete memory recovery in Tg4-42^{het} mice.
- The observed beneficial effects of cognitively and physically stimulating living conditions in Tg4-42^{het} mice are irrespective of a change in A β ₄₋₄₂ total brain levels and neurogenesis rates.
- Long-term enriched living induces genes involved in pathways yielding to neuroprotective events.

4.1.2 Part II: Lifelong environmental enrichment in combination with voluntary exercise has limited effects on the pathology of 5XFAD mice

4.1.2.1 Long-term enriched living conditions have a limited effect on the physiological status and the sensory-motor phenotype of 5XFAD mice

APP transgenic mouse models frequently exhibit a premature death phenotype caused by heavy amyloid deposition and subsequent cerebral vascular damage (Calhoun et al., 1999; Van Dorpe et al., 2000). As reported in previous studies, a reduced survival rate of 5XFAD SH mice could be observed in course of the current thesis (Heraud et al., 2014). However, this phenotype could not be attenuated upon enriched conditions (Figure 21A).

5XFAD mice display a reduced body weight starting with 9 months of age. The weight loss is aggravated over time, reaching a loss of 25% in comparison to WT littermates by the age of 12 months (Jawhar et al., 2012). Prolonged living in an enriched environment had no influence on the drastically reduced body weight of 5XFAD mice (Figure 21B). Therefore, no improvement in general health condition could be achieved by long-term physical and cognitive stimulation.

12-month-old 5XFAD mice are characterized by prominent amyloid plaque pathology in motor-related brain areas. Furthermore, accumulation of intraneuronal A β in motor neurons of the brain and spinal cord cause an impaired axonal transport with the

formation of axonal spheroids (Jawhar et al., 2012). Accordingly, severe sensory-motor impairments in the string suspension task and beam walking have been reported for 5XFAD mice starting with 9 months of age (Jawhar et al., 2012). This phenotype could not be rescued due to prolonged cognitive and physical stimulation (Figure 21C, D). However, as shown in previous studies, 5XFAD mice exhibit an abnormal rotarod performance with 12 months of age, which was completely rescued upon enriched living conditions (Figure 21E) (Shukla et al., 2013). As no amelioration in other motor tasks like string suspension and balance beam could be detected, the significant rescue of the rotarod performance points to a better overall motor coordination. This is likely based on a continuous interaction with the enriched environment, but not general muscular strength. Hence, the improved rotarod performance confirms the validity of the enrichment paradigm in the present study.

4.1.2.2 Enriched living conditions do not alter the behavioural phenotype of 5XFAD mice

Anxiety, disinhibition and depression belong to the neuropsychological changes that frequently accompany disease progression of AD patients (Mega et al., 1996; Lyketsos and Olin, 2002). Anxiety-related behaviour in mice can be studied using the elevated plus maze task. An increased time spent in open arms reflects reduced anxiety levels while more time spent in the closed arms is an indication of increased anxiety (Walf and Frye, 2007). Mechanistically, changes in the circuitries of the limbic system, susceptible to A β accumulation, seem to be involved in altered elevated plus maze behaviour (Lalonde et al., 2012). At the age of 6 months, 5XFAD mice demonstrate reduced anxiety levels, which further decrease in an age-dependent manner (Jawhar et al., 2012). Environmental enrichment in combination with exercise was not capable to compensate anxiety-related behavioural deficits (Figure 22A). Literature on the effect of EE on this phenotypic trait in AD mouse models is scarce. Therefore, the data gathered in the current thesis can only be confronted to a limited number of comparable studies. The present finding is consistent with recent data from our group demonstrating no changes in low levels of anxiety-like behaviour in the APP/PS1KI mouse model, which was unchanged after 4 months of EE (Cotel et al., 2012). In contrast, Verret and colleagues recently reported a restoration of an abnormal anxiety

phenotype in Tg2576 mice when EE occurred early in the animal's lifespan (Verret et al., 2013).

With 6 months of age, 5XFAD mice start to suffer from working memory deficits which further increase in an age-dependent manner (Oakley et al., 2006;Jawhar et al., 2012). To evaluate working memory deficits in rodents, spontaneous alternation tasks like the Y-, T- or cross-maze are used. These tasks are sensitive to lesions in the prefrontal cortex and hippocampus, making them suitable for AD pathology relevant impairments. Many studies on the effect of enriched environment in AD mouse models reported clearly improved performances in cognitive tests (Parachikova et al., 2008;Dao et al., 2013;Wang et al., 2013). However, no improvement in working memory performance upon enriched living conditions in 5XFAD mice could be assessed in course of this thesis (Figure 22C). This again is in good agreement with results from a study previously performed in our group, where standard- and enriched housed APP/PS1KI mice showed equally bad performances in the Y-maze task compared to age-matched WT controls (Cotel et al., 2012). It is worth mentioning that in most of the environmental enrichment studies, cognitive performances are assessed using the MWM test, which allows to analyse both spatial working, as well as reference memory capacities. Unfortunately, we were unable to perform the MWM test with 12-month-old 5XFAD mice, due to their massive impairments in swimming capability and their drastic motor phenotype at that age.

In summary, enriched housing combining cognitive enhancement and physical activity did not ameliorate the behavioural deficits seen in 12-month-old 5XFAD mice.

4.1.2.3 Standard- and enriched housed 5XFAD mice display similar levels of amyloid pathology

No differences in amyloid plaque pathology due to enriched environment living conditions were found between 5XFAD SH and EE mice in course of the present study (Figure 23A, B). Previous analyses on the influence of EE on extracellular plaque pathology in AD mouse models are inconsistent. Some investigations are in accordance with our observations reporting no effect of enriched living conditions on amyloid deposition (Arendash et al., 2004;Wolf et al., 2006;Parachikova et al., 2008;Cotel et al., 2012), while others found a reduction (Mirochnic et al., 2009;Ke et al., 2011;Liu et al., 2013) or even increased A β plaque deposition (Jankowsky et al., 2003). 5XFAD mice

harbour a robust plaque pathology which is preceded by intraneuronal accumulation of A β starting at the age of 6 weeks. With 2 months of age, first plaques appear in deep layers of the cortex and in the subiculum. During aging, amyloid deposition progresses and becomes present in the entire cortex, subiculum and hippocampus. To a lesser extent, plaques also become apparent in thalamus, olfactory bulb and brainstem (Oakley et al., 2006). The EE starting time point of the current study was chosen in the presymptomatic phase as there are studies showing that only when access to running wheels is given prior to disease onset, reduced plaque pathology can be observed (Adlard et al., 2005; Richter et al., 2008). However, no differences in A β plaque load were revealed in cortex, hippocampus, subiculum or thalamus between enriched and sedentary 5XFAD mice at 12 months of age. Notably, it has been reported earlier that there is a rapid increase in amyloid pathology in 5XFAD mice until the age of 6 months, which subsequently becomes less severe and reaches a certain plateau level at the age of 10 to 14 months, depending on the sex of the animal (Bhattacharya et al., 2014; Richard et al., 2015). Therefore, one cannot exclude that the enrichment paradigm leads to a certain delay in plaque deposition at earlier time points during disease progression, which, by the end of the treatment period is not visible anymore due to the reached plateau level of amyloid plaques. To test this hypothesis, plaque pathology could be analysed at earlier ages during the EE treatment period in a time-dependent manner.

Beauquis and colleagues recently reported lowered A β ₁₋₄₀ and A β ₁₋₄₂ levels upon enriched housing while the number and size of A β plaques did not change (Beauquis et al., 2013). These observations were further extended by Rao and colleagues, showing significantly decreased levels of soluble and insoluble A β ₁₋₄₀ and A β ₁₋₄₂ levels in both cortex and hippocampus upon voluntary exercise (Rao et al., 2015). There are multiple mechanisms described which could possibly be involved in lowering A β levels due to exercise and thereby improving cognitive abilities. For example, Rao et al. found reduced protein levels of β -secretase (BACE1) in active APP/PSEN mice compared to sedentary mice, which could be one mechanism explaining reduced A β levels. Moreover, increased levels of A β -degrading enzymes (ADEs) like neprilysin (NEP) and insulin-degrading enzyme (IDE) following EE paradigms have been reported, supposedly leading to an increased degradation of A β peptides (Lazarov et al., 2005; Briones et al., 2009). However, in the present study, no differences in soluble and

insoluble A β ₁₋₄₂ levels could be detected (Figure 23C, D). Accordingly, BACE1, NEP and IDE levels were unchanged between active and inactive 5XFAD mice (Figure 25).

Neuroinflammation, characterized by activation of astrocytes and microglia, is one of the major hallmarks of AD and develops concomitantly with amyloid deposition in the 5XFAD mouse model (Oakley et al., 2006). Many reports describe a decline in inflammatory markers like GFAP upon voluntary exercise accompanied by reduced A β levels (Nichol et al., 2007; Nichol et al., 2009; Kang et al., 2013; Souza et al., 2013). Corresponding to the comparable amyloid phenotype seen in the current study, our findings show no changes in the inflammatory status between enriched and sedentary 5XFAD mice in the analysed brain areas cortex, hippocampus and thalamus (Figure 24).

4.1.2.4 Induction of neuroprotective genes in physically active 5XFAD mice

As already mentioned earlier, numerous reports have shown elevated expression levels of the neurotrophic factor BDNF following voluntary exercise in both humans and rodents. Accordingly, active 5XFAD mice displayed significantly increased *BDNF* mRNA levels when compared to sedentary controls, which further indicates a successful EE protocol (Figure 25). An induction of BDNF due to physical activity is often paralleled by an enhanced cognitive performance, which supposes this neurotrophic factor as a key player in this process. However, in the present study, increased BDNF levels in 5XFAD EE mice were not associated with beneficial effects on cognitive impairment. Congruently, Liu and colleagues even found an exercise induced decrease of *BDNF* mRNA levels in APP/PS1 mice paralleled by a better cognitive performance and LTP (Liu et al., 2011). Next to BDNF, mRNA expression analyses revealed that members of the heat-shock protein family were upregulated in enriched housed 5XFAD mice compared to standard housed controls (Figure 25). In contrast to WT and Tg4-42^{het} mice, the induction of HSPs in 5XFAD was not accompanied by beneficial effects on the cognitive performance. This could be explained by the fact that the 5XFAD model represents a robust and aggressive mouse model of AD pathology, which is based on multiple mutations in AD-related genes. Even though neuroprotective genes like BDNF and HSPs are being induced upon exercise, the pathology of this familial AD model is too advanced to be attenuated.

4.1.2.5 Conclusions of Project I, Part II:

Based on the results of the current work:

- Long-term environmental enrichment has limited effects on the general health condition and sensory-motor phenotype of 5XFAD mice.
- Anxiety-related behavioural deficits and working memory impairments are not ameliorated due to physically and cognitively stimulating living conditions.
- Enriched-housed 5XFAD mice do not display diminished amyloid pathology and A β ₁₋₄₂ levels.
- The inflammatory response in brains of 5XFAD mice is not declined upon prolonged EE.
- Long-term enriched living induces genes involved in pathways yielding to neuroprotective events, however, without an effect on the pathology.

4.2 Project II: Neprilysin deficiency alters the neuropathological and behavioural phenotype in the 5XFAD model of Alzheimer's disease

5XFAD mice are characterized by amyloid plaque formation as early as two months of age, which is preceded by intraneuronal A β accumulation. Next to A β ₁₋₄₀, A β ₁₋₄₂ levels are tremendously increased due to the co-expression of five familial AD mutations in this double transgenic APP/PS1 mouse model (Oakley et al., 2006; Jawhar et al., 2012). 5XFAD mice therefore display a valuable tool recapitulating many AD-related phenotypes and represent a suitable model to analyse possible therapeutic strategies. During the last decades, numerous therapeutic approaches that target A β have been developed with the ultimate goal to diminish its toxic action in brains of AD patients. These approaches include the prevention of A β oligomerization, an improved clearance of the peptide through the blood brain barrier, the prevention or reduction of A β production, as well as enhanced degradation (Bates et al., 2009). A slowdown of A β degradation by A β -degrading enzymes (ADEs) is the major presumed cause of A β accumulation in sporadic AD cases (Iwata et al., 2005). Among a variety of ADEs, neprilysin (NEP) is considered to be one of the most important physiological enzymes regulating cerebral A β levels (Miners et al., 2011). Numerous *in vitro* studies described

the ability of NEP to cleave A β monomers and oligomers at several cleavage sites (Wang et al., 2006;Miners et al., 2011). A role of NEP has also been shown *in vivo*. A knock-out of the metalloprotease led to enhanced levels of soluble and oligomeric A β and subsequent impairments in synaptic plasticity as well as cognitive abnormalities in APP transgenic and WT mice (Huang et al., 2006;Madani et al., 2006). The primary objective of this part of the study was to evaluate the *in vivo* effect of NEP level reduction on the neuropathological and behavioural phenotype in young and aged 5XFAD mice. Therefore, the 5XFAD/NEP^{+/-} mouse model was generated by crossing NEP^{-/-} mice with 5XFAD mice (Lu et al., 1995;Oakley et al., 2006). It could be shown that young 5XFAD mice *per se* display strongly reduced NEP levels when compared to WT animals. In 6-month-old 5XFAD mice, reduced NEP levels were still present, albeit being not that distinct (Figure 26A, B) (Hüttenrauch et al., 2015). These results confirm recent findings from Ohno and colleagues, who observed reduced NEP levels in 12-month-old 5XFAD mice (Devi and Ohno, 2015). In accordance, NEP levels have been shown to decrease during normal aging, as well as during disease progression in human AD brains, further substantiating its crucial role during AD development (Iwata et al., 2002;Caccamo et al., 2005;Wang et al., 2010). In young and aged 5XFAD mice, a heterozygous NEP knock-out led to a further decrease in the *NEP* mRNA expression level, reaching only 7 or 8.5% of WT mice levels, respectively. A successful NEP depletion in 5XFAD/NEP^{+/-} mice could also be proven on the protein level by performing immunohistochemical stainings (Figure 26C).

Intriguingly, 5XFAD/NEP^{+/-} mice displayed deficits in spatial working memory at 6 months of age when compared to 5XFAD littermates (Figure 27) (Hüttenrauch et al., 2015). This is consistent with recently published data showing an impaired performance in the MWM task in a mouse model of amyloidosis with heterozygous NEP deficiency (Mohajeri and Wolfer, 2009). Moreover, Huang et al. observed behavioural deficits in the Y-maze and MWM in APP23 mice on a homozygous NEP knock-out background (Huang et al., 2006). Therefore, the inefficient removal of A β from the brain due to NEP depletion in the current study led to a diminished performance of 5XFAD/NEP^{+/-} mice in hippocampus-dependent cognitive tasks, further confirming previous results showing that a downregulation of NEP contributes to the pathophysiology of AD (Hüttenrauch et al., 2015).

In line with the altered memory performance, immunohistochemical stainings and subsequent quantifications revealed a significantly increased A β plaque load in the dentate gyrus, subiculum and spinal cord of 6-month-old 5XFAD/NEP^{+/-} mice when compared to 5XFAD controls (Figure 28A, B). Previous studies in J9 mice on a hemi- or homozygous NEP deficient background corroborate the findings of the current thesis. NEP depletion markedly increased the hippocampal amyloid plaque burden in this APP transgenic model (Farris et al., 2007). The fact that Thioflavin S-positive deposits were unchanged in all analysed brain areas between 5XFAD and 5XFAD/NEP^{+/-} mice, supports the hypothesis that NEP mainly degrades soluble A β peptides (Figure 28C) (Hüttenrauch et al., 2015). A related observation was reported in hAPP transgenic mice which were crossed with neprilysin transgenic mice. NEP overexpression in these mice reduced soluble A β levels but had no impact on amyloid plaque load (Meilandt et al., 2009). This is in line with higher A β ₁₋₄₂ levels in TBS-soluble brain fractions in the presence of unchanged SDS-soluble A β levels in 5XFAD/NEP^{+/-} mice in the current study (Figure 28E, F). It is noteworthy that the extracellular A β plaque load in 5XFAD and 5XFAD/NEP^{+/-} mice was unchanged in cortex and thalamus. However, the higher abundance of amyloid plaques in the dentate gyrus and subiculum of 5XFAD/NEP^{+/-} animals correlates well with the previously demonstrated intense NEP immunoreactivity in the hippocampal area of WT mice, suggesting that NEP deficiency has a stronger impact in this brain region than in regions like the cortex or thalamus (Fukami et al., 2002).

Surprisingly, at young ages 5XFAD mice displayed a 70% higher extracellular plaque load when compared to age-matched 5XFAD/NEP^{+/-} mice (Figure 30). Amyloid deposition is always accompanied by an inflammatory response. Accordingly, 2.5-month-old 5XFAD mice showed increased *GFAP* mRNA expression levels in comparison to all other experimental groups, while at older ages, *GFAP* levels were equally increased in 5XFAD and 5XFAD/NEP^{+/-} mice in comparison to healthy controls (Figure 29). This finding is in accordance with significantly increased insulin-degrading enzyme (*IDE*) mRNA levels in young 5XFAD mice when compared to WT and 5XFAD/NEP^{+/-} mice. IDE is another putative protease that has been shown to degrade A β peptides *in vivo* (Eckman and Eckman, 2005) and is known to be upregulated in response to increased A β production (Vepsäläinen et al., 2008). In older 5XFAD/NEP^{+/-} mice, IDE expression is increased up to the level of 5XFAD mice.

Intriguingly, expression analysis of the close NEP homologue endothelin-converting enzyme 1 (ECE1) revealed that this ADE is significantly increased in NEP-deficient mice compared to 5XFAD mice in young animals (Figure 31). ECE1 has been shown to degrade A β within intracellular compartments, which ultimately leads to a reduced secretion of the peptide and reduced extracellular accumulation (Eckman et al., 2001). As recently detected in SH-SY5Y cells, ECEs are capable of degrading at least two distinct pools of A β . One is intended for secretion, while the other is being produced and degraded within endosomes and lysosomes (Pacheco-Quinto and Eckman, 2013). The increased ECE1 levels in young 5XFAD/NEP^{+/-} mice correlate well with the strongly reduced extracellular A β signal compared to 5XFAD animals and suggest a reciprocal effect between ECE and NEP activities in A β degradation (Hüttenrauch et al., 2015). This is also supported by the reported expression profile of ECE1 in pyramidal neurons of cortical layer V (Pacheco-Quinto et al., 2013), the same layer that shows prominent intracellular accumulation of A β peptides in 5XFAD mice (Jawhar et al., 2012). The results of the current thesis provide *in vivo* evidence for a mutual regulation between the two ADEs NEP and ECE1, further supported by the observation that NEP^{+/-} and NEP^{-/-} mice display elevated ECE1 expression levels as well, with NEP^{-/-} animals showing the highest levels of ECE1 at this early time point. However, it warrants further investigation to delineate why ECE1 levels are normalized at older ages although NEP levels are still drastically reduced in hemi- and homozygous NEP-deficient mice.

4.2.1 Conclusions of Project II:

Based on the results of the current work:

- 5XFAD mice display strongly reduced neprilysin levels compared to WT mice.
- Neprilysin deficiency leads to spatial working memory deficits in 6-month-old 5XFAD mice.
- Aged 5XFAD/NEP^{+/-} mice demonstrate region-specific increases in extracellular A β deposition, overall increased levels of soluble A β ₁₋₄₂ and an elevated astrocytosis in all studied brain areas.
- In young 5XFAD/NEP^{+/-} mice, extracellular A β plaque pathology is delayed when compared with age-matched 5XFAD animals.

- 2.5-month-old 5XFAD/NEP^{+/-}, NEP^{+/-} and NEP^{-/-} display elevated levels of ECE1, suggesting a compensatory upregulation upon NEP depletion.

5 SUMMARY & CONCLUSIONS

There is substantial evidence for a protective role of physical and cognitive activity on the risk and progression of Alzheimer's disease (AD). Although numerous studies in rodent models have explored beneficial effects of an enriched environment (EE) combined with voluntary exercise on AD pathology, it is difficult to draw clear-cut conclusions. Confounding variables are variations in study design regarding the type of enrichment, different durations and extent of physical activity, different ages at which animals are exposed to EE, as well as differences in the used AD models. Most studies were conducted in models overexpressing mutant forms of human APP, presenilin 1/2, or a combination of both. Even though all of these AD models develop typical pathological hallmarks of AD, it is hard to translate findings to the situation of sporadic AD patients, which neither possess any mutations nor APP overexpression. Furthermore, despite massive research, relatively little is known about the effect of physical activity on neurodegenerative processes in the hippocampus, a brain region being one of the first and most severely affected during AD progression. This is likely due to the fact that only a small number of AD mouse models display a reliable hippocampal neuron loss.

The goal of the first part of the present work was to investigate the effect of long-term enriched environment, combining cognitive enhancement and physical activity, on the newly-developed Tg4-42 mouse model. This model overexpresses A β ₄₋₄₂ without any mutations and develops an age-dependent hippocampal neuron loss associated with a severe memory decline. Tg4-42 mice therefore represent a valid AD mouse model which reflects the key features of sporadic AD. By using unbiased, design-based stereology, it was demonstrated that long-term physical stimulation exerts a preventive effect on hippocampal CA1 neuron loss induced by intraneuronal A β ₄₋₄₂ expression in Tg4-42^{het} and Tg4-42^{hom} mice. Behavioural analyses revealed that the diminished neuronal cell death was accompanied by an improved motor performance and a complete memory recovery. Furthermore, lifelong exercise induced gene expression pathways yielding to neuroprotective events. These effects were irrespective of total A β ₄₋₄₂ brain levels and increased neurogenesis rates. Taken together, the present study provides evidence for the first time that enhanced cognitive

and physical activity counteracts hippocampal neuron loss and behavioural deficits in a transgenic AD mouse model without mutations and APP overexpression. Furthermore, we found evidence that changes in gene-expression programs play a substantial role in the observed effects. These results underscore the relevance of a challenging lifestyle in combination with regular exercise as a potential strategy in the prevention of sporadic AD.

In contrast to Tg4-42 mice, 5XFAD mice represent a conventional model with an early, robust and aggressive AD pathology. Although vast literature is reporting about beneficial effects of EE on the pathology of familial AD models, no study investigated the widely-used 5XFAD model so far. In the present work, despite of partial benefits in motor performance, no effect on anxiety levels, working memory performance, plaque deposition, A β ₁₋₄₂ levels or inflammatory status could be observed upon prolonged enriched living conditions. Therefore, a lifelong cognitive and physical stimulation has no therapeutic benefit on the Alzheimer-like pathophysiology of 5XFAD mice.

Taken together, the results of the first part of this thesis support that physical activity and environmental enrichment can counteract disease progression in the Tg4-42 mouse model, which likely represents a model more suitable for the most common sporadic form of AD. In contrast, the 5XFAD model represents a robust and aggressive model of familial AD incorporating five different mutations. The disease phenotype of 5XFAD mice cannot be counteracted efficiently by a rather mild intervention like EE and voluntary exercise.

The deposition of A β in form of soluble oligomers, insoluble fibrils or neuritic plaques is one of the major hallmarks of AD. In familial AD cases, an enhanced production of A β caused by mutations in genes encoding APP and presenilins leads to an enhanced accumulation of the peptide. In sporadic AD cases, however, the cause of increased A β accumulation is likely due to decelerated degradation. The metalloprotease neprilysin (NEP) is one of the major A β -degrading enzymes (ADEs) as shown by numerous *in vitro*, *in vivo* and reverse genetic studies. This second part of the current thesis aimed on gaining deeper knowledge about the role of neprilysin during the progression of AD. Therefore, 5XFAD mice were crossed with homozygous NEP knock-out mice (NEP^{-/-}). It was shown that 5XFAD mice *per se* exhibit reduced NEP levels when compared to WT mice. 5XFAD/NEP^{+/-} animals displayed an even stronger NEP level reduction resulting in an impaired spatial working memory. Furthermore, hemizygous NEP

deficiency led to region-specific increases in extracellular amyloid deposition, overall increased levels of A β ₄₂ and an enhanced inflammatory response in all studied brain areas. In contrast, young 5XFAD/NEP^{+/-} mice showed cortical A β plaque pathology to a much lesser extent than age-matched 5XFAD animals. This finding was accompanied by elevated levels of endothelin-converting enzyme 1 (ECE1) in young 5XFAD/NEP^{+/-}, NEP^{+/-} and NEP^{-/-} mice, suggesting a mutual regulation of ECE1 and NEP in 2.5-month-old animals. In total, these observations support previous *in vivo* data indicating that NEP is one of the main A β -degrading peptidases. Hence, the current findings provide evidence for a reciprocal effect between NEP and ECE1 activities in A β degradation.

6 BIBLIOGRAPHY

- Adlard, P.A., Perreau, V.M., Pop, V., and Cotman, C.W. (2005). Voluntary exercise decreases amyloid load in a transgenic model of Alzheimer's disease. *J Neurosci* 25, 4217-4221.
- Alexandru, A., Jagla, W., Graubner, S., Becker, A., Bauscher, C., Kohlmann, S., Sedlmeier, R., Raber, K.A., Cynis, H., Ronicke, R., Reymann, K.G., Petrasch-Parwez, E., Hartlage-Rubsamen, M., Waniek, A., Rossner, S., Schilling, S., Osmand, A.P., Demuth, H.U., and Von Horsten, S. (2011). Selective Hippocampal Neurodegeneration in Transgenic Mice Expressing Small Amounts of Truncated A β Is Induced by Pyroglutamate-A β Formation. *J Neurosci* 31, 12790-12801.
- Allinquant, B., Hantraye, P., Maillieux, P., Moya, K., Bouillot, C., and Prochiantz, A. (1995). Downregulation of amyloid precursor protein inhibits neurite outgrowth in vitro. *J Cell Biol* 128, 919-927.
- Alonso, M., Medina, J.H., and Pozzo-Miller, L. (2004). ERK1/2 activation is necessary for BDNF to increase dendritic spine density in hippocampal CA1 pyramidal neurons. *Learn Mem* 11, 172-178.
- Alzheimer, A. (1907). Über eine eigenartige Erkrankung der Hirnrinde. *Allg. Zeitsch. Psychiatrie Psychisch-gerichtliches Med.* 64, 146-148.
- Alzheimer's Association (2015). 2015 Alzheimer's disease facts and figures. *Alzheimer's and Dementia* 11, 332-384.
- Anderson, K.W., Mast, N., Pikuleva, I.A., and Turko, I.V. (2015). Histone H3 Ser57 and Thr58 phosphorylation in the brain of 5XFAD mice. *FEBS Open Bio* 5, 550-556.
- Annaert, W., and De Strooper, B. (2002). A cell biological perspective on Alzheimer's disease. *Annu Rev Cell Dev Biol* 18, 25-51.
- Antonios, G., Borgers, H., Richard, B.C., Brauss, A., Meissner, J., Weggen, S., Pena, V., Pillot, T., Davies, S.L., Bakrania, P., Matthews, D., Brownlees, J., Bouter, Y., and Bayer, T.A. (2015). Alzheimer therapy with an antibody against N-terminal Abeta 4-X and pyroglutamate Abeta 3-X. *Sci Rep* 5, 17338.
- Aoki, M., Volkman, I., Tjernberg, L.O., Winblad, B., and Bogdanovic, N. (2008). Amyloid beta-peptide levels in laser capture microdissected cornu ammonis 1 pyramidal neurons of Alzheimer's brain. *Neuroreport* 19, 1085-1089.
- Arendash, G.W., Garcia, M.F., Costa, D.A., Cracchiolo, J.R., Wefes, I.M., and Potter, H. (2004). Environmental enrichment improves cognition in aged Alzheimer's transgenic mice despite stable beta-amyloid deposition. *Neuroreport* 15, 1751-1754.
- Arendash, G.W., King, D.L., Gordon, M.N., Morgan, D., Hatcher, J.M., Hope, C.E., and Diamond, D.M. (2001). Progressive, age-related behavioral impairments in transgenic mice carrying both mutant amyloid precursor protein and presenilin-1 transgenes. *Brain Res.* 891, 42-53.
- Arnold, S.E., Hyman, B.T., Flory, J., Damasio, A.R., and Van Hoesen, G.W. (1991). The topographical and neuroanatomical distribution of neurofibrillary tangles and neuritic plaques in the cerebral cortex of patients with Alzheimer's disease. *Cereb Cortex.* 1, 103-116.
- Backman, L., Jones, S., Berger, A.K., Laukka, E.J., and Small, B.J. (2004). Multiple cognitive deficits during the transition to Alzheimer's disease. *J Intern Med* 256, 195-204.
- Barak, B., Shvarts-Serebro, I., Modai, S., Gilam, A., Okun, E., Michaelson, D.M., Mattson, M.P., Shomron, N., and Ashery, U. (2013). Opposing actions of environmental enrichment and Alzheimer's disease on the expression of hippocampal microRNAs in mouse models. *Transl Psychiatry* 3, e304.
- Barker, W.W., Luis, C.A., Kashuba, A., Luis, M., Harwood, D.G., Loewenstein, D., Waters, C., Jimison, P., Shepherd, E., Sevush, S., Graff-Radford, N., Newland, D., Todd, M., Miller, B., Gold, M., Heilman, K., Doty, L., Goodman, I., Robinson, B., Pearl, G., Dickson, D., and

- Duara, R. (2002). Relative frequencies of Alzheimer disease, Lewy body, vascular and frontotemporal dementia, and hippocampal sclerosis in the State of Florida Brain Bank. *Alzheimer Dis Assoc Disord* 16, 203-212.
- Barnes, D.E., Whitmer, R.A., and Yaffe, K. (2007). Physical activity and dementia: The need for prevention trials. *Exerc Sport Sci Rev* 35, 24-29.
- Barnes, D.E., and Yaffe, K. (2011). The projected effect of risk factor reduction on Alzheimer's disease prevalence. *The Lancet Neurology* 10, 819-828.
- Bates, K.A., Verdile, G., Li, Q.X., Ames, D., Hudson, P., Masters, C.L., and Martins, R.N. (2009). Clearance mechanisms of Alzheimer's amyloid-beta peptide: implications for therapeutic design and diagnostic tests. *Mol Psychiatry* 14, 469-486.
- Bayer, T.A., Cappai, R., Masters, C.L., Beyreuther, K., and Multhaup, G. (1999). It all sticks together--the APP-related family of proteins and Alzheimer's disease. *Mol Psychiatry* 4, 524-528.
- Bayer, T.A., and Wirths, O. (2010). Intracellular accumulation of amyloid-beta - a predictor for synaptic dysfunction and neuron loss in Alzheimer's disease. *Frontiers in Aging Neuroscience* 2, 1-10.
- Beauquis, J., Pavía, P., Pomilio, C., Vinuesa, A., Podlutskaya, N., Galvan, V., and Saravia, F. (2013). Environmental enrichment prevents astroglial pathological changes in the hippocampus of APP transgenic mice, model of Alzheimer's disease. *Experimental Neurology* 239, 28-37.
- Bennett, J.C., Mcrae, P.A., Levy, L.J., and Frick, K.M. (2006). Long-term continuous, but not daily, environmental enrichment reduces spatial memory decline in aged male mice. *Neurobiol Learn Mem* 85, 139-152.
- Bertram, L., and Tanzi, R.E. (2005). The genetic epidemiology of neurodegenerative disease. *J Clin Invest* 115, 1449-1457.
- Beydoun, M.A., Beydoun, H.A., and Wang, Y. (2008). Obesity and central obesity as risk factors for incident dementia and its subtypes: a systematic review and meta-analysis. *Obes Rev* 9, 204-218.
- Bhattacharya, S., Haertel, C., Maelicke, A., and Montag, D. (2014). Galantamine Slows Down Plaque Formation and Behavioral Decline in the 5XFAD Mouse Model of Alzheimer's Disease. *PLoS ONE* 9, e89454.
- Bickel, H. (2012). Epidemiologie und Gesundheitsökonomie. In: Wallesch, C.-W. & Förstl, H. (Hrsg.) *Demenzen*. 2. Auflage. Georg Thieme Verlag, Stuttgart, 18-35.
- Black, J.E., Isaacs, K.R., Anderson, B.J., Alcantara, A.A., and Greenough, W.T. (1990). Learning causes synaptogenesis, whereas motor activity causes angiogenesis, in cerebellar cortex of adult rats. *Proc Natl Acad Sci U S A* 87, 5568-5572.
- Borchelt, D.R., Ratovitski, T., Van Lare, J., Lee, M.K., Gonzales, V., Jenkins, N.A., Copeland, N.G., Price, D.L., and Sisodia, S.S. (1997). Accelerated amyloid deposition in the brains of transgenic mice coexpressing mutant presenilin 1 and amyloid precursor proteins. *Neuron* 19, 939-945.
- Bottino, C.M., Castro, C.C., Gomes, R.L., Buchpiguel, C.A., Marchetti, R.L., and Neto, M.R. (2002). Volumetric MRI measurements can differentiate Alzheimer's disease, mild cognitive impairment, and normal aging. *Int Psychogeriatr* 14, 59-72.
- Boutajangout, A., and Wisniewski, T. (2013). The innate immune system in Alzheimer's disease. *Int J Cell Biol* 2013, 576383.
- Bouter, Y., Dietrich, K., Wittnam, J.L., Rezaei-Ghaleh, N., Pillot, T., Papot-Couturier, S., Lefebvre, T., Sprenger, F., Wirths, O., Zweckstetter, M., and Bayer, T.A. (2013). N-truncated amyloid beta (A β) 4-42 forms stable aggregates and induces acute and long-lasting behavioral deficits. *Acta Neuropathol* 126, 189-205.
- Bouter, Y., Kacprowski, T., Weissmann, R., Dietrich, K., Borgers, H., Brauss, A., Sperling, C., Wirths, O., Albrecht, M., Jensen, L.R., Kuss, A.W., and Bayer, T.A. (2014). Deciphering the molecular profile of plaques, memory decline and neuron loss in two mouse models for Alzheimer's disease by deep sequencing. *Front Aging Neurosci* 6, 75.

- Braak, H., Alafuzoff, I., Arzberger, T., Kretschmar, H., and Del Tredici, K. (2006). Staging of Alzheimer disease-associated neurofibrillary pathology using paraffin sections and immunocytochemistry. *Acta Neuropathol (Berl)* 112, 389-404.
- Braak, H., and Braak, E. (1991). Neuropathological staging of Alzheimer-related changes. *Acta Neuropathol (Berl)* 82, 239-259.
- Briones, T.L., Rogozinska, M., and Woods, J. (2009). Environmental experience modulates ischemia-induced amyloidogenesis and enhances functional recovery. *J Neurotrauma* 26, 613-625.
- Broadbent, N.J., Gaskin, S., Squire, L.R., and Clark, R.E. (2010). Object recognition memory and the rodent hippocampus. *Learn Mem* 17, 5-11.
- Broadbent, N.J., Squire, L.R., and Clark, R.E. (2004). Spatial memory, recognition memory, and the hippocampus. *Proc Natl Acad Sci U S A* 101, 14515-14520.
- Brooks, S.P., Trueman, R.C., and Dunnett, S.B. (2012). Assessment of Motor Coordination and Balance in Mice Using the Rotarod, Elevated Bridge, and Footprint Tests. *Curr Protoc Mouse Biol* 2, 37-53.
- Buchman, A.S., and Bennett, D.A. (2011). Loss of motor function in preclinical Alzheimer's disease. *Expert Rev Neurother* 11, 665-676.
- Caccamo, A., Oddo, S., Sugarman, M.C., Akbari, Y., and Laferla, F.M. (2005). Age- and region-dependent alterations in A β -degrading enzymes: implications for A β -induced disorders. *Neurobiology of Aging* 26, 645-654.
- Calhoun, M.E., Burgermeister, P., Phinney, A.L., Stalder, M., Tolnay, M., Wiederhold, K.H., Abramowski, D., Sturchler-Pierrat, C., Sommer, B., Staufenbiel, M., and Jucker, M. (1999). Neuronal overexpression of mutant amyloid precursor protein results in prominent deposition of cerebrovascular amyloid. *Proc Natl Acad Sci U S A* 96, 14088-14093.
- Campion, D., Dumanchin, C., Hannequin, D., Dubois, B., Belliard, S., Puel, M., Thomas-Anterion, C., Michon, A., Martin, C., Charbonnier, F., Raux, G., Camuzat, A., Penet, C., Mesnage, V., Martinez, M., Clerget-Darpoux, F., Brice, A., and Frebourg, T. (1999). Early-onset autosomal dominant Alzheimer disease: prevalence, genetic heterogeneity, and mutation spectrum. *Am J Hum Genet* 65, 664-670.
- Caroni, P. (1997). Overexpression of growth-associated proteins in the neurons of adult transgenic mice. *J Neurosci Methods* 71, 3-9.
- Carter, J., and Lippa, C.F. (2001). Beta-amyloid, neuronal death and Alzheimer's disease. *Curr Mol Med* 1, 733-737.
- Casas, C., Sergeant, N., Itier, J.M., Blanchard, V., Wirths, O., Van Der Kolk, N., Vingtdeux, V., Van De Steeg, E., Ret, G., Canton, T., Drobecq, H., Clark, A., Bonici, B., Delacourte, A., Benavides, J., Schmitz, C., Tremp, G., Bayer, T.A., Benoit, P., and Pradier, L. (2004). Massive CA1/2 neuronal loss with intraneuronal and N-terminal truncated Abeta42 accumulation in a novel Alzheimer transgenic model. *Am J Pathol* 165, 1289-1300.
- Castellano, J.M., Kim, J., Stewart, F.R., Jiang, H., Demattos, R.B., Patterson, B.W., Fagan, A.M., Morris, J.C., Mawuenyega, K.G., Cruchaga, C., Goate, A.M., Bales, K.R., Paul, S.M., Bateman, R.J., and Holtzman, D.M. (2011). Human apoE Isoforms Differentially Regulate Brain Amyloid- β Peptide Clearance. *Sci Transl Med* 3, 89ra57.
- Cataldo, J.K., Prochaska, J.J., and Glantz, S.A. (2010). Cigarette smoking is a risk factor for Alzheimer's Disease: an analysis controlling for tobacco industry affiliation. *J Alzheimers Dis* 19, 465-480.
- Catlow, B.J., Rowe, A.R., Clearwater, C.R., Mamcarz, M., Arendash, G.W., and Sanchez-Ramos, J. (2009). Effects of environmental enrichment and physical activity on neurogenesis in transgenic PS1/APP mice. *Brain Res* 1256, 173-179.
- Chapillon, P., Manneche, C., Belzung, C., and Caston, J. (1999). Rearing environmental enrichment in two inbred strains of mice: 1. Effects on emotional reactivity. *Behav Genet* 29, 41-46.
- Chishti, M.A., Yang, D.S., Janus, C., Phinney, A.L., Horne, P., Pearson, J., Strome, R., Zuker, N., Loukides, J., French, J., Turner, S., Lozza, G., Grilli, M., Kunicki, S., Morissette, C., Paquette,

- J., Gervais, F., Bergeron, C., Fraser, P.E., Carlson, G.A., George-Hyslop, P.S., and Westaway, D. (2001). Early-onset amyloid deposition and cognitive deficits in transgenic mice expressing a double mutant form of amyloid precursor protein 695. *J Biol Chem* 276, 21562-21570.
- Cho, W.-H., Park, J.-C., Kim, D.-H., Kim, M.-S., Lee, S.-Y., Park, H., Kang, J.-H., Yeon, S.-W., and Han, J.-S. (2014). ID1201, the ethanolic extract of the fruit of *Melia toosendan* ameliorates impairments in spatial learning and reduces levels of amyloid beta in 5XFAD mice. *Neuroscience Letters* 583, 170-175.
- Citron, M., Teplow, D.B., and Selkoe, D.J. (1995). Generation of amyloid beta protein from its precursor is sequence specific. *Neuron* 14, 661-670.
- Connor, J.R., Wang, E.C., and Diamond, M.C. (1982). Increased length of terminal dendritic segments in old adult rats' somatosensory cortex: an environmentally induced response. *Exp Neurol* 78, 466-470.
- Cook, D.G., Leverenz, J.B., Mcmillan, P.J., Kulstad, J.J., Ericksen, S., Roth, R.A., Schellenberg, G.D., Jin, L.W., Kovacina, K.S., and Craft, S. (2003). Reduced hippocampal insulin-degrading enzyme in late-onset Alzheimer's disease is associated with the apolipoprotein E-epsilon4 allele. *Am J Pathol* 162, 313-319.
- Costa, D.A., Cracchiolo, J.R., Bachstetter, A.D., Hughes, T.F., Bales, K.R., Paul, S.M., Mervis, R.F., Arendash, G.W., and Potter, H. (2007). Enrichment improves cognition in AD mice by amyloid-related and unrelated mechanisms. *Neurobiol Aging* 28, 831-844.
- Cotel, M.C., Jawhar, S., Christensen, D.Z., Bayer, T.A., and Wirths, O. (2012). Environmental enrichment fails to rescue working memory deficits, neuron loss, and neurogenesis in APP/PS1KI mice. *Neurobiol Aging* 33, 96-107.
- Cotman, C.W., Berchtold, N.C., and Christie, L.A. (2007). Exercise builds brain health: key roles of growth factor cascades and inflammation. *Trends Neurosci* 30, 464-472.
- Couillard-Despres, S., Winner, B., Schaubek, S., Aigner, R., Vroemen, M., Weidner, N., Bogdahn, U., Winkler, J., Kuhn, H.G., and Aigner, L. (2005). Doublecortin expression levels in adult brain reflect neurogenesis. *Eur J Neurosci* 21, 1-14.
- Cras, P., Smith, M.A., Richey, P.L., Siedlak, S.L., Mulvihill, P., and Perry, G. (1995). Extracellular neurofibrillary tangles reflect neuronal loss and provide further evidence of extensive protein cross-linking in Alzheimer disease. *Acta Neuropathol* 89, 291-295.
- D'andrea, M.R., Nagele, R.G., Wang, H.Y., Peterson, P.A., and Lee, D.H. (2001). Evidence that neurones accumulating amyloid can undergo lysis to form amyloid plaques in Alzheimer's disease. *Histopathology* 38, 120-134.
- D'hooge, R., and De Deyn, P.P. (2001). Applications of the Morris water maze in the study of learning and memory. *Brain Res Brain Res Rev* 36, 60-90.
- Dao, A.T., Zagaar, M.A., Levine, A.T., Salim, S., Eriksen, J.L., and Alkadhi, K.A. (2013). Treadmill exercise prevents learning and memory impairment in Alzheimer's disease-like pathology. *Curr Alzheimer Res* 10, 507-515.
- Deane, R., Du Yan, S., Subramanian, R.K., Larue, B., Jovanovic, S., Hogg, E., Welch, D., Manness, L., Lin, C., Yu, J., Zhu, H., Ghiso, J., Frangione, B., Stern, A., Schmidt, A.M., Armstrong, D.L., Arnold, B., Liliensiek, B., Nawroth, P., Hofman, F., Kindy, M., Stern, D., and Zlokovic, B. (2003). RAGE mediates amyloid-beta peptide transport across the blood-brain barrier and accumulation in brain. *Nat Med* 9, 907-913.
- Deane, R., and Zlokovic, B.V. (2007). Role of the blood-brain barrier in the pathogenesis of Alzheimer's disease. *Curr Alzheimer Res* 4, 191-197.
- Dehle, F.C., Ecroyd, H., Musgrave, I.F., and Carver, J.A. (2010). alphaB-Crystallin inhibits the cell toxicity associated with amyloid fibril formation by kappa-casein and the amyloid-beta peptide. *Cell Stress Chaperones* 15, 1013-1026.
- Dekosky, S.T., and Scheff, S.W. (1990). Synapse loss in frontal cortex biopsies in Alzheimer's disease: correlation with cognitive severity. *Ann Neurol* 27, 457-464.
- Devi, L., and Ohno, M. (2015). A combination Alzheimer's therapy targeting BACE1 and neprilysin in 5XFAD transgenic mice. *Mol Brain* 8, 19.

- Diamond, M.C., Ingham, C.A., Johnson, R.E., Bennett, E.L., and Rosenzweig, M.R. (1976). Effects of environment on morphology of rat cerebral cortex and hippocampus. *J Neurobiol* 7, 75-85.
- Dickson, D.W. (1997). The pathogenesis of senile plaques. *J Neuropathol Exp Neurol* 56, 321-339.
- Ding, Q., Vaynman, S., Souda, P., Whitelegge, J.P., and Gomez-Pinilla, F. (2006). Exercise affects energy metabolism and neural plasticity-related proteins in the hippocampus as revealed by proteomic analysis. *Eur J Neurosci* 24, 1265-1276.
- Donovan, M.H., Yazdani, U., Norris, R.D., Games, D., German, D.C., and Eisch, A.J. (2006). Decreased adult hippocampal neurogenesis in the PDAPP mouse model of Alzheimer's disease. *J Comp Neurol* 495, 70-83.
- Drechsel, D.N., Hyman, A.A., Cobb, M.H., and Kirschner, M.W. (1992). Modulation of the dynamic instability of tubulin assembly by the microtubule-associated protein tau. *Mol Biol Cell* 3, 1141-1154.
- Duckworth, W.C., Bennett, R.G., and Hamel, F.G. (1998). Insulin degradation: progress and potential. *Endocr Rev* 19, 608-624.
- Duyckaerts, C., Delatour, B., and Potier, M.C. (2009). Classification and basic pathology of Alzheimer disease. *Acta Neuropathol* 118, 5-36.
- Duyckaerts, C., Potier, M.C., and Delatour, B. (2008). Alzheimer disease models and human neuropathology: similarities and differences. *Acta Neuropathol* 115, 5-38.
- Eckman, E.A., and Eckman, C.B. (2005). Abeta-degrading enzymes: modulators of Alzheimer's disease pathogenesis and targets for therapeutic intervention. *Biochem Soc Trans* 33, 1101-1105.
- Eckman, E.A., Reed, D.K., and Eckman, C.B. (2001). Degradation of the Alzheimer's Amyloid β Peptide by Endothelin-converting Enzyme. *Journal of Biological Chemistry* 276, 24540-24548.
- Eckman, E.A., Watson, M., Marlow, L., Sambamurti, K., and Eckman, C.B. (2003). Alzheimer's Disease β -Amyloid Peptide Is Increased in Mice Deficient in Endothelin-converting Enzyme. *Journal of Biological Chemistry* 278, 2081-2084.
- Edbauer, D., Winkler, E., Regula, J.T., Pesold, B., Steiner, H., and Haass, C. (2003). Reconstitution of gamma-secretase activity. *Nat Cell Biol* 5, 486-488.
- Eimer, W.A., and Vassar, R. (2013). Neuron loss in the 5XFAD mouse model of Alzheimer's disease correlates with intraneuronal Abeta42 accumulation and Caspase-3 activation. *Mol Neurodegener* 8, 2.
- Ekdahl, C.T., Claasen, J.H., Bonde, S., Kokaia, Z., and Lindvall, O. (2003). Inflammation is detrimental for neurogenesis in adult brain. *Proc Natl Acad Sci USA* 100, 13632-13637.
- Elder, G.A., Gama Sosa, M.A., and De Gasperi, R. (2010). Transgenic mouse models of Alzheimer's disease. *Mt Sinai J Med* 77, 69-81.
- Etnier, J.L., Caselli, R.J., Reiman, E.M., Alexander, G.E., Sibley, B.A., Tessier, D., and Mclemore, E.C. (2007). Cognitive performance in older women relative to ApoE-epsilon4 genotype and aerobic fitness. *Med Sci Sports Exerc* 39, 199-207.
- Evans, C.G., Wisen, S., and Gestwicki, J.E. (2006). Heat shock proteins 70 and 90 inhibit early stages of amyloid beta-(1-42) aggregation in vitro. *J Biol Chem* 281, 33182-33191.
- Farrer, L.A., Cupples, L.A., Haines, J.L., Hyman, B., Kukull, W.A., Mayeux, R., Myers, R.H., Pericak-Vance, M.A., Risch, N., and Van Duijn, C.M. (1997). Effects of age, sex, and ethnicity on the association between apolipoprotein E genotype and Alzheimer disease. A meta-analysis. APOE and Alzheimer Disease Meta Analysis Consortium. *JAMA* 278, 1349-1356.
- Farris, W., Mansourian, S., Chang, Y., Lindsley, L., Eckman, E.A., Frosch, M.P., Eckman, C.B., Tanzi, R.E., Selkoe, D.J., and Guénette, S. (2003). Insulin-degrading enzyme regulates the levels of insulin, amyloid β -protein, and the β -amyloid precursor protein intracellular domain in vivo. *Proceedings of the National Academy of Sciences* 100, 4162-4167.
- Farris, W., Schütz, S.G., Cirrito, J.R., Shankar, G.M., Sun, X., George, A., Leissring, M.A., Walsh, D.M., Qiu, W.Q., Holtzman, D.M., and Selkoe, D.J. (2007). Loss of Nephilysin Function Promotes

- Amyloid Plaque Formation and Causes Cerebral Amyloid Angiopathy. *The American Journal of Pathology* 171, 241-251.
- Feng, R., Rampon, C., Tang, Y.P., Shrom, D., Jin, J., Kyin, M., Sopher, B., Miller, M.W., Ware, C.B., Martin, G.M., Kim, S.H., Langdon, R.B., Sisodia, S.S., and Tsien, J.Z. (2001). Deficient neurogenesis in forebrain-specific presenilin-1 knockout mice is associated with reduced clearance of hippocampal memory traces. *Neuron* 32, 911-926.
- Forstl, H., and Kurz, A. (1999). Clinical features of Alzheimer's disease. *Eur Arch Psychiatry Clin Neurosci* 249, 288-290.
- Francis, R., Mcgrath, G., Zhang, J., Ruddy, D.A., Sym, M., Apfeld, J., Nicoll, M., Maxwell, M., Hai, B., Ellis, M.C., Parks, A.L., Xu, W., Li, J., Gurney, M., Myers, R.L., Himes, C.S., Hiebsch, R., Ruble, C., Nye, J.S., and Curtis, D. (2002). *aph-1* and *pen-2* are required for Notch pathway signaling, gamma-secretase cleavage of betaAPP, and presenilin protein accumulation. *Dev Cell* 3, 85-97.
- Frank, E.M. (1994). Effect of Alzheimer's disease on communication function. *J S C Med Assoc* 90, 417-423.
- Fukami, S., Watanabe, K., Iwata, N., Haraoka, J., Lu, B., Gerard, N.P., Gerard, C., Fraser, P., Westaway, D., St George-Hyslop, P., and Saido, T.C. (2002). Abeta-degrading endopeptidase, neprilysin, in mouse brain: synaptic and axonal localization inversely correlating with Abeta pathology. *Neurosci Res* 43, 39-56.
- Furini, C.R., Rossato, J.I., Bitencourt, L.L., Medina, J.H., Izquierdo, I., and Cammarota, M. (2010). Beta-adrenergic receptors link NO/sGC/PKG signaling to BDNF expression during the consolidation of object recognition long-term memory. *Hippocampus* 20, 672-683.
- Games, D., Adams, D., Alessandrini, R., Barbour, R., Berthelette, P., Blackwell, C., Carr, T., Clemens, J., Donaldson, T., Gillespie, F., and Et Al. (1995). Alzheimer-type neuropathology in transgenic mice overexpressing V717F beta-amyloid precursor protein. *Nature* 373, 523-527.
- Gatz, M., Reynolds, C.A., Fratiglioni, L., Johansson, B., Mortimer, J.A., Berg, S., Fiske, A., and Pedersen, N.L. (2006). Role of genes and environments for explaining Alzheimer disease. *Arch Gen Psychiatry* 63, 168-174.
- Glabe, C.G., and Kaye, R. (2006). Common structure and toxic function of amyloid oligomers implies a common mechanism of pathogenesis. *Neurology*. 66, S74-78.
- Greenough, W.T., and Volkmar, F.R. (1973). Pattern of dendritic branching in occipital cortex of rats reared in complex environments. *Exp Neurol* 40, 491-504.
- Guzman, E.A., Bouter, Y., Richard, B.C., Lannfelt, L., Ingelsson, M., Paetau, A., Verkkoniemi-Ahola, A., Wirths, O., and Bayer, T.A. (2014). Abundance of Abeta5-x like immunoreactivity in transgenic 5XFAD, APP/PS1KI and 3xTG mice, sporadic and familial Alzheimer's disease. *Mol Neurodegener* 9, 13.
- Gyure, K.A., Durham, R., Stewart, W.F., Smialek, J.E., and Troncoso, J.C. (2001). Intraneuronal abeta-amyloid precedes development of amyloid plaques in Down syndrome. *Arch Pathol Lab Med* 125, 489-492.
- Haass, C., Hung, A.Y., Schlossmacher, M.G., Teplow, D.B., and Selkoe, D.J. (1993). beta-Amyloid peptide and a 3-kDa fragment are derived by distinct cellular mechanisms. *J Biol Chem* 268, 3021-3024.
- Haass, C., Kaether, C., Thinakaran, G., and Sisodia, S. (2012). Trafficking and Proteolytic Processing of APP. *Cold Spring Harb Perspect Med* 2, a006270.
- Haass, C., Schlossmacher, M.G., Hung, A.Y., Vigo-Pelfrey, C., Mellon, A., Ostaszewski, B.L., Lieberburg, I., Koo, E.H., Schenk, D., Teplow, D.B., and Selkoe, D.J. (1992). Amyloid [beta]-peptide is produced by cultured cells during normal metabolism. *Nature* 359, 322-325.
- Haass, C., and Selkoe, D.J. (2007). Soluble protein oligomers in neurodegeneration: lessons from the Alzheimer's amyloid [beta]-peptide. *Nat Rev Mol Cell Biol* 8, 101-112.
- Hama, E., Shirotani, K., Iwata, N., and Saido, T.C. (2004). Effects of neprilysin chimeric proteins targeted to subcellular compartments on amyloid beta peptide clearance in primary neurons. *J Biol Chem* 279, 30259-30264.

- Hardy, J., and Allsop, D. (1991). Amyloid deposition as the central event in the aetiology of Alzheimer's disease. *Trends Pharmacol Sci* 12, 383-388.
- Harold, D., Abraham, R., Hollingworth, P., Sims, R., Gerrish, A., Hamshere, M.L., Pahwa, J.S., Moskvina, V., Dowzell, K., Williams, A., Jones, N., Thomas, C., Stretton, A., Morgan, A.R., Lovestone, S., Powell, J., Proitsi, P., Lupton, M.K., Brayne, C., Rubinsztein, D.C., Gill, M., Lawlor, B., Lynch, A., Morgan, K., Brown, K.S., Passmore, P.A., Craig, D., McGuinness, B., Todd, S., Holmes, C., Mann, D., Smith, A.D., Love, S., Kehoe, P.G., Hardy, J., Mead, S., Fox, N., Rossor, M., Collinge, J., Maier, W., Jessen, F., Schurmann, B., Heun, R., Van Den Bussche, H., Heuser, I., Kornhuber, J., Wiltfang, J., Dichgans, M., Frolich, L., Hampel, H., Hull, M., Rujescu, D., Goate, A.M., Kauwe, J.S., Cruchaga, C., Nowotny, P., Morris, J.C., Mayo, K., Sleegers, K., Bettens, K., Engelborghs, S., De Deyn, P.P., Van Broeckhoven, C., Livingston, G., Bass, N.J., Gurling, H., Mcquillin, A., Gwilliam, R., Deloukas, P., Al-Chalabi, A., Shaw, C.E., Tsolaki, M., Singleton, A.B., Guerreiro, R., Muhleisen, T.W., Nothen, M.M., Moebus, S., Jockel, K.H., Klopp, N., Wichmann, H.E., Carrasquillo, M.M., Pankratz, V.S., Younkin, S.G., Holmans, P.A., O'donovan, M., Owen, M.J., and Williams, J. (2009). Genome-wide association study identifies variants at CLU and PICALM associated with Alzheimer's disease. *Nat Genet* 41, 1088-1093.
- Harris-White, M.E., and Frautschy, S.A. (2005). Low density lipoprotein receptor-related proteins (LRPs), Alzheimer's and cognition. *Curr Drug Targets CNS Neurol Disord* 4, 469-480.
- Hashimoto, M., Bogdanovic, N., Volkman, I., Aoki, M., Winblad, B., and Tjernberg, L.O. (2010). Analysis of microdissected human neurons by a sensitive ELISA reveals a correlation between elevated intracellular concentrations of Abeta42 and Alzheimer's disease neuropathology. *Acta Neuropathol* 119, 543-554.
- Heraud, C., Goufak, D., Ando, K., Leroy, K., Suain, V., Yilmaz, Z., De Decker, R., Authelet, M., Laporte, V., Octave, J.N., and Brion, J.P. (2014). Increased misfolding and truncation of tau in APP/PS1/tau transgenic mice compared to mutant tau mice. *Neurobiol Dis* 62, 100-112.
- Heyn, P., Abreu, B.C., and Ottenbacher, K.J. (2004). The effects of exercise training on elderly persons with cognitive impairment and dementia: A meta-analysis. *Archives of Physical Medicine and Rehabilitation* 85, 1694-1704.
- Hillmann, A., Hahn, S., Schilling, S., Hoffmann, T., Demuth, H.U., Bulic, B., Schneider-Axmann, T., Bayer, T.A., Weggen, S., and Wirths, O. (2012). No improvement after chronic ibuprofen treatment in the 5XFAD mouse model of Alzheimer's disease. *Neurobiol Aging* 33, 833.e39-50.
- Holcomb, L., Gordon, M.N., McGowan, E., Yu, X., Benkovic, S., Jantzen, P., Wright, K., Saad, I., Mueller, R., Morgan, D., Sanders, S., Zehr, C., K, O.C., Hardy, J., Prada, C.M., Eckman, C., Younkin, S., Hsiao, K., and Duff, K. (1998). Accelerated Alzheimer-type phenotype in transgenic mice carrying both mutant amyloid precursor protein and presenilin 1 transgenes. *Nat Med* 4, 97-100.
- Hoozemans, J.J., Chafekar, S.M., Baas, F., Eikelenboom, P., and Scheper, W. (2006). Always around, never the same: pathways of amyloid beta induced neurodegeneration throughout the pathogenic cascade of Alzheimer's disease. *Curr Med Chem.* 13, 2599-2605.
- Hsiao, K.K., Chapman, P., Nilsen, S., Eckman, C., Harigaya, Y., Younkin, S., Yang, F., and Cole, G. (1996). Correlative memory deficits, Abeta elevation and amyloid plaques in transgenic mice. *Science* 274, 99-102.
- Hu, Y.-S., Long, N., Pigino, G., Brady, S.T., and Lazarov, O. (2013). Molecular Mechanisms of Environmental Enrichment: Impairments in Akt/GSK3 β , Neurotrophin-3 and CREB Signaling. *PLoS ONE* 8, e64460.
- Huang, E.J., and Reichardt, L.F. (2001). Neurotrophins: roles in neuronal development and function. *Annu Rev Neurosci* 24, 677-736.
- Huang, S.M., Mouri, A., Kokubo, H., Nakajima, R., Suemoto, T., Higuchi, M., Staufenbiel, M., Noda, Y., Yamaguchi, H., Nabeshima, T., Saido, T.C., and Iwata, N. (2006). Nephrilysin-sensitive

- synapse-associated amyloid-beta peptide oligomers impair neuronal plasticity and cognitive function. *J Biol Chem* 281, 17941-17951.
- Hüttenrauch, M., Baches, S., Gerth, J., Bayer, T.A., Weggen, S., Wirths, O. (2015). Neprilysin deficiency alters the neuropathological and behavioral phenotype in the 5XFAD mouse model of Alzheimer's disease. *J Alzheimers Dis* 44, 1291-302.
- Hüttenrauch, M., Brauß, A., Kurdakova, A., Borgers, H., Klinker, F., Liebetanz, D., Salinas-Riester, G., Wiltfang, J., Klafki, H., Wirths, O. (2016). Physical activity delays hippocampal neurodegeneration and rescues memory deficits in an Alzheimer disease mouse model. *Transl Psychiatry*. In press
- Ickes, B.R., Pham, T.M., Sanders, L.A., Albeck, D.S., Mohammed, A.H., and Granholm, A.C. (2000). Long-term environmental enrichment leads to regional increases in neurotrophin levels in rat brain. *Exp Neurol* 164, 45-52.
- Iijima-Ando, K., Hearn, S.A., Granger, L., Shenton, C., Gatt, A., Chiang, H.C., Hakker, I., Zhong, Y., and Iijima, K. (2008). Overexpression of neprilysin reduces alzheimer amyloid-beta42 (Abeta42)-induced neuron loss and intraneuronal Abeta42 deposits but causes a reduction in cAMP-responsive element-binding protein-mediated transcription, age-dependent axon pathology, and premature death in Drosophila. *J Biol Chem* 283, 19066-19076.
- Ingelsson, M., Fukumoto, H., Newell, K.L., Growdon, J.H., Hedley-Whyte, E.T., Frosch, M.P., Albert, M.S., Hyman, B.T., and Irizarry, M.C. (2004). Early Abeta accumulation and progressive synaptic loss, gliosis, and tangle formation in AD brain. *Neurology* 62, 925-931.
- Iso-Markku, P., Waller, K., Kujala, U.M., and Kaprio, J. (2015). Physical activity and dementia: Long-term follow-up study of adult twins. *Ann Med*, 1-7.
- Itagaki, S., McGeer, P.L., Akiyama, H., Zhu, S., and Selkoe, D. (1989). Relationship of microglia and astrocytes to amyloid deposits of Alzheimer disease. *J Neuroimmunol* 24, 173-182.
- Itnner, L.M., and Gotz, J. (2011). Amyloid-beta and tau--a toxic pas de deux in Alzheimer's disease. *Nat Rev Neurosci* 12, 65-72.
- Iwata, N., Higuchi, M., and Saido, T.C. (2005). Metabolism of amyloid-beta peptide and Alzheimer's disease. *Pharmacol Ther* 108, 129-148.
- Iwata, N., Takaki, Y., Fukami, S., Tsubuki, S., and Saido, T.C. (2002). Region-specific reduction of A beta-degrading endopeptidase, neprilysin, in mouse hippocampus upon aging. *J Neurosci Res* 70, 493-500.
- Iwata, N., Tsubuki, S., Takaki, Y., Shirotani, K., Lu, B., Gerard, N.P., Gerard, C., Hama, E., Lee, H.J., and Saido, T.C. (2001). Metabolic regulation of brain Abeta by neprilysin. *Science* 292, 1550-1552.
- Iwata, N., Tsubuki, S., Takaki, Y., Watanabe, K., Sekiguchi, M., Hosoki, E., Kawashima-Morishima, M., Lee, H.J., Hama, E., Sekine-Aizawa, Y., and Saido, T.C. (2000). Identification of the major Abeta1-42-degrading catabolic pathway in brain parenchyma: suppression leads to biochemical and pathological deposition. *Nat Med* 6, 143-150.
- Jack, C.R., Jr., Shiung, M.M., Weigand, S.D., O'Brien, P.C., Gunter, J.L., Boeve, B.F., Knopman, D.S., Smith, G.E., Ivnik, R.J., Tangalos, E.G., and Petersen, R.C. (2005). Brain atrophy rates predict subsequent clinical conversion in normal elderly and amnesic MCI. *Neurology* 65, 1227-1231.
- Jankowsky, J.L., Xu, G., Fromholt, D., Gonzales, V., and Borchelt, D.R. (2003). Environmental enrichment exacerbates amyloid plaque formation in a transgenic mouse model of Alzheimer disease. *J Neuropathol Exp Neurol* 62, 1220-1227.
- Jawhar, S., Trawicka, A., Jenneckens, C., Bayer, T.A., and Wirths, O. (2012). Motor deficits, neuron loss, and reduced anxiety coinciding with axonal degeneration and intraneuronal Abeta aggregation in the 5XFAD mouse model of Alzheimer's disease. *Neurobiol Aging* 33, 196.e29-40.
- Jay, P., Rougeulle, C., Massacrier, A., Moncla, A., Mattei, M.G., Malzac, P., Roeckel, N., Taviaux, S., Lefranc, J.L., Cau, P., Berta, P., Lalande, M., and Muscatelli, F. (1997). The human necdin

- gene, NDN, is maternally imprinted and located in the Prader-Willi syndrome chromosomal region. *Nat Genet* 17, 357-361.
- Ji, Y., Gong, Y., Gan, W., Beach, T., Holtzman, D.M., and Wisniewski, T. (2003). Apolipoprotein E isoform-specific regulation of dendritic spine morphology in apolipoprotein E transgenic mice and Alzheimer's disease patients. *Neuroscience* 122, 305-315.
- Kanemitsu, H., Tomiyama, T., and Mori, H. (2003). Human neprilysin is capable of degrading amyloid beta peptide not only in the monomeric form but also the pathological oligomeric form. *Neurosci Lett* 350, 113-116.
- Kang, E.B., Kwon, I.S., Koo, J.H., Kim, E.J., Kim, C.H., Lee, J., Yang, C.H., Lee, Y.I., Cho, I.H., and Cho, J.Y. (2013). Treadmill exercise represses neuronal cell death and inflammation during Abeta-induced ER stress by regulating unfolded protein response in aged presenilin 2 mutant mice. *Apoptosis* 18, 1332-1347.
- Karl, T., Pabst, R., and Von Horsten, S. (2003). Behavioral phenotyping of mice in pharmacological and toxicological research. *Exp Toxicol Pathol.* 55, 69-83.
- Katzman, R. (1993). Education and the prevalence of dementia and Alzheimer's disease. *Neurology* 43, 13-20.
- Katzman, R., Terry, R., DeTeresa, R., Brown, T., Davies, P., Fuld, P., Renbing, X., and Peck, A. (1988). Clinical, pathological, and neurochemical changes in dementia: a subgroup with preserved mental status and numerous neocortical plaques. *Ann Neurol* 23, 138-144.
- Ke, H.-C., Huang, H.-J., Liang, K.-C., and Hsieh-Li, H.M. (2011). Selective improvement of cognitive function in adult and aged APP/PS1 transgenic mice by continuous non-shock treadmill exercise. *Brain Research* 1403, 1-11.
- Kempermann, G. (2002). Why new neurons? Possible functions for adult hippocampal neurogenesis. *J Neurosci* 22, 635-638.
- Kempermann, G., Fabel, K., Ehninger, D., Babu, H., Leal-Galicia, P., Garthe, A., and Wolf, S.A. (2010). Why and how physical activity promotes experience-induced brain plasticity. *Front Neurosci* 4, 189.
- Kempermann, G., Kuhn, H.G., and Gage, F.H. (1997). More hippocampal neurons in adult mice living in an enriched environment. *Nature* 386, 493-495.
- Kempermann, G., Kuhn, H.G., and Gage, F.H. (1998). Experience-induced neurogenesis in the senescent dentate gyrus. *J Neurosci* 18, 3206-3212.
- Kennelly, S.P., Lawlor, B.A., and Kenny, R.A. (2009). Blood pressure and dementia - a comprehensive review. *Ther Adv Neurol Disord* 2, 241-260.
- Kidd, M. (1963). Paired helical filaments in electron microscopy of Alzheimer's disease. *Nature* 197, 192-193.
- Kobilo, T., Liu, Q.R., Gandhi, K., Mughal, M., Shaham, Y., and Van Praag, H. (2011). Running is the neurogenic and neurotrophic stimulus in environmental enrichment. *Learn Mem* 18, 605-609.
- Kuhn, H.G., Dickinson-Anson, H., and Gage, F.H. (1996). Neurogenesis in the dentate gyrus of the adult rat: age-related decrease of neuronal progenitor proliferation. *J Neurosci* 16, 2027-2033.
- Kuhn, P.H., Wang, H., Dislich, B., Colombo, A., Zeitschel, U., Ellwart, J.W., Kremmer, E., Rossner, S., and Lichtenthaler, S.F. (2010). ADAM10 is the physiologically relevant, constitutive alpha-secretase of the amyloid precursor protein in primary neurons. *EMBO J* 29, 3020-3032.
- Lalonde, R., Fukuchi, K., and Strazielle, C. (2012). APP transgenic mice for modelling behavioural and psychological symptoms of dementia (BPSD). *Neurosci Biobehav Rev* 36, 1357-1375.
- Lancaster, G.I., Moller, K., Nielsen, B., Secher, N.H., Febbraio, M.A., and Nybo, L. (2004). Exercise induces the release of heat shock protein 72 from the human brain in vivo. *Cell Stress Chaperones* 9, 276-280.
- Landel, V., Baranger, K., Virard, I., Loriod, B., Khrestchatsky, M., Rivera, S., Benesch, P., and Feron, F. (2014). Temporal gene profiling of the 5XFAD transgenic mouse model

- highlights the importance of microglial activation in Alzheimer's disease. *Mol Neurodegener* 9, 33.
- Lazarov, O., Robinson, J., Tang, Y.P., Hairston, I.S., Korade-Mirnic, Z., Lee, V.M., Hersh, L.B., Sapolsky, R.M., Mirnic, K., and Sisodia, S.S. (2005). Environmental enrichment reduces Abeta levels and amyloid deposition in transgenic mice. *Cell* 120, 701-713.
- Leggio, M.G., Mandolesi, L., Federico, F., Spirito, F., Ricci, B., Gelfo, F., and Petrosini, L. (2005). Environmental enrichment promotes improved spatial abilities and enhanced dendritic growth in the rat. *Behav Brain Res* 163, 78-90.
- Leissring, M.A. (2014). Aβ degradation--the inside story. *Frontiers in Aging Neuroscience* 6, 229.
- Leissring, M.A., Farris, W., Chang, A.Y., Walsh, D.M., Wu, X., Sun, X., Frosch, M.P., and Selkoe, D.J. (2003). Enhanced proteolysis of beta-amyloid in APP transgenic mice prevents plaque formation, secondary pathology, and premature death. *Neuron* 40, 1087-1093.
- Lesne, S., Kotilinek, L., and Ashe, K.H. (2008). Plaque-bearing mice with reduced levels of oligomeric amyloid-beta assemblies have intact memory function. *Neuroscience* 151, 745-749.
- Levi, O., and Michaelson, D.M. (2007). Environmental enrichment stimulates neurogenesis in apolipoprotein E3 and neuronal apoptosis in apolipoprotein E4 transgenic mice. *J Neurochem* 100, 202-210.
- Li, C., Niu, W., Jiang, C.H., and Hu, Y. (2007). Effects of enriched environment on gene expression and signal pathways in cortex of hippocampal CA1 specific NMDAR1 knockout mice. *Brain Res Bull* 71, 568-577.
- Linnarsson, S., Bjorklund, A., and Ernfors, P. (1997). Learning deficit in BDNF mutant mice. *Eur J Neurosci* 9, 2581-2587.
- Liu, H.-L., Zhao, G., Cai, K., Zhao, H.-H., and Shi, L.-D. (2011). Treadmill exercise prevents decline in spatial learning and memory in APP/PS1 transgenic mice through improvement of hippocampal long-term potentiation. *Behavioural Brain Research* 218, 308-314.
- Liu, H.-L., Zhao, G., Zhang, H., and Shi, L.-D. (2013). Long-term treadmill exercise inhibits the progression of Alzheimer's disease-like neuropathology in the hippocampus of APP/PS1 transgenic mice. *Behavioural Brain Research* 256, 261-272.
- Liu, Y., and Chang, A. (2008). Heat shock response relieves ER stress. *EMBO J* 27, 1049-1059.
- Lu, B., Gerard, N.P., Kolakowski, L.F., Jr., Bozza, M., Zurakowski, D., Finco, O., Carroll, M.C., and Gerard, C. (1995). Neutral endopeptidase modulation of septic shock. *J Exp Med* 181, 2271-2275.
- Lu, F.P., Lin, K.P., and Kuo, H.K. (2009). Diabetes and the risk of multi-system aging phenotypes: a systematic review and meta-analysis. *PLoS One* 4, e4144.
- Luong, T.N., Carlisle, H.J., Southwell, A., and Patterson, P.H. (2011). Assessment of motor balance and coordination in mice using the balance beam. *J Vis Exp* 49, 2376.
- Lyketsos, C.G., and Olin, J. (2002). Depression in Alzheimer's disease: overview and treatment. *Biol Psychiatry* 52, 243-252.
- Madani, R., Poirier, R., Wolfer, D.P., Welzl, H., Groscurth, P., Lipp, H.P., Lu, B., El Mouedden, M., Mercken, M., Nitsch, R.M., and Mohajeri, M.H. (2006). Lack of neprilysin suffices to generate murine amyloid-like deposits in the brain and behavioral deficit in vivo. *J Neurosci Res* 84, 1871-1878.
- Magrane, J., Smith, R.C., Walsh, K., and Querfurth, H.W. (2004). Heat shock protein 70 participates in the neuroprotective response to intracellularly expressed beta-amyloid in neurons. *J Neurosci* 24, 1700-1706.
- Makizako, H., Liu-Ambrose, T., Shimada, H., Doi, T., Park, H., Tsutsumimoto, K., Uemura, K., and Suzuki, T. (2014). Moderate-Intensity Physical Activity, Hippocampal Volume, and Memory in Older Adults With Mild Cognitive Impairment. *J Gerontol A Biol Sci Med Sci* 70, 480-6.
- Mandolesi, L., De Bartolo, P., Foti, F., Gelfo, F., Federico, F., Leggio, M.G., and Petrosini, L. (2008). Environmental enrichment provides a cognitive reserve to be spent in the case of brain lesion. *J Alzheimers Dis* 15, 11-28.

- Mandrekar-Colucci, S., and Landreth, G.E. (2010). Microglia and inflammation in Alzheimer's disease. *CNS Neurol Disord Drug Targets* 9, 156-167.
- Mansson, C., Arosio, P., Hussein, R., Kampinga, H.H., Hashem, R.M., Boelens, W.C., Dobson, C.M., Knowles, T.P., Linse, S., and Emanuelsson, C. (2014). Interaction of the molecular chaperone DNAJB6 with growing amyloid-beta 42 (Abeta42) aggregates leads to substoichiometric inhibition of amyloid formation. *J Biol Chem* 289, 31066-31076.
- Marlatt, M.W., Potter, M.C., Bayer, T.A., Van Praag, H., and Lucassen, P.J. (2013). Prolonged running, not fluoxetine treatment, increases neurogenesis, but does not alter neuropathology, in the 3xTg mouse model of Alzheimer's disease. *Curr Top Behav Neurosci* 15, 313-340.
- Marlatt, M.W., Potter, M.C., Lucassen, P.J., and Van Praag, H. (2012). Running throughout middle-age improves memory function, hippocampal neurogenesis, and BDNF levels in female C57BL/6J mice. *Developmental Neurobiology* 72, 943-952.
- Masters, C.L., Multhaup, G., Simms, G., Pottgiesser, J., Martins, R.N., and Beyreuther, K. (1985). Neuronal origin of a cerebral amyloid: neurofibrillary tangles of Alzheimer's disease contain the same protein as the amyloid of plaque cores and blood vessels. *Embo J* 4, 2757-2763.
- Matsas, R., Kenny, A.J., and Turner, A.J. (1986). An immunohistochemical study of endopeptidase-24.11 ("enkephalinase") in the pig nervous system. *Neuroscience* 18, 991-1012.
- Mattson, M.P. (1997). Cellular actions of beta-amyloid precursor protein and its soluble and fibrillogenic derivatives. *Physiol Rev* 77, 1081-1132.
- Mattson, M.P., Duan, W., Wan, R., and Guo, Z. (2004). Prophylactic activation of neuroprotective stress response pathways by dietary and behavioral manipulations. *NeuroRx* 1, 111-116.
- Mawuenyega, K.G., Sigurdson, W., Ovod, V., Munsell, L., Kasten, T., Morris, J.C., Yarasheski, K.E., and Bateman, R.J. (2010). Decreased clearance of CNS beta-amyloid in Alzheimer's disease. *Science* 330, 1774.
- Mcallister, A.K., Katz, L.C., and Lo, D.C. (1999). Neurotrophins and synaptic plasticity. *Annu Rev Neurosci* 22, 295-318.
- Mega, M.S., Cummings, J.L., Fiorello, T., and Gornbein, J. (1996). The spectrum of behavioral changes in Alzheimer's disease. *Neurology* 46, 130-135.
- Meilandt, W.J., Cisse, M., Ho, K., Wu, T., Esposito, L.A., Scarce-Levie, K., Cheng, I.H., Yu, G.Q., and Mucke, L. (2009). Neprilysin overexpression inhibits plaque formation but fails to reduce pathogenic Abeta oligomers and associated cognitive deficits in human amyloid precursor protein transgenic mice. *J Neurosci* 29, 1977-1986.
- Meshi, D., Drew, M.R., Saxe, M., Ansorge, M.S., David, D., Santarelli, L., Malapani, C., Moore, H., and Hen, R. (2006). Hippocampal neurogenesis is not required for behavioral effects of environmental enrichment. *Nat Neurosci* 9, 729-731.
- Miners, J.S., Barua, N., Kehoe, P.G., Gill, S., and Love, S. (2011). Abeta-degrading enzymes: potential for treatment of Alzheimer disease. *J Neuropathol Exp Neurol* 70, 944-959.
- Mirochnic, S., Wolf, S., Staufenbiel, M., and Kempermann, G. (2009). Age effects on the regulation of adult hippocampal neurogenesis by physical activity and environmental enrichment in the APP23 mouse model of Alzheimer disease. *Hippocampus* 19, 1008-1018.
- Mizuno, M., Yamada, K., Olariu, A., Nawa, H., and Nabeshima, T. (2000). Involvement of brain-derived neurotrophic factor in spatial memory formation and maintenance in a radial arm maze test in rats. *J Neurosci* 20, 7116-7121.
- Mohajeri, M.H., and Wolfer, D.P. (2009). Neprilysin deficiency-dependent impairment of cognitive functions in a mouse model of amyloidosis. *Neurochem Res* 34, 717-726.
- Monro, O.R., Mackic, J.B., Yamada, S., Segal, M.B., Ghiso, J., Maurer, C., Calero, M., Frangione, B., and Zlokovic, B.V. (2002). Substitution at codon 22 reduces clearance of Alzheimer's amyloid-beta peptide from the cerebrospinal fluid and prevents its transport from the central nervous system into blood. *Neurobiol Aging* 23, 405-412.

- Moran, P.M., Higgins, L.S., Cordell, B., and Moser, P.C. (1995). Age-related learning deficits in transgenic mice expressing the 751-amino acid isoform of human beta-amyloid precursor protein. *Proc Natl Acad Sci U S A* 92, 5341-5345.
- Morris, J.C., Storandt, M., Mckeel, D.W., Jr., Rubin, E.H., Price, J.L., Grant, E.A., and Berg, L. (1996). Cerebral amyloid deposition and diffuse plaques in "normal" aging: Evidence for presymptomatic and very mild Alzheimer's disease. *Neurology* 46, 707-719.
- Morris, R. (1984). Developments of a water-maze procedure for studying spatial learning in the rat. *J Neurosci Methods*. 11, 47-60.
- Muscatelli, F., Abrous, D.N., Massacrier, A., Boccaccio, I., Le Moal, M., Cau, P., and Cremer, H. (2000). Disruption of the mouse Necdin gene results in hypothalamic and behavioral alterations reminiscent of the human Prader-Willi syndrome. *Hum Mol Genet* 9, 3101-3110.
- Nagahara, A.H., Mateling, M., Kovacs, I., Wang, L., Eggert, S., Rockenstein, E., Koo, E.H., Masliah, E., and Tuszynski, M.H. (2013). Early BDNF Treatment Ameliorates Cell Loss in the Entorhinal Cortex of APP Transgenic Mice. *The Journal of Neuroscience* 33, 15596-15602.
- Nagamatsu, L.S., Chan, A., Davis, J.C., Beattie, B.L., Graf, P., Voss, M.W., Sharma, D., and Liu-Ambrose, T. (2013). Physical activity improves verbal and spatial memory in older adults with probable mild cognitive impairment: a 6-month randomized controlled trial. *J Aging Res* 2013, 861893.
- Nalivaeva, N.N., Belyaev, N.D., Kerridge, C., and Turner, A.J. (2014). Amyloid-clearing proteins and their epigenetic regulation as a therapeutic target in Alzheimer's disease. *Front Aging Neurosci* 6, 235.
- Namba, Y., Tomonaga, M., Kawasaki, H., Otomo, E., and Ikeda, K. (1991). Apolipoprotein E immunoreactivity in cerebral amyloid deposits and neurofibrillary tangles in Alzheimer's disease and kuru plaque amyloid in Creutzfeldt-Jakob disease. *Brain Res* 541, 163-166.
- Neeper, S.A., Gómez-Pinilla, F., Choi, J., and Cotman, C.W. (1996). Physical activity increases mRNA for brain-derived neurotrophic factor and nerve growth factor in rat brain. *Brain Research* 726, 49-56.
- Nichol, K., Deeny, S.P., Seif, J., Camaclang, K., and Cotman, C.W. (2009). Exercise improves cognition and hippocampal plasticity in APOE ϵ 4 mice. *Alzheimer's & Dementia* 5, 287-294.
- Nichol, K.E., Parachikova, A.I., and Cotman, C.W. (2007). Three weeks of running wheel exposure improves cognitive performance in the aged Tg2576 mouse. *Behav Brain Res* 184, 124-132.
- Nickerson, M., Elphick, G.F., Campisi, J., Greenwood, B.N., and Fleshner, M. (2005). Physical activity alters the brain Hsp72 and IL-1beta responses to peripheral E. coli challenge. *Am J Physiol Regul Integr Comp Physiol* 289, R1665-1674.
- Nithianantharajah, J., and Hannan, A.J. (2006). Enriched environments, experience-dependent plasticity and disorders of the nervous system. *Nat Rev Neurosci* 7, 697-709.
- Norton, S., Matthews, F.E., Barnes, D.E., Yaffe, K., and Brayne, C. (2014). Potential for primary prevention of Alzheimer's disease: an analysis of population-based data. *The Lancet Neurology* 13, 788-794.
- O'callaghan, R.M., Ohle, R., and Kelly, A.M. (2007). The effects of forced exercise on hippocampal plasticity in the rat: A comparison of LTP, spatial- and non-spatial learning. *Behav Brain Res* 176, 362-366.
- Oakley, H., Cole, S.L., Logan, S., Maus, E., Shao, P., Craft, J., Guillozet-Bongaarts, A., Ohno, M., Disterhoft, J., Van Eldik, L., Berry, R., and Vassar, R. (2006). Intraneuronal beta-amyloid aggregates, neurodegeneration, and neuron loss in transgenic mice with five familial Alzheimer's disease mutations: potential factors in amyloid plaque formation. *J Neurosci*. 26, 10129-10140.
- Ohia-Nwoko, O., Montazari, S., Lau, Y.S., and Eriksen, J.L. (2014). Long-term treadmill exercise attenuates tau pathology in P301S tau transgenic mice. *Mol Neurodegener* 9, 54.

- Ou-Yang, M.H., and Van Nostrand, W.E. (2013). The absence of myelin basic protein promotes neuroinflammation and reduces amyloid beta-protein accumulation in Tg-5xFAD mice. *J Neuroinflammation* 10, 134.
- Ownby, R.L., Crocco, E., Acevedo, A., John, V., and Loewenstein, D. (2006). Depression and risk for Alzheimer disease: systematic review, meta-analysis, and metaregression analysis. *Arch Gen Psychiatry* 63, 530-538.
- Pacheco-Quinto, J., and Eckman, E.A. (2013). Endothelin-converting Enzymes Degrade Intracellular β -Amyloid Produced within the Endosomal/Lysosomal Pathway and Autophagosomes. *Journal of Biological Chemistry* 288, 5606-5615.
- Pacheco-Quinto, J., Herdt, A., Eckman, C.B., and Eckman, E.A. (2013). Endothelin-Converting Enzymes and Related Metalloproteases in Alzheimer's Disease. *Alzheimer's Disease: Advances For A New Century* IOS Press, Amsterdam, 101-110.
- Paillard-Borg, S., Fratiglioni, L., Xu, W., Winblad, B., and Wang, H.X. (2012). An active lifestyle postpones dementia onset by more than one year in very old adults. *J Alzheimers Dis* 31, 835-842.
- Pang, P.T., and Lu, B. (2004). Regulation of late-phase LTP and long-term memory in normal and aging hippocampus: role of secreted proteins tPA and BDNF. *Ageing Res Rev* 3, 407-430.
- Parachikova, A., Nichol, K.E., and Cotman, C.W. (2008). Short-term exercise in aged Tg2576 mice alters neuroinflammation and improves cognition. *Neurobiology of Disease* 30, 121-129.
- Pimplikar, S.W. (2009). Reassessing the amyloid cascade hypothesis of Alzheimer's disease. *Int J Biochem Cell Biol* 41, 1261-1268.
- Pitkälä, K.H., Pöysti, M.M., Laakkonen, M., and Et Al. (2013). Effects of the finnish alzheimer disease exercise trial (finalex): A randomized controlled trial. *JAMA Internal Medicine* 173, 894-901.
- Plassman, B.L., Havlik, R.J., Steffens, D.C., Helms, M.J., Newman, T.N., Drosdick, D., Phillips, C., Gau, B.A., Welsh-Bohmer, K.A., Burke, J.R., Guralnik, J.M., and Breitner, J.C. (2000). Documented head injury in early adulthood and risk of Alzheimer's disease and other dementias. *Neurology* 55, 1158-1166.
- Poirier, R., Wolfer, D.P., Welzl, H., Tracy, J., Galsworthy, M.J., Nitsch, R.M., and Mohajeri, M.H. (2006). Neuronal neprilysin overexpression is associated with attenuation of A β -related spatial memory deficit. *Neurobiology of Disease* 24, 475-483.
- Polito, L., Chierchia, A., Tunesi, M., Bouybayoune, I., Kehoe, P.G., Albani, D., and Forloni, G. (2014). Environmental Enrichment Lessens Cognitive Decline in APP23 Mice Without Affecting Brain Sirtuin Expression. *J Alzheimers Dis* 42, 851-864.
- Poo, M.M. (2001). Neurotrophins as synaptic modulators. *Nat Rev Neurosci* 2, 24-32.
- Portelius, E., Bogdanovic, N., Gustavsson, M.K., Volkman, I., Brinkmalm, G., Zetterberg, H., Winblad, B., and Blennow, K. (2010). Mass spectrometric characterization of brain amyloid beta isoform signatures in familial and sporadic Alzheimer's disease. *Acta Neuropathol* 120, 185-193.
- Priller, C., Bauer, T., Mitteregger, G., Krebs, B., Kretschmar, H.A., and Herms, J. (2006). Synapse formation and function is modulated by the amyloid precursor protein. *J Neurosci* 26, 7212-7221.
- Profenno, L.A., Porsteinsson, A.P., and Faraone, S.V. (2010). Meta-analysis of Alzheimer's disease risk with obesity, diabetes, and related disorders. *Biol Psychiatry* 67, 505-512.
- Querfurth, H.W., and Laferla, F.M. (2010). Alzheimer's disease. *N Engl J Med* 362, 329-344.
- Rademakers, R., and Rovelet-Lecrux, A. (2009). Recent insights into the molecular genetics of dementia. *Trends Neurosci* 32, 451-461.
- Rao, S.K., Ross, J.M., Harrison, F.E., Bernardo, A., Reiserer, R.S., Reiserer, R.S., Mobley, J.A., and McDonald, M.P. (2015). Differential proteomic and behavioral effects of long-term voluntary exercise in wild-type and APP-overexpressing transgenics. *Neurobiology of Disease* 78, 45-55.

- Redolat, R., and Mesa-Gresa, P. (2012). Potential benefits and limitations of enriched environments and cognitive activity on age-related behavioural decline. *Curr Top Behav Neurosci* 10, 293-316.
- Renkawek, K., Voorter, C.E., Bosman, G.J., Van Workum, F.P., and De Jong, W.W. (1994). Expression of alpha B-crystallin in Alzheimer's disease. *Acta Neuropathol* 87, 155-160.
- Renner, M., Lacor, P.N., Velasco, P.T., Xu, J., Contractor, A., Klein, W.L., and Triller, A. (2010). Deleterious effects of amyloid beta oligomers acting as an extracellular scaffold for mGluR5. *Neuron* 66, 739-754.
- Richard, B.C., Kurdakova, A., Baches, S., Bayer, T.A., Weggen, S., and Wirths, O. (2015). Gene Dosage Dependent Aggravation of the Neurological Phenotype in the 5XFAD Mouse Model of Alzheimer's Disease. *J Alzheimers Dis* 45, 1223-1236.
- Richter, H., Ambree, O., Lewejohann, L., Herring, A., Keyvani, K., Paulus, W., Palme, R., Touma, C., Schabitz, W.R., and Sachser, N. (2008). Wheel-running in a transgenic mouse model of Alzheimer's disease: protection or symptom? *Behav Brain Res* 190, 74-84.
- Richter, S.H., Gass, P., and Fuss, J. (2014). Resting Is Rusting: A Critical View on Rodent Wheel-Running Behavior. *The Neuroscientist* 20, 313-325.
- Rogers, J., Strohmeyer, R., Kovelowski, C.J., and Li, R. (2002). Microglia and inflammatory mechanisms in the clearance of amyloid beta peptide. *Glia* 40, 260-269.
- Rosenzweig, M.R., Krech, D., Bennett, E.L., and Zolman, J.F. (1962). Variation in environmental complexity and brain measures. *J Comp Physiol Psychol* 55, 1092-1095.
- Rossi, C., Angelucci, A., Costantin, L., Braschi, C., Mazzantini, M., Babbini, F., Fabbri, M.E., Tessarollo, L., Maffei, L., Berardi, N., and Caleo, M. (2006). Brain-derived neurotrophic factor (BDNF) is required for the enhancement of hippocampal neurogenesis following environmental enrichment. *Eur J Neurosci* 24, 1850-1856.
- Rovio, S., Kareholt, I., Helkala, E.L., Viitanen, M., Winblad, B., Tuomilehto, J., Soininen, H., Nissinen, A., and Kivipelto, M. (2005). Leisure-time physical activity at midlife and the risk of dementia and Alzheimer's disease. *Lancet Neurol* 4, 705-711.
- Roy, V., Belzung, C., Delarue, C., and Chapillon, P. (2001). Environmental enrichment in BALB/c mice: effects in classical tests of anxiety and exposure to a predatory odor. *Physiol Behav* 74, 313-320.
- Saarelainen, T., Pussinen, R., Koponen, E., Alhonen, L., Wong, G., Sirvio, J., and Castren, E. (2000). Transgenic mice overexpressing truncated trkB neurotrophin receptors in neurons have impaired long-term spatial memory but normal hippocampal LTP. *Synapse* 38, 102-104.
- Sabo, S.L., Ikin, A.F., Buxbaum, J.D., and Greengard, P. (2003). The amyloid precursor protein and its regulatory protein, FE65, in growth cones and synapses in vitro and in vivo. *J Neurosci* 23, 5407-5415.
- Sagare, A., Deane, R., Bell, R.D., Johnson, B., Hamm, K., Pendu, R., Marky, A., Lenting, P.J., Wu, Z., Zarcone, T., Goate, A., Mayo, K., Perlmutter, D., Coma, M., Zhong, Z., and Zlokovic, B.V. (2007). Clearance of amyloid-beta by circulating lipoprotein receptors. *Nat Med* 13, 1029-1031.
- Saitoh, T., Sundsmo, M., Roch, J.M., Kimura, N., Cole, G., Schubert, D., Oltersdorf, T., and Schenk, D.B. (1989). Secreted form of amyloid beta protein precursor is involved in the growth regulation of fibroblasts. *Cell* 58, 615-622.
- Sale, A., Berardi, N., and Maffei, L. (2014). Environment and Brain Plasticity: Towards an Endogenous Pharmacotherapy. *Physiological Reviews* 94, 189-234.
- Salkovic-Petrisic, M., Tribl, F., Schmidt, M., Hoyer, S., and Riederer, P. (2006). Alzheimer-like changes in protein kinase B and glycogen synthase kinase-3 in rat frontal cortex and hippocampus after damage to the insulin signalling pathway. *J Neurochem* 96, 1005-1015.
- Sarasa, M., and Pesini, P. (2009). Natural non-transgenic animal models for research in Alzheimer's disease. *Curr Alzheimer Res* 6, 171-178.

- Scarmeas, N., Hadjigeorgiou, G.M., Papadimitriou, A., Dubois, B., Sarazin, M., Brandt, J., Albert, M., Marder, K., Bell, K., Honig, L.S., Wegesin, D., and Stern, Y. (2004). Motor signs during the course of Alzheimer disease. *Neurology* 63, 975-982.
- Scarmeas, N., Luchsinger, J.A., Brickman, A.M., Cosentino, S., Schupf, N., Xin-Tang, M., Gu, Y., and Stern, Y. (2011). Physical activity and Alzheimer disease course. *Am J Geriatr Psychiatry* 19, 471-481.
- Scarmeas, N., Luchsinger, J.A., Schupf, N., Brickman, A.M., Cosentino, S., Tang, M.X., and Stern, Y. (2009). Physical activity, diet, and risk of Alzheimer disease. *Jama* 302, 627-637.
- Scheff, S.W., Price, D.A., Schmitt, F.A., Dekosky, S.T., and Mufson, E.J. (2007). Synaptic alterations in CA1 in mild Alzheimer disease and mild cognitive impairment. *Neurology* 68, 1501-1508.
- Scheuner, D., Eckman, C., Jensen, M., Song, X., Citron, M., Suzuki, N., Bird, T.D., Hardy, J., Hutton, M., Kukull, W., Larson, E., Levy-Lahad, E., Viitanen, M., Peskind, E., Poorkaj, P., Schellenberg, G., Tanzi, R., Wasco, W., Lannfelt, L., Selkoe, D., and Younkin, S. (1996). Secreted amyloid beta-protein similar to that in the senile plaques of Alzheimer's disease is increased in vivo by the presenilin 1 and 2 and APP mutations linked to familial Alzheimer's disease. *Nat Med* 2, 864-870.
- Schmittgen, T.D., and Livak, K.J. (2008). Analyzing real-time PCR data by the comparative C(T) method. *Nat Protoc* 3, 1101-1108.
- Schwab, C., Klegeris, A., and McGeer, P.L. (2010). Inflammation in transgenic mouse models of neurodegenerative disorders. *Biochimica et Biophysica Acta (BBA) - Molecular Basis of Disease* 1802, 889-902.
- Selkoe, D.J. (2001). Alzheimer's disease: genes, proteins, and therapy. *Physiol Rev* 81, 741-766.
- Serrano-Pozo, A., Frosch, M.P., Masliah, E., and Hyman, B.T. (2011). Neuropathological Alterations in Alzheimer Disease. *Cold Spring Harbor Perspectives in Medicine* 1, a006189.
- Shammas, S.L., Waudby, C.A., Wang, S., Buell, A.K., Knowles, T.P., Ecroyd, H., Welland, M.E., Carver, J.A., Dobson, C.M., and Meehan, S. (2011). Binding of the molecular chaperone alphaB-crystallin to Abeta amyloid fibrils inhibits fibril elongation. *Biophys J* 101, 1681-1689.
- Shibata, M., Yamada, S., Kumar, S.R., Calero, M., Bading, J., Frangione, B., Holtzman, D.M., Miller, C.A., Strickland, D.K., Ghiso, J., and Zlokovic, B.V. (2000). Clearance of Alzheimer's amyloid-ss(1-40) peptide from brain by LDL receptor-related protein-1 at the blood-brain barrier. *J Clin Invest* 106, 1489-1499.
- Shimohama, S. (2000). Apoptosis in Alzheimer's disease--an update. *Apoptosis* 5, 9-16.
- Shinohara, H., Inaguma, Y., Goto, S., Inagaki, T., and Kato, K. (1993). Alpha B crystallin and HSP28 are enhanced in the cerebral cortex of patients with Alzheimer's disease. *J Neurol Sci* 119, 203-208.
- Shukla, V., Zheng, Y.L., Mishra, S.K., Amin, N.D., Steiner, J., Grant, P., Kesavapany, S., and Pant, H.C. (2013). A truncated peptide from p35, a Cdk5 activator, prevents Alzheimer's disease phenotypes in model mice. *FASEB J* 27, 174-186.
- Silvers, J.M., Harrod, S.B., Mactutus, C.F., and Booze, R.M. (2007). Automation of the novel object recognition task for use in adolescent rats. *J Neurosci Methods* 166, 99-103.
- Sisodia, S.S. (1992). Beta-amyloid precursor protein cleavage by a membrane-bound protease. *Proc Natl Acad Sci U S A* 89, 6075-6079.
- Small, G.W. (1998). The pathogenesis of Alzheimer's disease. *J Clin Psychiatry* 59 Suppl 9, 7-14.
- Snowdon, D.A. (2003). Healthy aging and dementia: findings from the Nun Study. *Ann Intern Med* 139, 450-454.
- Souza, L.C., Filho, C.B., Goes, A.T., Fabbro, L.D., De Gomes, M.G., Savegnago, L., Oliveira, M.S., and Jesse, C.R. (2013). Neuroprotective effect of physical exercise in a mouse model of Alzheimer's disease induced by beta-amyloid(1)(-)(4)(0) peptide. *Neurotox Res* 24, 148-163.
- Sperling, R.A., Aisen, P.S., Beckett, L.A., Bennett, D.A., Craft, S., Fagan, A.M., Iwatsubo, T., Jack, C.R., Jr., Kaye, J., Montine, T.J., Park, D.C., Reiman, E.M., Rowe, C.C., Siemers, E., Stern, Y.,

- Yaffe, K., Carrillo, M.C., Thies, B., Morrison-Bogorad, M., Wagster, M.V., and Phelps, C.H. (2011). Toward defining the preclinical stages of Alzheimer's disease: recommendations from the National Institute on Aging-Alzheimer's Association workgroups on diagnostic guidelines for Alzheimer's disease. *Alzheimers Dement* 7, 280-292.
- Squire, L.R., Zola-Morgan, S., and Clark, R.E. (2007). Recognition memory and the medial temporal lobe: a new perspective. *Nat Rev Neurosci* 8, 872-883.
- Squire, L.R., and Zola-Morgan, S. (1991). The medial temporal lobe memory system. *Science* 253, 1380-1386.
- Stern, Y. (2002). What is cognitive reserve? Theory and research application of the reserve concept. *J Int Neuropsychol Soc* 8, 448-460.
- Stern, Y. (2009). Cognitive reserve. *Neuropsychologia* 47, 2015-2028.
- Strittmatter, W.J., Saunders, A.M., Schmechel, D., Pericak-Vance, M., Enghild, J., Salvesen, G.S., and Roses, A.D. (1993). Apolipoprotein E: high-avidity binding to beta-amyloid and increased frequency of type 4 allele in late-onset familial Alzheimer disease. *Proc Natl Acad Sci U S A* 90, 1977-1981.
- Tanzi, R.E. (2012). The Genetics of Alzheimer Disease. *Cold Spring Harb Perspect Med* 2, a006296.
- Tapia-Rojas, C., Aranguiz, F., Varela-Nallar, L., and Inestrosa, N.C. (2015). Voluntary Running Attenuates Memory Loss, Decreases Neuropathological Changes and Induces Neurogenesis in a Mouse Model of Alzheimer's Disease. *Brain Pathology* 26, 62-74.
- Tarasoff-Conway, J.M., Carare, R.O., Osorio, R.S., Glodzik, L., Butler, T., Fieremans, E., Axel, L., Rusinek, H., Nicholson, C., Zlokovic, B.V., Frangione, B., Blennow, K., Menard, J., Zetterberg, H., Wisniewski, T., and De Leon, M.J. (2015). Clearance systems in the brain-implications for Alzheimer disease. *Nat Rev Neurol* 11, 457-470.
- Thal, D.R., Rub, U., Orantes, M., and Braak, H. (2002). Phases of A beta-deposition in the human brain and its relevance for the development of AD. *Neurology* 58, 1791-1800.
- Thiriet, N., Amar, L., Toussay, X., Lardeux, V., Ladenheim, B., Becker, K.G., Cadet, J.L., Solinas, M., and Jaber, M. (2008). Environmental enrichment during adolescence regulates gene expression in the striatum of mice. *Brain Res* 1222, 31-41.
- Tolwani, R.J., Buckmaster, P.S., Varma, S., Cosgaya, J.M., Wu, Y., Suri, C., and Shooter, E.M. (2002). BDNF overexpression increases dendrite complexity in hippocampal dentate gyrus. *Neuroscience* 114, 795-805.
- Tong, L., Shen, H., Perreau, V.M., Balazs, R., and Cotman, C.W. (2001). Effects of exercise on gene-expression profile in the rat hippocampus. *Neurobiol Dis* 8, 1046-1056.
- Turner, A.J., Isaac, R.E., and Coates, D. (2001). The neprilysin (NEP) family of zinc metalloendopeptidases: genomics and function. *Bioessays* 23, 261-269.
- Turner, A.M., and Greenough, W.T. (1985). Differential rearing effects on rat visual cortex synapses. I. Synaptic and neuronal density and synapses per neuron. *Brain Res* 329, 195-203.
- Turner, P.R., O'connor, K., Tate, W.P., and Abraham, W.C. (2003). Roles of amyloid precursor protein and its fragments in regulating neural activity, plasticity and memory. *Prog Neurobiol* 70, 1-32.
- Tyas, S.L., Salazar, J.C., Snowden, D.A., Desrosiers, M.F., Riley, K.P., Mendiondo, M.S., and Kryscio, R.J. (2007a). Transitions to mild cognitive impairments, dementia, and death: findings from the Nun Study. *Am J Epidemiol* 165, 1231-1238.
- Tyas, S.L., Snowden, D.A., Desrosiers, M.F., Riley, K.P., and Markesbery, W.R. (2007b). Healthy ageing in the Nun Study: definition and neuropathologic correlates. *Age Ageing* 36, 650-655.
- Um, H.-S., Kang, E.-B., Koo, J.-H., Kim, H.-T., Jin, L., Kim, E.-J., Yang, C.-H., An, G.-Y., Cho, I.-H., and Cho, J.-Y. (2011). Treadmill exercise represses neuronal cell death in an aged transgenic mouse model of Alzheimer's disease. *Neuroscience Research* 69, 161-173.

- Uylings, H.B., Kuypers, K., Diamond, M.C., and Veltman, W.A. (1978). Effects of differential environments on plasticity of dendrites of cortical pyramidal neurons in adult rats. *Exp Neurol* 62, 658-677.
- Valenzuela, M.J. (2008). Brain reserve and the prevention of dementia. *Curr Opin Psychiatry* 21, 296-302.
- Valla, J., Yaari, R., Wolf, A.B., Kusne, Y., Beach, T.G., Roher, A.E., Corneveaux, J.J., Huentelman, M.J., Caselli, R.J., and Reiman, E.M. (2010). Reduced posterior cingulate mitochondrial activity in expired young adult carriers of the APOE epsilon4 allele, the major late-onset Alzheimer's susceptibility gene. *J Alzheimers Dis* 22, 307-313.
- Van Dorpe, J., Smeijers, L., Dewachter, I., Nuyens, D., Spittaels, K., Van Den Haute, C., Mercken, M., Moechars, D., Laenen, I., Kuiperi, C., Bruynseels, K., Tesseur, I., Loos, R., Vanderstichele, H., Checler, F., Sciot, R., and Van Leuven, F. (2000). Prominent cerebral amyloid angiopathy in transgenic mice overexpressing the london mutant of human APP in neurons. *Am J Pathol* 157, 1283-1298.
- Van Praag, H., Kempermann, G., and Gage, F.H. (1999). Running increases cell proliferation and neurogenesis in the adult mouse dentate gyrus. *Nat Neurosci* 2, 266-270.
- Van Praag, H., Kempermann, G., and Gage, F.H. (2000). Neural consequences of environmental enrichment. *Nat Rev Neurosci* 1, 191-198.
- Van Praag, H., Shubert, T., Zhao, C., and Gage, F.H. (2005). Exercise enhances learning and hippocampal neurogenesis in aged mice. *J Neurosci* 25, 8680-8685.
- Vandal, M., Bourassa, P., and Calon, F. (2015). Can insulin signaling pathways be targeted to transport Abeta out of the brain? *Front Aging Neurosci* 7, 114.
- Vassar, R., Bennett, B.D., Babu-Khan, S., Kahn, S., Mendiaz, E.A., Denis, P., Teplow, D.B., Ross, S., Amarante, P., Loeloff, R., Luo, Y., Fisher, S., Fuller, J., Edenson, S., Lile, J., Jarosinski, M.A., Biere, A.L., Curran, E., Burgess, T., Louis, J.C., Collins, F., Treanor, J., Rogers, G., and Citron, M. (1999). Beta-secretase cleavage of Alzheimer's amyloid precursor protein by the transmembrane aspartic protease BACE. *Science* 286, 735-741.
- Veena, J., Srikumar, B.N., Raju, T.R., and Shankaranarayana Rao, B.S. (2009). Exposure to enriched environment restores the survival and differentiation of new born cells in the hippocampus and ameliorates depressive symptoms in chronically stressed rats. *Neurosci Lett* 455, 178-182.
- Vepsäläinen, S., Hiltunen, M., Helisalmi, S., Wang, J., Van Groen, T., Tanila, H., and Soininen, H. (2008). Increased expression of A β degrading enzyme IDE in the cortex of transgenic mice with Alzheimer's disease-like neuropathology. *Neuroscience Letters* 438, 216-220.
- Verret, L., Krezymon, A., Halley, H., Trouche, S., Zerwas, M., Lazouret, M., Lassalle, J.-M., and Rampon, C. (2013). Transient enriched housing before amyloidosis onset sustains cognitive improvement in Tg2576 mice. *Neurobiology of Aging* 34, 211-225.
- Vorhees, C.V., and Williams, M.T. (2006). Morris water maze: procedures for assessing spatial and related forms of learning and memory. *Nat Protoc* 1, 848-858.
- Voss, M.W., Prakash, R.S., Erickson, K.I., Basak, C., Chaddock, L., Kim, J.S., Alves, H., Heo, S., Szabo, A., White, S.M., Wojcicki, T.R., Mailey, E.L., Gothe, N., Olson, E.A., Mcauley, E., and Kramer, A.F. (2010). Plasticity of brain networks in a randomized intervention trial of exercise training in older adults. *Frontiers in Aging Neuroscience* 2, 32.
- Walf, A.A., and Frye, C.A. (2007). The use of the elevated plus maze as an assay of anxiety-related behavior in rodents. *Nat Protoc* 2, 322-328.
- Walsh, D.M., and Selkoe, D.J. (2007). A β Oligomers – a decade of discovery. *Journal of Neurochemistry* 101, 1172-1184.
- Wang, D.S., Dickson, D.W., and Malter, J.S. (2006). beta-Amyloid degradation and Alzheimer's disease. *J Biomed Biotechnol* 2006, 58406.
- Wang, Q., Xu, Z., Tang, J., Sun, J., Gao, J., Wu, T., and Xiao, M. (2013). Voluntary exercise counteracts A β 25-35-induced memory impairment in mice. *Behavioural Brain Research* 256, 618-625.
- Wang, S., Wang, R., Chen, L., Bennett, D.A., Dickson, D.W., and Wang, D.S. (2010). Expression and functional profiling of neprilysin, insulin-degrading enzyme, and endothelin-

- converting enzyme in prospectively studied elderly and Alzheimer's brain. *J Neurochem* 115, 47-57.
- Wasco, W., Bupp, K., Magendantz, M., Gusella, J.F., Tanzi, R.E., and Solomon, F. (1992). Identification of a mouse brain cDNA that encodes a protein related to the Alzheimer disease-associated amyloid beta protein precursor. *Proc Natl Acad Sci U S A* 89, 10758-10762.
- Weidemann, A., König, G., Bunke, D., Fischer, P., Salbaum, J.M., Masters, C.L., and Beyreuther, K. (1989). Identification, biogenesis, and localization of precursors of Alzheimer's disease A4 amyloid protein. *Cell* 57, 115-126.
- Weller, R.O., Massey, A., Kuo, Y.M., and Roher, A.E. (2000). Cerebral amyloid angiopathy: accumulation of A beta in interstitial fluid drainage pathways in Alzheimer's disease. *Ann NY Acad Sci* 903, 110-117.
- Wietrzych, M., Meziane, H., Sutter, A., Ghyselinck, N., Chapman, P.F., Chambon, P., and Krężel, W. (2005). Working memory deficits in retinoid X receptor γ -deficient mice. *Learning & Memory* 12, 318-326.
- Wilhelmus, M.M., De Waal, R.M., and Verbeek, M.M. (2007). Heat shock proteins and amateur chaperones in amyloid-Beta accumulation and clearance in Alzheimer's disease. *Mol Neurobiol* 35, 203-216.
- Winters, B.D., Saksida, L.M., and Bussey, T.J. (2008). Object recognition memory: neurobiological mechanisms of encoding, consolidation and retrieval. *Neurosci Biobehav Rev* 32, 1055-1070.
- Wirh's, O., and Bayer, T.A. (2010). Neuron Loss in Transgenic Mouse Models of Alzheimer's Disease. *Int J Alzheimers Dis* 2010, pii: 723782.
- Wirh's, O., Erck, C., Martens, H., Harmeier, A., Geumann, C., Jawhar, S., Kumar, S., Multhaup, G., Walter, J., Ingelsson, M., Degerman-Gunnarsson, M., Kalimo, H., Huitinga, I., Lannfelt, L., and Bayer, T.A. (2010). Identification of low molecular weight pyroglutamate A β oligomers in Alzheimer disease: a novel tool for therapy and diagnosis. *Journal of Biological Chemistry* 285, 41517-41524.
- Wirh's, O., Multhaup, G., and Bayer, T.A. (2004). A modified beta-amyloid hypothesis: intraneuronal accumulation of the beta-amyloid peptide - the first step of a fatal cascade. *J Neurochem* 91, 513-520.
- Wisniewski, K.E., Wisniewski, H.M., and Wen, G.Y. (1985). Occurrence of neuropathological changes and dementia of Alzheimer's disease in Down's syndrome. *Ann Neurol* 17, 278-282.
- Witnam, J.L. (2012). The contribution of N-terminally modified amyloid beta to the etiology of Alzheimer's disease. PhD-Thesis, Georg-August-Universität Göttingen.
- Wolf, S.A., Kronenberg, G., Lehmann, K., Blankenship, A., Overall, R., Staufenbiel, M., and Kempermann, G. (2006). Cognitive and physical activity differently modulate disease progression in the amyloid precursor protein (APP)-23 model of Alzheimer's disease. *Biol Psychiatry*. 60, 1314-1323.
- Wolfe, M.S., Xia, W., Ostaszewski, B.L., Diehl, T.S., Kimberly, W.T., and Selkoe, D.J. (1999). Two transmembrane aspartates in presenilin-1 required for presenilin endoproteolysis and gamma-secretase activity. *Nature* 398, 513-517.
- Wyss-Coray, T., Loike, J.D., Brionne, T.C., Lu, E., Anankov, R., Yan, F., Silverstein, S.C., and Husemann, J. (2003). Adult mouse astrocytes degrade amyloid-beta in vitro and in situ. *Nat Med* 9, 453-457.
- Wyss-Coray, T., and Rogers, J. (2012). Inflammation in Alzheimer Disease—A Brief Review of the Basic Science and Clinical Literature. *Cold Spring Harbor Perspectives in Medicine* 2, a006346.
- Yamaguchi, H., Hirai, S., Morimatsu, M., Shoji, M., and Ihara, Y. (1988). A variety of cerebral amyloid deposits in the brains of the Alzheimer-type dementia demonstrated by beta protein immunostaining. *Acta Neuropathol* 76, 541-549.

- Yamazaki, T., Koo, E.H., and Selkoe, D.J. (1997). Cell surface amyloid beta-protein precursor colocalizes with beta 1 integrins at substrate contact sites in neural cells. *J Neurosci* 17, 1004-1010.
- Yasojima, K., Akiyama, H., Mcgeer, E.G., and Mcgeer, P.L. (2001). Reduced neprilysin in high plaque areas of Alzheimer brain: a possible relationship to deficient degradation of beta-amyloid peptide. *Neurosci Lett* 297, 97-100.
- Yoo, B.C., Kim, S.H., Cairns, N., Fountoulakis, M., and Lubec, G. (2001). Deranged expression of molecular chaperones in brains of patients with Alzheimer's disease. *Biochem Biophys Res Commun* 280, 249-258.
- Yoshikai, S., Sasaki, H., Doh-Ura, K., Furuya, H., and Sakaki, Y. (1990). Genomic organization of the human amyloid beta-protein precursor gene. *Gene* 87, 257-263.
- Yuede, C.M., Zimmerman, S.D., Dong, H., Kling, M.J., Bero, A.W., Holtzman, D.M., Timson, B.F., and Csernansky, J.G. (2009). Effects of voluntary and forced exercise on plaque deposition, hippocampal volume, and behavior in the Tg2576 mouse model of Alzheimer's disease. *Neurobiol Dis* 35, 426-432.
- Zhang, Z., Liu, X., Schroeder, J.P., Chan, C.-B., Song, M., Yu, S.P., Weinshenker, D., and Ye, K. (2014). 7,8-Dihydroxyflavone Prevents Synaptic Loss and Memory Deficits in a Mouse Model of Alzheimer's Disease. *Neuropsychopharmacology* 39, 638-650.
- Zheng, H., and Koo, E.H. (2011). Biology and pathophysiology of the amyloid precursor protein. *Mol Neurodegener* 6, 27.
- Zou, L.-B., Mouri, A., Iwata, N., Saido, T.C., Wang, D., Wang, M.-W., Mizoguchi, H., Noda, Y., and Nabeshima, T. (2006). Inhibition of Neprilysin by Infusion of Thiorphan into the Hippocampus Causes an Accumulation of Amyloid β and Impairment of Learning and Memory. *Journal of Pharmacology and Experimental Therapeutics* 317, 334-340.

CURRICULUM VITAE

Melanie Hüttenrauch

Kurze Straße 16 · 37073 Göttingen · Germany

Phone: +49 (0)160-97349717

E-Mail: huettenrauch.melanie@gmail.com

Date of Birth: May 14, 1989

Place of Birth: Heilbad Heiligenstadt

Citizenship: German

Education

- | | |
|-------------------|--|
| 05/2013 to date | Doctoral studies
University Medicine Göttingen (UMG), Department of Molecular Psychiatry
Thesis: „Alzheimer-like pathology in murine transgenic models: disease modification by environmental and genetic interventions“
Advisor: PD Dr. Oliver Wirths
Date of submission: March, 2015 |
| 10/2010 - 07/2012 | Master of Science (Biomedicine)
University of Würzburg
Thesis: „Studies on the regulatory effect of the PI3-kinase/mTOR inhibitor BEZ235 on the activity of the MAP-kinase signaling pathway“ (Theodor Boveri Institute, Biocenter, University of Würzburg)
Advisor: Prof. Dr. Martin Eilers
Overall Grade: 1.0 (excellent) |
| 10/2007 - 07/2010 | Bachelor of Science (Biomedicine)
University of Würzburg
Thesis: „Studies on platelet activity in genetically modified mice“ (Rudolf Virchow Center for Experimental Biomedicine, University of Würzburg)
Advisor: Prof. Dr. Bernhard Nieswandt
Overall Grade: 1.7 (good) |
| 06/2007 | High-School Diploma (Abitur)
Johann-Georg-Lingemann Gymnasium, Heilbad Heiligenstadt
Major subjects: Biology, German
Overall Grade: 1.2 |

Professional experience

03/2013 - 04/2013

Industrial Internship

IBA-Solutions for Life Sciences, Göttingen, Germany

Product Management/Marketing

Advisor: Bettina Renker

08/2012 - 03/2013

Research Associate

Theodor Boveri Institute, Biocenter, University of Würzburg, Germany

Topic: The effect of small molecule inhibitors on the activity of the MAP-kinase signaling pathway

Advisor: Prof. Dr. Martin Eilers

04/2011 - 07/2011

Research Internship

Karolinska Institutet, Stockholm, Sweden

Department for Cell and Molecular Biology

Topic: Effects of mutant Thyroid Hormone Receptor $\alpha 1$ on hypothalamic gene expression

Advisor: Prof. Dr. Jens Mittag

09/2010 - 10/2010

Research Internship

Max-Planck-Institute of Molecular Biomedicine, Münster, Germany

Department of Vascular Cell Biology

Topic: The role of CD99 and CD99L2 in leucocyte diapedesis

Advisor: Prof. Dr. Dietmar Vestweber

Publications

Hüttenrauch M, Brauß A, Kurdakova A, Borgers H, Klinker F, Liebetanz D, Salinas-Riester G, Wiltfang J, Klafki H, Wirths O. (2016)

Physical activity delays hippocampal neurodegeneration and rescues memory deficits in an Alzheimer disease mouse model.

Transl Psychiatry. 6:e800

Weissmann R*, **Hüttenrauch M***, Kacprowski T, Bouter Y, Pradier L, Bayer TA, Kuss AW, Wirths O. (2015)

Gene expression profiling in the APP/PS1KI mouse model of familial Alzheimer's disease.

J Alzheimers Dis. 50(2):397-409

* equal contribution

Wiegering A, Uthe FW, Jamieson T, Ruoss Y, **Hüttenrauch M**, Küspert M, Pfann C, Nixon C, Herold S, Walz S, Taranets L, Germer CT, Rosenwald A, Samson OJ, Eilers M. (2015) Targeting Translation Initiation Bypasses Signaling Crosstalk Mechanisms That Maintain High MYC levels in Colorectal Cancer. *Cancer Discov.* 5(7):768-81.

Hüttenrauch M, Baches S, Gerth J, Bayer TA, Weggen S, Wirths O. (2015) Neprilysin deficiency alters the neuropathological and behavioral phenotype in the 5XFAD mouse model of Alzheimer's disease. *J Alzheimers Dis.* 44(4):1291-302.

Wiegering A, Uthe FW, **Hüttenrauch M**, Mühling B, Linnebacher M, Krummenast F, Germer CT, Thalheimer A, Otto C. (2014) The impact of pyrvinium pamoate on colon cancer cell viability. *Int J Colorectal Dis.* 29(10):1189-98.

Christensen DZ, **Huettenrauch M**, Mitkowski M, Pradier L, Wirths O. (2014) Axonal degeneration in an Alzheimer mouse model is PS1 gene dose dependent and linked to intraneuronal A β accumulation. *Front Aging Neurosci.* 6:139

Reinert J, Martens H, **Huettenrauch M**, Kolbow T, Lannfelt L, Ingelsson M, Pateau A, Verkkoniemi-Ahola A, Bayer TA, Wirths O. 2014 A β 38 in the brains of patients with sporadic and familial Alzheimer's disease and transgenic mouse models. *J Alzheimers Dis.* 39(4):871-81

Memberships, Stipends and Awards

05/2013 to date	Göttingen Graduate School for Neurosciences, Biophysics and Molecular Biosciences (GGNB), Program: Molecular Physiology of the brain (CMPB)
05/2013 to date	PhD stipend Gerhard Hunsmann Foundation
03/2013	Travel grant for a poster abstract entitled "The translation inhibitor Silvestrol can abolish the induction of c-Myc in colorectal cancer" at the 2 nd International Meeting on Molecular-Based Treatment of GI-Cancer, Göttingen, Germany
08/2012 - 03/2013	Research fellowship Graduate college 1048 (Molecular basis of organ development in vertebrates), University of Würzburg

Additional Skills and Qualifications

Communication skills	<p>Presented research results on international conferences</p> <ul style="list-style-type: none">- Arbeitsgemeinschaft für Neuropsychopharmakologie und Pharmakopsychiatrie (AGNP) Symposium, September 2015, Munich, Germany (Poster)- Conference on Alzheimer's and Parkinson's Diseases (AD/PD), March 2015, Nice, France (Poster)- 2nd International Meeting on Molecular-Based Treatment of GI-Cancer, March 2013, Göttingen, Germany (Poster) <p>Laboratory trainings and supervision of internships and theses for BSc/MSc/Medical doctor programs</p> <p>Well experienced and confident in giving oral presentations</p>
Language skills	German (native), English (fluent)
Computer skills	Standard Microsoft Office applications, GraphPad Prism, ImageJ, Inkscape, Adobe Illustrator
Additional qualifications	Laboratory Animal Science Certificate according to FELASA B (03/2010)

Göttingen, March 2016